1-1-2017

Approach Towards The Development Of Novel Disease Modifying Therapeutics For Parkinson's Disease

Dan Luo
Wayne State University,

APPROACH TOWARDS THE DEVELOPMENT OF NOVEL DISEASE MODIFYING THERAPEUTICS FOR PARKINSON'S DISEASE

by

DAN LUO

DISSERTATION

Submitted to the Graduate School

of Wayne State University,

Detroit, Michigan

in partial fulfillment of the requirements

for the degree of

DOCTOR OF PHILOSOPHY

2017

MAJOR: PHARMACEUTICAL SCIENCES

Approved By:

_____

Advisor Date

_____

_____

_____

DEDICATION

This work is dedicated to my parents, who have always been there for me.

ACKNOWLEDGMENTS

I would like to express my sincere gratitude to my advisor Dr. Aloke Dutta for allowing me to pursue my research in his laboratory. I am grateful for his generous guidance, support, and encouragement throughout my study and research. Writing of this dissertation would have never been successful without his constant guidance and careful review.

I am grateful to my dissertation committee members, Dr. Sokol Todi, Dr. Timothy Stemmler, and Dr. Zhihui Qin for their insightful advice and suggestions for completing my research and dissertation.

I would also like to express my thanks to our collaborator, Dr. Maarteen Reith from New York University School of medicine for performing the *in vitro* receptor assays.

Thank you to all the past and present members in Dr. Dutta's group. I would like to thank Dr. Horrick Sharma, Dr. Banibrata Das, Dr. Deepthi Yedlapudi, and Ms. Liping Xu for their valuable guidance. I am also thankful to Dr. Bidyut Dinda, Dr. Chandrashekhar Voshavar, Dr. Seenuvasan Vedachalam, Dr. Soumava Santra, Dr. Mrudang Shah, Dr. Gyan Modi, Mr. Fahd Dholkawala, Ms. Asma Elmabruk, and Mr. Pranay Ravipati, for their advice and support.

I would like to express my gratitude towards the department Pharmaceutical Sciences at Wayne State University for offering me the opportunity to continue my graduate study here. My sincere thanks also go to all the faculty, staff and student members.

I would like to thank the financial support from the National Institute of Health (NIH/NS047198, AKD) for this study.

Last but not least, I thank my family and friends for their encouragement and support.

TABLE OF CONTENTS

LIST OF TABLES

LIST OF FIGURES

LIST OF SCHEMES

CHAPTER 1 INTRODUCTION

1.1. Parkinson's disease

Parkinson's disease (PD), which was first described by Dr. James Parkinson in 1817 (Parkinson 2002), is an age-related neurodegenerative disease that mainly affects the motor system. It has four cardinal symptoms, namely, bradykinesia, rigidity, resting tremor, and postural instability (Moustafa et al. 2016, Jankovic 2008). In addition, this disease affects the non-motor system as well and gives rise to symptoms such as mood changes, cognitive decline, pain, sleep disturbance, and autonomic dysfunction (Politis et al. 2010). The severity of both motor and non-motor symptoms progresses during the course of the disease (Alves, Forsaa, Pedersen, Gjerstad, et al. 2008).

Two pathological hallmarks of PD have been described in literature. One is the progressive loss of dopaminergic neurons in the substantia nigra cons compacta (SNpc); the other is the presence of intraneuronal proteinaceous deposits named Lewy bodies (LBs) or Lewy neurites (LNs) (Dauer and Przedborski 2003). The neuropathological-clinical correlations based on multiple studies have suggested that the initial motor signs in PD may occur when experiencing around 30% of total substantia nigra neurons loss (Grosch, Winkler, and Kohl 2016).

1.2. Statistics about PD

PD is the second most common neurodegenerative disorder following Alzheimer's disease and affects around ten million people worldwide (Parkinson's

Disease Foundation). In the industrialized countries, the prevalence of PD is estimated to be approximately 0.3% in the entire population or 1% of the population over the age 60 (de Lau and Breteler 2006).

According to the World Health Organization, the age-adjusted incidence rate of PD ranges from 9.7 to 13.8 per 100,000 population per year (World Health Organization 2006). This rate in the developed countries is estimated to be approximately 14 per 100,000 population per year in the total population or about 160 per 100,000 population per year for the population aged 65 years or over (Ascherio and Schwarzschild 2016). It has also been suggested that the incidence rate of PD increases with age (Hirsch et al. 2016).

The economic burden of PD in the United States has been estimated to be 15.5 billion per year, which covers direct medical costs and indirect costs including reduced employment, workdays lost due to illness, reduced household income, higher disability payments (Gooch, Pracht, and Borenstein 2017). Moreover, the economic burden of PD is expected to escalate further in the coming decades (Kowal et al. 2013).

1.3. Pathogenesis of PD

This section reviews the studies on PD pathogenesis as they serve as the foundation of rational drug design and development. Although the etiology of PD is still not well-understood, multiple pathological factors including oxidative stress, mitochondrial dysfunction, α-synuclein (αSN) protein aggregation, as well as genetic and environmental aspects are strongly implicated in the disease

progression (Hwang 2013, Bose and Beal 2016, Stefanis 2012, Corti, Lesage, and Brice 2011, Goldman 2014).

1.3.1. Oxidative stress

Oxidative stress refers to the redox imbalance due to excess reactive oxygen species (ROS) production over the capability of antioxidant response (Ray, Huang, and Tsuji 2012). Under physiological conditions, the endogenous generation of ROS in general involves direct interactions with redox-active metals and oxygen species through reactions including the Fenton and Haber-Weiss reactions, in combination with indirect pathways that are mediated by both mitochondrial and non-mitochondrial ROS-generating enzymes, including monoamine oxidase (MAO) and nicotinamide adenine dinucleotide phosphate (NADPH) oxidase (NOX) (Dias, Junn, and Mouradian 2013, Kim et al. 2015).

The consumption of oxygen by brain comprises approximately 20% of the oxygen supply of the whole body, a large portion of which is converted to ROS (Johnson, Wilson-Delfosse, and Mieyal 2012). Both the ROS-generating enzymes and dopamine (DA), an autoxidizable neurotransmitter, render the dopaminergic neurons more susceptible to oxidative stress (Hwang 2013, Halliwell 2006). DA itself has been suggested to be a possible source of oxidative stress due to the fact that excess cytosolic DA can be readily metabolized and generate ROS (Blesa et al. 2015). Under normal conditions, the vesicular monoamine transporter (VMAT) sequesters more than 90% of intracellular DA into storage vesicles and prevent it from excessive accumulation and subsequent

degradation in the intracellular compartment, which produces neurotoxic species (Eisenhofer, Kopin, and Goldstein 2004, Caudle et al. 2008). However, in the presence of insults such as αSN protofibrils, oxidative stress, and certain weak base compounds, disruption of vesicular DA storage may cause the exposure of dopamine and promote its metabolism through two pathways leading to the ROS production (Hastings 2009) (**Figure 1**). The autoxidation of DA, which may be facilitated by the presence of transition metal ions, can generate electron-deficient DA quinone species that can react readily with cellular nucleophiles (Lotharius and Brundin 2002, Hastings 2009). It has been suggested that the covalent modification of proteins by DA quinones often results in inactivation of protein functions (Hastings 2009). Moreover, the enzymatic degradation of DA by MAO-B enzyme produces the reactive 3,4-dihydroxyphenylacetaldehyde (DOPAL), which undergoes further inactivation, and hydrogen peroxide (Meiser, Weindl, and Hiller 2013). The generated hydrogen peroxide can be further converted to hydroxyl radical by the Fenton reaction mediated by iron leading to cytotoxicity (Lotharius and Brundin 2002). Additionally, the level of iron in SN has been reported to be significantly higher than in other brain regions due to its binding affinity to neuromelanin, and it was further elevated in the SN of PD patients (Lotharius and Brundin 2002).

In addition to mechanisms involving DA metabolism, several studies have suggested a role for NOX enzymes, which mainly reside on the cellular membrane and can generate superoxide anions by coupling NADPH-derived

electrons with oxygen (Sorce, Krause, and Jaquet 2012, Zhao et al. 2017). It has also been proposed that the elevation of NOX1 and NOX2 may contribute to the dopaminergic neuronal loss in PD brain via NOX-derived ROS (Ma et al. 2017).

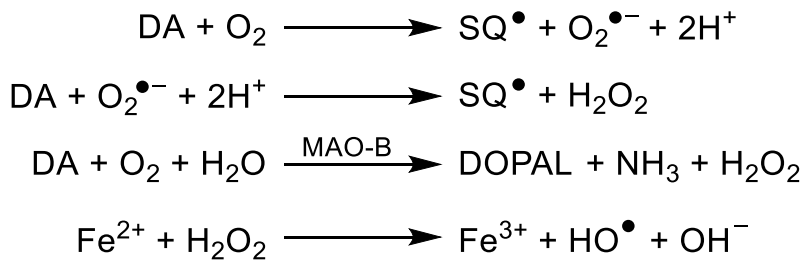

Figure 1. Non-enzymatic and enzymatic metabolism of DA (modified based on Lotharius and Brundin 2002). DA can undergo autoxidation and lead to the formation of ROS, including dopamine quinone species (SQ•), superoxide anion (O_2•-), and hydrogen peroxide (H_2O_2). It can also be metabolized by MAO-B enzyme and produce hydrogen peroxide that can be further converted by the Fenton reaction.

As for the ROS removal, several postmortem studies have revealed a decrease in the amount of reduced glutathione (GSH), which is a major component of cellular antioxidant defenses, relative to glutathione disulfide (GSSG) (GSH:GSSG ratio) in the SN of the PD brain compared to the controls (Dias, Junn, and Mouradian 2013, Martin and Teismann 2009). Furthermore, altered GSH-dependent enzyme activity caused by the mutations that correlate with PD has also been reported, such as the mutation of Glutathione S-Transferases P1 (GSTP1), an enzyme that has an important role in dopaminergic nerve cell survival (Johnson, Wilson-Delfosse, and Mieyal 2012). The effect of GSH depletion includes the inhibition of mitochondrial complex I, E1 ubiquitin

ligase, and proteasome activity and also the activation of the JNK pathway, leading to an inflammatory response (Martin and Teismann 2009).

As a consequence of oxidative stress, increased levels of oxidized protein, lipid, and DNA have been observed in the SN of PD subjects (Limongi and Baldelli 2016). Furthermore, the structures and functions of macromolecules have been proposed to be altered by ROS through direct or indirect oxidative modifications of small molecules that either comprise or interact with the macromolecules, which can disturb nucleic acid stability, protein homeostasis, the functionality of ion channels, and cellular self-defenses leading to the neurodegeneration of PD (Zhao et al. 2017).

1.3.2. Mitochondrial dysfunction

Mitochondria is where oxidative phosphorylation takes place (Winklhofer and Haass 2010). A reduced activity of mitochondrial complex I has been observed in the SN, platelets, and skeletal muscle of PD subjects (Schapira 2006, Hauser and Hastings 2013). A number of observations, including defects in the activity of the mitochondrial electron transport complex, a reduction of mitochondria movement, and an increase in the mitochondrial permeability transition have been reported in the toxin models of mitochondrial dysfunction (Bose and Beal 2016). Studies have also suggested that defects in mitochondria, especially complex I, can lead to neurodegeneration as they result in an elevated ROS level and a decreased ATP level (Moore et al. 2005, Winklhofer and Haass 2010).

Certain gene mutations that can cause mitochondrial dysfunction are known to play a role in familial forms of PD (Bose and Beal 2016). Point mutations and deletions in gene *Parkin*, *PINK1*, and *DJ-1* have been reported to cause familial/early-onset PD (Subramaniam and Chesselet 2013, Hauser and Hastings 2013).

1.3.3. Protein aggregation

In addition to oxidative stress and mitochondrial dysfunction, protein aggregation has also been suggested to be critically involved in PD pathogenesis (Stefanis 2012). As a part of neurodegenerative process, the accumulation of proteins will result in the formation of proteinaceous inclusions (LBs or LNs), whose presence is one of the pathological hallmarks of PD (Dauer and Przedborski 2003). The main component of these inclusions has been identified to be αSN through immunohistochemical staining in the early studies (Spillantini et al. 1997, Spillantini et al. 1998). Furthermore, to date six N-terminal missense mutations (A30P, E46K, H50Q, G51D, A53E, A53T) in the α-synuclein gene (*SNCA*) as well as duplication and triplication of the *SNCA* locus have been linked to the autosomal dominant forms of familial PD (Kruger et al. 1998, Zarranz et al. 2004, Proukakis et al. 2013, Lesage et al. 2013, Pasanen et al. 2014, Polymeropoulos et al. 1997, Chartier-Harlin et al. 2004, Singleton et al. 2003, Wong and Krainc 2017). While the penetrance of *SNCA* duplication has been estimated to be approximately 40%, it has been reported to be close to 100% for triplications and missense mutations (Schulte and Gasser 2011, Goedert

2015). In addition, the genome-wide association studies (GWAS) on the sporadic PD patients have revealed a strong association of the *SNCA* locus and the sporadic form of PD (Venda et al. 2010). These findings indicate the important role of αSN in the disease pathogenesis.

1.3.3.1. Structure and physiological function of αSN

αSN, encoded by the *SNCA* gene that resides on chromosome 4q21.3-q22, is a 14.5 kDa presynaptic protein (Chen et al. 1995, Siddiqui, Pervaiz, and Abbasi 2016). It consists of 140 amino acids and can be structurally divided into three domains (**Figure 2a**). The amphipathic N-terminal domain (from residue 1 to 60) and the hydrophobic non-amyloid component (NAC) domain (from residue 61 to 95) contain seven imperfect 11-residue repeats with a consensus motif (KTKEGV), which share structural similarity with the class A2 apolipoproteins and are capable of lipid binding through the formation of helical structures (Jo et al. 2000). The NAC domain can form β-sheets and is believed to be responsible for the protein aggregation (Giasson et al. 2001, Tuttle et al. 2016). The acidic C-terminal domain (from residue 96 to 140) is rich in glutamate, aspartate, and proline residues and is highly charged (Barrett and Timothy Greenamyre 2015). This region has been suggested to have a critical role in interaction with other proteins and small molecules (Mor et al. 2016). During the interaction with membranes, the N-terminus helical structure can serve as a membrane anchor, while the central region has the capacity to modulate the affinity to the

membranes through acting as a sensor for the lipid properties; however, the C-terminal domain will remain unstructured (**Figure 2b**) (Fusco et al. 2014).

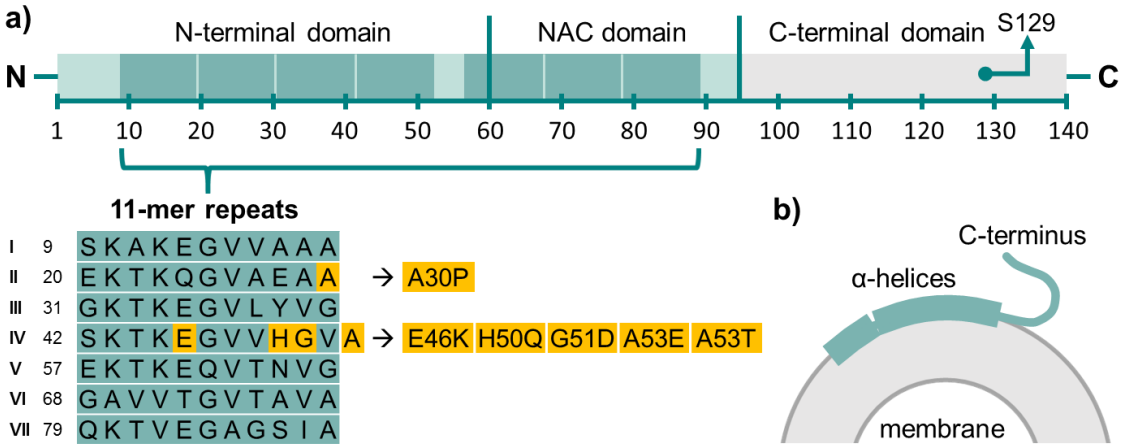

Figure 2. αSN structure and domains. **a)** Schematic depiction of the primary structure of αSN. The N-terminal domain and the non-amyloid component (NAC) domain are illustrated in light green; the C-terminal domain is shown in grey. The 11-mer imperfect repeats with a consensus motif (KTKEGV) are depicted as green boxes, and their sequences are listed below as well. Currently identified disease-associated point mutations are highlighted in yellow. A common spot for post translational modification (PTM) is indicated. **b)** Schematic drawing of αSN bond to the negatively charged membrane.

αSN is traditionally viewed as an intrinsically disordered protein (IDP), which does not possess defined three-dimensional structures, based on the biophysical characterization of recombinant αSN purified from E. coli using techniques such as circular dichroism (CD) spectroscopy and Fourier-transform infrared (FTIR) spectroscopy (Weinreb et al. 1996, Wang et al. 2016). This disordered monomeric structure has been reported to be independent of cell lysis method and heating/acidification for protein purification (Coelho-Cerqueira et al. 2013), and it is also able to adopt α-helical secondary structure upon lipid binding

(Davidson et al. 1998). In addition, the native αSN purified from mouse brain without boiling or detergents has been shown as a largely unstructured monomer that is prone to aggregation (Burre et al. 2013). However, in recent years an ongoing debate on the native conformation of αSN started. Endogenous αSN isolated from cell lines, brain tissue and living human cells under non-denaturing conditions has been proposed to exist mainly as a folded tetramer that resists aggregation (Bartels, Choi, and Selkoe 2011). Other evidence has demonstrated that αSN forms physiological multimers, principally tetramers, that have α-helical conformation (Wang et al. 2011, Dettmer et al. 2015). In another study, αSN has been observed to exist in a stable monomeric form, in which the NAC domain is shielded to prevent spontaneous aggregation (Theillet et al. 2016). These contradicting observations have led to the current postulation that αSN with great structural flexibility may exist in a dynamic equilibrium between multiple forms depending on the cellular localization, environment and binding partners (Jain et al. 2013, Wang et al. 2016, Wong and Krainc 2017).

Although the physiological role of αSN, which predominantly exists in the presynaptic terminals, is still not fully understood (Calo et al. 2016), it has been suggested that αSN is importantly involved in synaptic maintenance (Mor et al. 2016). It can participate in synaptic vesicle trafficking (Esposito, Ana Clara, and Verstreken 2012). αSN may also act as molecular chaperones by cooperating with Cysteine-string protein α (CSPα). This idea is further supported by the observation of sequence homology between αSN and 14-3-3 protein chaperones

and its ability to prevent denatured protein aggregation *in vitro* (Mor et al. 2016). Moreover, modulatory role of αSN in dopamine neurotransmission through the function of soluble NSF attachment protein receptor (SNARE) complex assembly has been reported (Mor et al. 2016, Gallegos et al. 2015). In addition, αSN may have a putative role in neurotransmitter synthesis and reuptake through the modulation of tyrosine hydroxylase (TH), vesicular monoamine transporter 2 (VMAT2), dopamine transporter (DAT) trafficking (Butler, Sambo, and Khoshbouei 2016, Mor et al. 2016).

1.3.3.2. Misfolding and aggregation of αSN

As stated earlier, αSN possesses a great degree of structural flexibility, which can adopt various conformations in different conditions and exert versatile functions (Wang et al. 2016). Due to the presence of central hydrophobic region, αSN can be misfolded into β-sheet enriched αSN assembly that varies in size, stability, morphology, and potential for further aggregation; this process can be influenced by factors including the interactions with lipids, small molecules such as dopamine, or metals such as iron, mutations, post-translational modification (PTM), oxidative stress and truncation (Lashuel et al. 2013, Majd, Power, and Grantham 2015, Breydo, Wu, and Uversky 2012) (**Figure 3**).

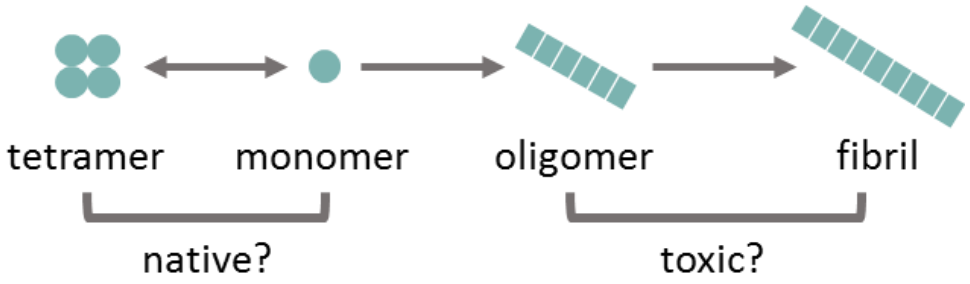

Figure 3. Schematic drawing of αSN misfolding and aggregation (modified based on Wong and Krainc 2017). Drawings are not to scale. The native protein is depicted as circles, and the aberrant form is indicated by rectangular shape. The native αSN may exist in a dynamic equilibrium between multiple conformations. Under the conditions such as oxidative stress or the presence of metals, αSN can be misfolded into abnormal β-sheets and tends to aggregate.

Redox-active metal ions can affect the αSN misfolding and aggregation either through direct interaction that leads to conformational change or via oxidation (Breydo, Wu, and Uversky 2012). Mutations in the imperfect repeats extending to the hydrophobic domain may reduce the membrane binding and cause αSN dissociation, which can subsequently lead to the accumulation of unfolding forms that favors the formation of oligomeric and/or fibrillar species (Luna and Luk 2015). Among various PTMs in αSN, phosphorylation of Serine 129 (**Figure 2a**) is the most well studied, and has been suggested to be the most pathologically relevant to PD (Barrett and Timothy Greenamyre 2015). Autopsy of PD brains revealed that about 90% of αSN found in LB is phosphorylated at S129 in contrast to 4% or less in the normal brain, which suggests a link between phosphorylation and aggregation (Majd, Power, and Grantham 2015, Tyson, Steiner, and Brundin 2016, Xu, Deng, and Qing 2015). It has also been

suggested that phosphorylation of αSN may act as a signal for degradation (Tyson, Steiner, and Brundin 2016).

1.3.3.3. Propagation of αSN

The progression of αSN pathology in sporadic PD adopts a distinct pattern, which can be characterized into six stages and is termed as “Braak staging” (Braak et al. 2003). This pathology starts from olfactory bulb, the anterior olfactory nucleus and/or the dorsal motor nuclei of the vagal and glossopharyngeal nerves in the brainstem and gradually expands to less vulnerable nuclear grays and cortical areas (Braak et al. 2003, Goedert et al. 2013). Continuing study based on the “Braak staging” proposed that this spreading is caused by a neurotropic pathogen that enters the central nervous system (CNS) through retrograde axonal and transneuronal transport (Hawkes, Del Tredici, and Braak 2007).

Following these findings, the observation of LB like inclusions in the grafted neurons in the PD brain years after implantation by two independent studies suggested “host-to-graft” transmission of αSN pathology (Li et al. 2008, Kordower et al. 2008). In addition, based on the initial clinical observations, various *in vitro* and *in vivo* models have been developed to simulate αSN propagation (Rey, George, and Brundin 2016, Gallegos et al. 2015, Hasegawa, Nonaka, and Masuda-Suzukake 2017). These studies indicated that in addition to the traditional cell-autonomous mechanism, which means independent occurrence of protein misfolding and assemblies in many cells, cell non-

autonomous mechanism may also exist in αSN propagation. (Goedert, Clavaguera, and Tolnay 2010, Goedert 2015). Moreover, the “prion-like” propagation has been hypothesized, which suggested that the aberrant αSN has prion-like properties to convert the normal proteins into abnormal forms and spread throughout the brain via cell-to-cell transmission (Hasegawa, Nonaka, and Masuda-Suzukake 2017).

The early *in vitro* studies and recent models in αSN propagation gave rise to the “seeding” concept, which was first used to describe Prion protein (PrP) (Oueslati, Ximerakis, and Vekrellis 2014). As illustrated in **Figure 4a**, seeding is a nucleation-dependent mechanism, in which the seeds (the pathogenic species) generated from rate-limiting nucleation step can recruit adjacent soluble monomers and serve as a template to accelerate the assembly (Oueslati, Ximerakis, and Vekrellis 2014).

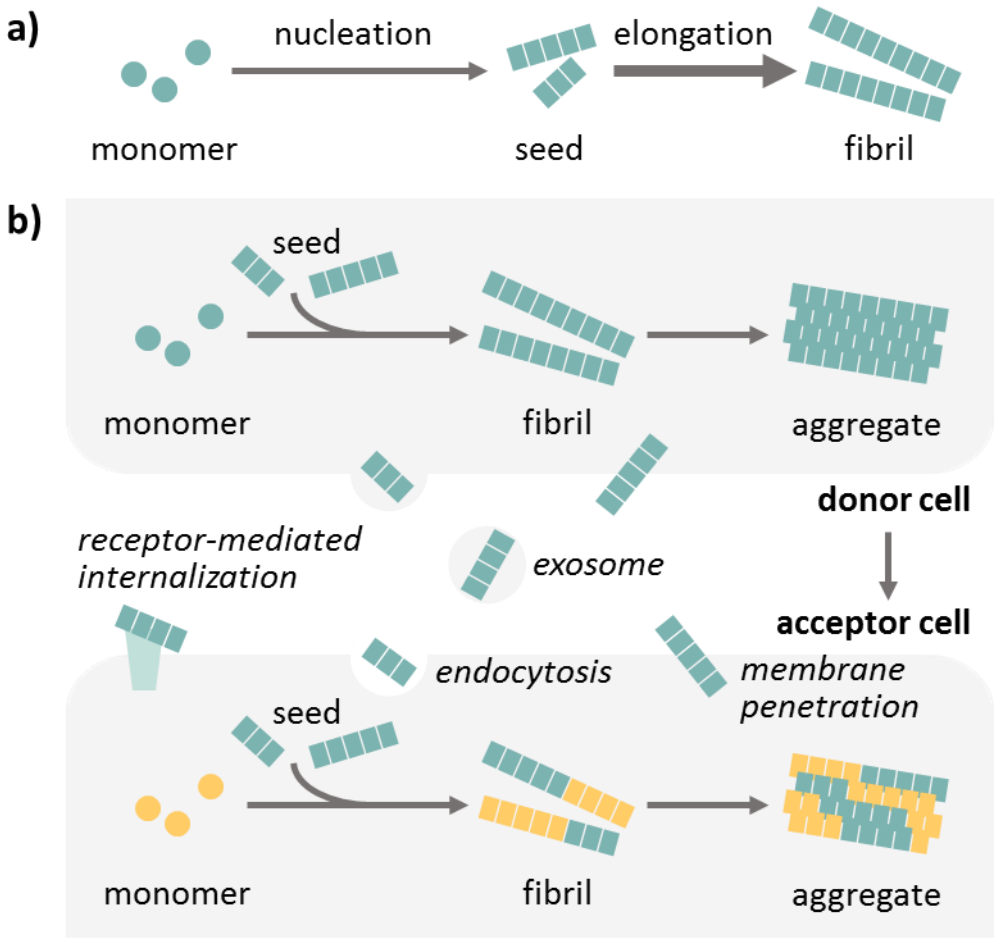

Figure 4. Schematic drawing of αSN seeding and propagation mechanism. Drawings are not to scale. The native protein is depicted as circle, and the aberrant form is indicated by rectangular shape. **a)** Seeding of αSN is a nucleation-dependent mechanism. **b)** Propagation of αSN via cell-to-cell transmission (adapted from Oueslati, Ximerakis, and Vekrellis 2014). The donor cell can release seeds through non-classic secretory pathway or direct release, and the acceptor cell can internalize them by mechanisms including classical endocytosis, exosomal transport, receptor-mediated internalization, and direct membrane penetration.

The transmission of αSN from donor cells to acceptor cells involves multiple molecular mechanisms (**Figure 4b**). Studies have shown that αSN can be released via non-classic secretory pathway, including exocytotic vesicles and

exosomes, and direct release from injured/dying neurons (Recasens and Dehay 2014, Oueslati, Ximerakis, and Vekrellis 2014). Failure of intracellular clearance pathways may further exacerbate the pathological release (Recasens and Dehay 2014, Gallegos et al. 2015). Moreover, the uptake of αSN can be achieved through classical endocytosis, exosomal transport, receptor-mediated internalization, and direct membrane penetration (Gallegos et al. 2015, Recasens and Dehay 2014, Oueslati, Ximerakis, and Vekrellis 2014).

1.3.3.4. Toxicity of αSN

The removal of abnormal proteins is critical for the cell survival and cellular function (Tyson, Steiner, and Brundin 2016). However, A30P and A53T mutations have been reported to inhibit chaperone-mediated autophagy (CMA); familial mutations and overexpression of αSN as well as LB-like αSN inclusions have been shown to inhibit macro autophagy (Tyson, Steiner, and Brundin 2016). Moreover, defects in quality control and protein degradation machinery may result in an elevated intracellular αSN concentration, an increase in cell autonomous aggregation and the chance of seeding by exogenous αSN (Luna and Luk 2015). In addition, in compromised cells or in cells expressing aggregation-prone familial forms of αSN, the overwhelmed protein degradation system may lead to a cascade of pathological events that cause cellular dysfunction and cell death (Tyson, Steiner, and Brundin 2016).

There is an ongoing debate on whether oligomeric species or fibrils are the toxic form of αSN. Studies have suggested that PD-linked A53T and A30P

mutations can accelerate oligomerization rather than fibrillization, and an increased level of soluble, lipid-dependent oligomers has been observed in both αSN transgenic mice and PD brains comparing to the controls (Wong and Krainc 2017). The annular protofibrils have been shown to alter membrane permeability and increase influx of calcium from the extracellular to intracellular space, leading to cell death (Lashuel et al. 2013). Other studies have demonstrated that fibrils, when injected into rat SNpc, can significantly induce motor impairment, dopaminergic cell loss and synaptic impairment, suggesting they might be more toxic than their precursors (Wong and Krainc 2017).

Both toxic gain-of-function and loss-of-function mechanisms have been proposed to play a significant role in αSN pathology (Collier et al. 2016, Winklhofer, Tatzelt, and Haass 2008). The misfolding of αSN caused by conformational changes can reduce the capacity of αSN in vesicular trafficking and modulating neurotransmission (Majd, Power, and Grantham 2015). Furthermore, αSN overexpression can contribute to the impairment of mitochondrial homeostasis leading to oxidative stress and dopamine oxidation (Majd, Power, and Grantham 2015). Studies have suggested that oligomers and aggregates spanning through the cell body and neurites, may cause disruption of cellular function, including organelle dysfunction, defects in interorganelle contacts and dysfunctional organelle dynamics (**Figure 5**) (Wong and Krainc 2017).

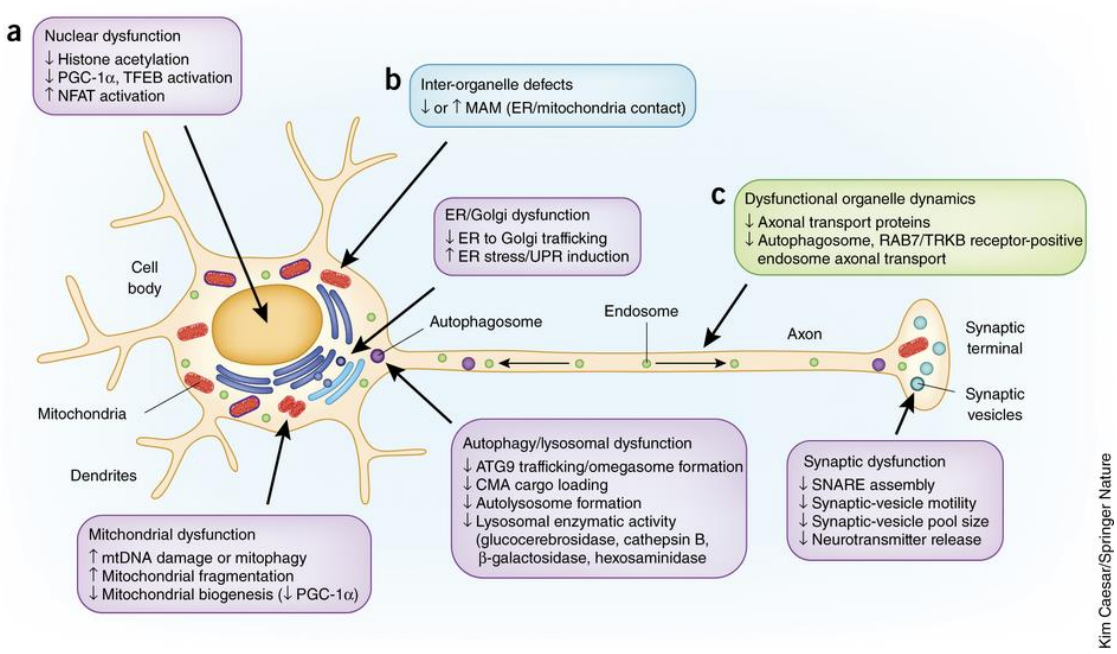

Figure 5. Pathways implicated in α-synuclein toxicity (Wong and Krainc 2017).

1.3.4. Genetic factors

Compared to sporadic PD, familial/early-onset PD, which constitutes less than 10% of total PD cases, is more tightly associated with genetic factors (Schapira 2006, Wirdefeldt et al. 2011, Alves, Forsaa, Pedersen, Gjerstad, et al. 2008, Lesage and Brice 2009). Till this decade, more than 16 loci and 11 genes including aforementioned *Parkin*, *PINK1*, *DJ-1*, and *SNCA* have been associated with PD (Corti, Lesage, and Brice 2011, Hernandez, Reed, and Singleton 2016, Ferreira and Massano 2017).

1.3.5. Environmental factors

The environmental factors include rural living, drinking well water, farming, and using herbicides or pesticides (Priyadarshi et al. 2001, Schapira 2006,

Goldman 2014). These risk factors may lead to an increased exposure to exogenic toxins, many of which are known to have neurotoxicity and can produce Parkinsonian syndromes in animals (Burbulla and Kruger 2011, Schapira 2006).

It needs to be emphasized that the pathogenesis of PD is multifactorial. As shown above, all these pathogenic factors are interrelated. A single pathogenic event may lead to another and initiate a vicious cycle. This provides a great challenge in PD treatment, which is discussed briefly in the next section.

1.4. PD treatments

This section reviews the current status of anti-parkinsonian agents in use. The present treatments available for PD generally fall into four major categories, namely dopamine replacement therapy, MAO-B inhibitors, catechol-*O*-methyl transferase (COMT) inhibitors, and dopamine agonists (**Figure 6, 7**) (Schapira 2009, Factor 2008).

1.4.1. Dopamine replacement therapy

Levodopa, an orally active precursor of DA, remains the gold standard of PD treatment (Mercuri and Bernardi 2005, Poewe et al. 2010). Due to the peripherrial levodopa decarboxylation, which causes limited bioavailability and poor tolerability, levodopa is commonly admistrated with carbidopa, a DOPA decarboxylase (DDC) inhibitor (Gershanik 2015). However, the long-term use of levodopa may induce motor complications, such as motor fluctuations and dyskinesia, due to the erratic stimulation of DA receptors (Jankovic and Aguilar 2008, Blandini and Armentero 2014). Over the years, interventions, including the

use of oral, transdermal, and subcutaneous DA agonists, MAO-B or COMT inhibitors, have been developed to manage motor complications by extending the duration of striatal DA receptors stimulation (Rascol, Perez-Lloret, and Ferreira 2015).

1.4.2. MAO-B inhibitors

MAO-B is a mitochondrial enzyme that catalyzes the oxidative deamination of a group of monoamines including DA (Youdim, Edmondson, and Tipton 2006). MAO-B inhibitors have been suggested to be a class of medication that is relatively safe and well tolerated (Robakis and Fahn 2015). The first FDA approved selective irreversible MAO-B inhibitor, selegiline, is commonly used as either monotherapy or an adjunct in moderately advanced PD; however, its L-amphetamine-like metabolic products can cause sympathomimetic side effects such as insomnia (Robakis and Fahn 2015, Teo and Ho 2013). Rasagiline, a second generation propargylamine-based selective irreversible MAO-B inhibitor, in contrast to selegiline, is free from generating such metabolic products (Teo and Ho 2013). It is usually used alone or with other PD medications in early-to-late stages of PD (Robakis and Fahn 2015). They function by delaying the metabolism of DA and reducing the generation of ROS (Jankovic and Aguilar 2008). In March 2017, safinamide, a selective reversible MAO-B inhibitor with additional pharmacologic properties including blocking of voltage-dependent sodium channels and inhibiting glutamate release, has been approved by FDA as

an adjuvant therapy to levodopa/carbidopa for PD patients experiencing “off” episodes (Stocchi and Torti 2016, The Food and Drug Administration).

1.4.3. COMT inhibitors

Agents such as entacapone and tolcapone have been used as adjuvants to increase levodopa bioavailability and prolong DA response by inhibiting COMT, which is an enzyme involved in DA degradation (Jankovic and Aguilar 2008, Bonifacio et al. 2007). When levodopa/DDC inhibitor formulations used in combination with COMT inhibitors, more continuous plasma behaviour and weakening in levodopa/DDC inhibitor related homocysteine increase, a biomarker for an impaired methylation capacity, have been observed (Muller 2015).

1.4.4. Dopamine agonists

Dopamine agonists, which mimic DA, can directly activate dopaminergic receptors (Lev, Djaldetti, and Melamed 2007). They can be used as monotherapy mainly in the early stage of PD in order to delay levodopa-induced motor complications or combined with levodopa in advanced PD (Jankovic and Aguilar 2008, Blandini and Armentero 2014). Currently, the clinical use of ergot dopamine agonists has been drastically reduced due to side effects (Factor 2008, Blandini and Armentero 2014). Non-ergot dopamine agonists, such as pramipexole (PPX) and ropinirole, have been shown to be effective in the early stage of PD (Jankovic and Aguilar 2008). Furthermore, in addition to being effective for treating drug-resistant tremor in PD, studies have also suggested

that PPX is able to inhibit the phosphorylation of αSN induced by inhibition of the ubiquitin proteasomal system through a machnism independent of DA receptor activation (Constantinescu 2008, Chau, Cooper, and Schapira 2013).

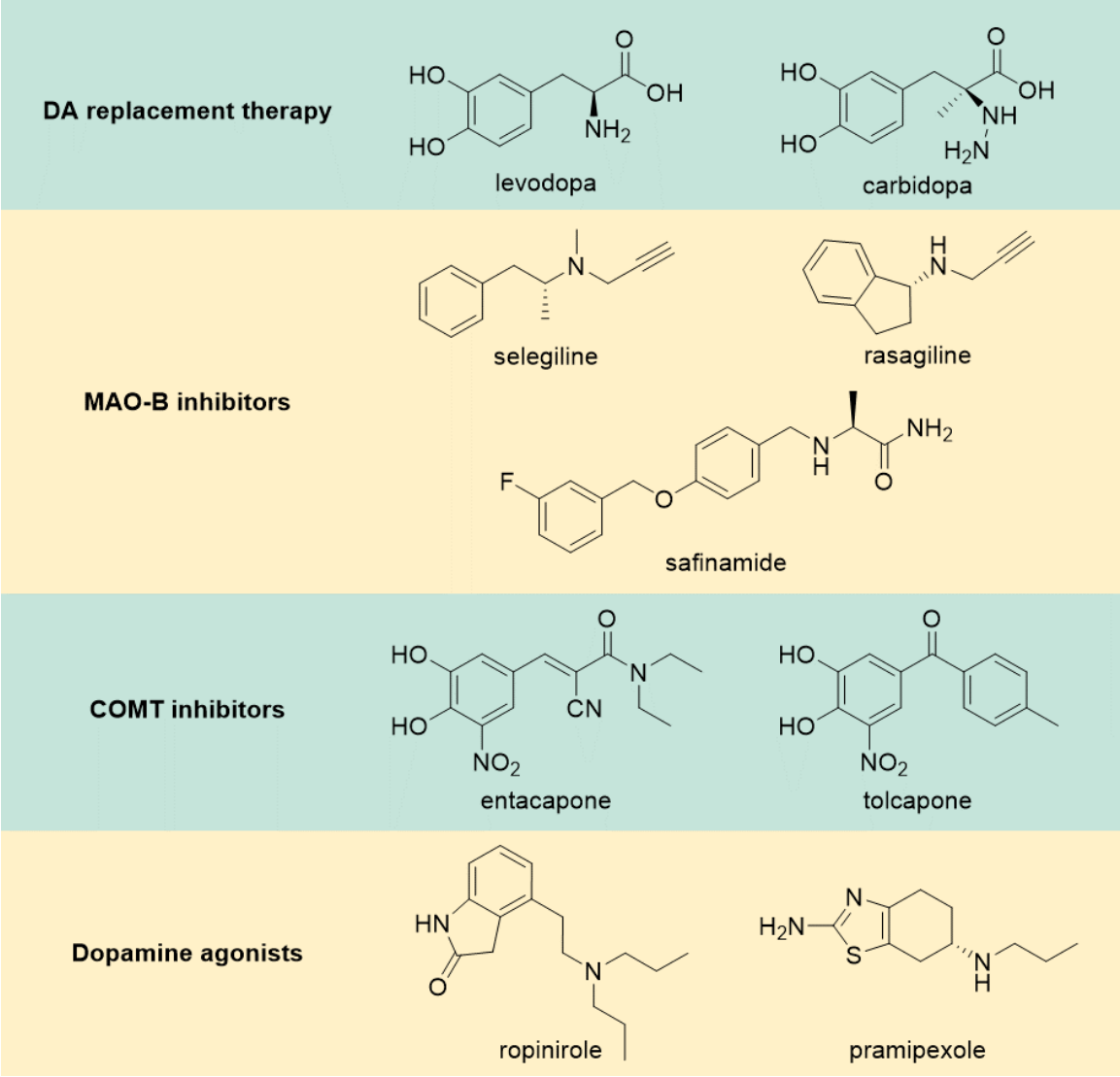

Figure 6. Chemical structures of pharmacological treatments for PD.

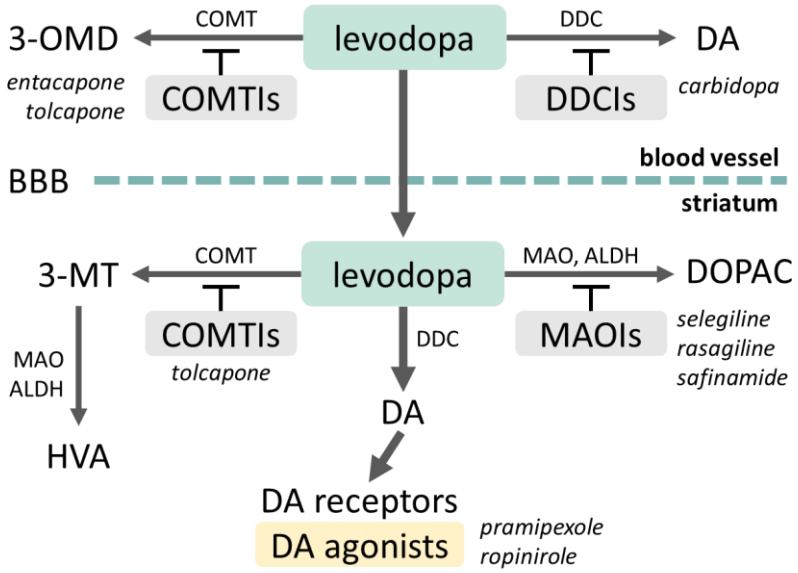

Figure 7. Mechanism of treatments available for PD (adapted based on Jankovic and Aguilar 2008). Abbreviations: COMT, catechol-*O*-methyl-transferase; 3-OMD, 3-*O*-methyldopa; DDC: DOPA decarboxylase; DA, dopamine; BBB, blood-brain barrier; 3-MT, 3-methoxytramine; MAO, monoamine oxidase; ALDH, aldehyde dehydrogenase; HVA, homovanillic acid; DOPAC, 3,4-dihydroxyphenylacetic acid.

Although great progress has been made in PD research throughout the years, the benefits provided by these current treatments are mostly symptom relieving and there are still no curative treatments for PD (Jones, Moussaud, and McLean 2014). Furthermore, these anti-parkinsonian agents suffer from the loss of efficacy as the disease progresses (Jankovic and Aguilar 2008, Blandini and Armentero 2014). Thus, there is still a great unmet need for the development of neuroprotective and disease-modifying therapeutics, which can delay or halt the disease progression. Rationally designed anti-parkinsonian agents that target the

aforementioned pathogenic factors are desirable in terms of providing more effective and safe treatment for PD.

1.5. Potential therapeutic targets and treatments under development

This section reviews the potential therapeutic targets that have been identified and proposed for PD treatment as well as the development of newer generation of therapeutic agents. Events such as oxidative stress, mitochondrial dysfunction, and αSN protein aggregation have been proposed as major potential therapeutic targets to combat PD due to their significant involvement in the PD pathogenesis (Jiang, Sun, and Chen 2016, Moreira et al. 2010, Dehay et al. 2015, Lee and Trojanowski 2006, Hwang 2013, Bose and Beal 2016, Stefanis 2012).

For targeting oxidative stress, the use of antioxidants, which scavenge reactive species, has been suggested, and both direct-acting or indirect-acting methods have been explored (Jiang, Sun, and Chen 2016, Tarazi et al. 2014, Patel 2016). Moreover, the mitochondrial dysfunction has been targeted by mechanisms including the modulations of PD-related genetic mutants, mitochondrial proteins, and the consequences of mitochondrial dysfunction (Luo et al. 2015). Here, the therapeutic development strategies and rationale for targeting αSN aggregation and MAO-B enzyme are discussed in detail below.

1.5.1. Therapeutic development targeting αSN aggregation

As described previously, the identification of αSN as the main component in LBs or LNs and the genetic association of αSN with familial PD have

suggested the critical involvement of αSN in PD pathogenesis and thus, a highly relevant target for therapeutic development (Stefanis 2012, Dehay et al. 2015).

In general, the strategies that have been proposed to combat αSN toxicity include reducing αSN production, increasing αSN clearance, modulating αSN aggregation either directly or indirectly via small molecules (Yacoubian and Standaert 2009, Dehay et al. 2015). The reducing αSN production approach has been proposed by applying techniques such as small interfering RNA (siRNA) or microRNA (miRNA) (Lashuel et al. 2013). Furthermore, activation of proteosomal or lysosomal pathways, promotion of chaperone function, and vaccine-based therapies have been commonly proposed for increasing αSN clearance (Yacoubian and Standaert 2009). Here, only the αSN aggregation modulation strategy is discussed, and the molecules targeting αSN aggregation, especially the polyphenolic compounds and derivatives, are focused on.

1.5.1.1. Polyphenolic compounds as αSN aggregation modulators

Over the years, naturally occurring polyphenolic compounds and their derivatives, such as epigallocatechin gallate (EGCG), baicalein, curcumin, gallic acid, and resveratrol (**Figure 8**), have been substantially investigated for their modulatory effect on αSN aggregation. It has been proposed that polyphenolic compounds, such as EGCG, baicalein, and curcumin, in general may function by inducing the formation of soluble non-toxic oligomers (Ardah et al. 2014). However, there are still variations in their effects. Baicalein has been found to inhibit oligomer formation and disaggregate existing oligomers (Hu et al. 2016).

Studies have suggested that EGCG may function by immobilizing the C-terminal region of αSN and moderately reducing the binding of oligomers to membranes, and gallic acid may function by stabilizing the non-toxic oligomeric αSN through oligomer binding (Lorenzen et al. 2014, Ardah et al. 2014). Recently, the optimized cocktail of curcumin and β-cyclodextrin (β-CD) has been shown to inhibit aggregation and greatly disaggregate preformed aggregates (Gautam et al. 2014). In addition, the similar effect has been reported for the polyphenol–β-CD combinations formed by baicalein, EGCG, and resveratrol (Gautam et al. 2017).

Furthermore, rifampicin (**Figure 8**), an antibiotic, has also demonstrated to preferentially stabilize the non-toxic monomeric and soluble oligomeric forms of αSN (Li et al. 2004).

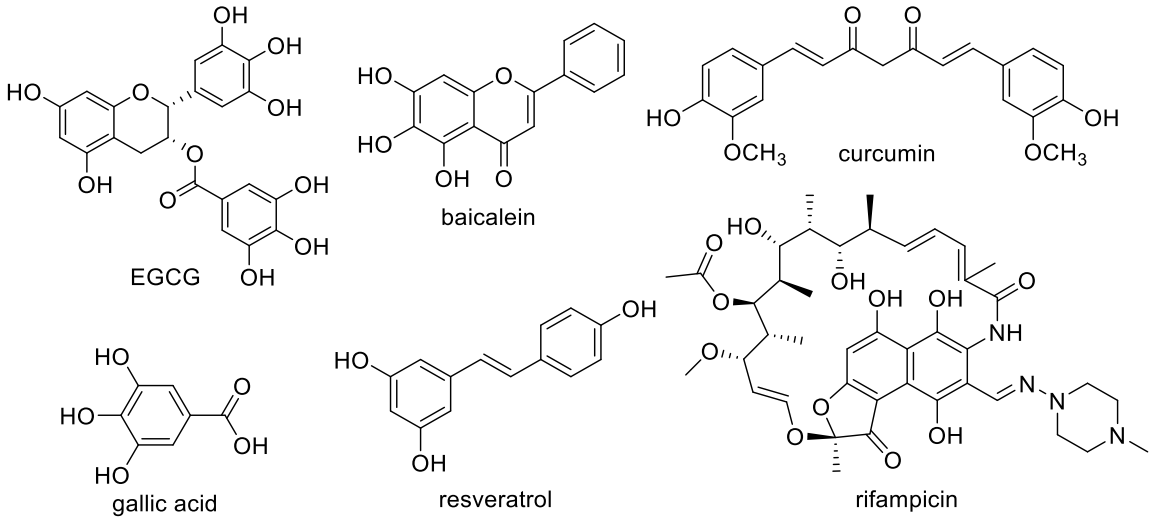

Figure 8. Examples of known αSN aggregation modulators

The mechanism of action (**Figure 9**) of these polyphenolic compounds has been speculated to be that they can be readily converted into quinone

structure to interact with αSN and alter the aggregation pathway (Ardah et al. 2014). Further analysis has suggested that the lysine (Lys) residues on αSN can undergo nucleophilic attack towards the electrophilic center of the quinone group (Li et al. 2005, Labenski et al. 2009). In addition, these polyphenolic compounds may be viewed as candidates of pathologically activated therapeutic, as they can be activated in response to oxidative stress, which plays a crucial role in the pathogenesis of PD (**Figure 10**) (Lipton 2007).

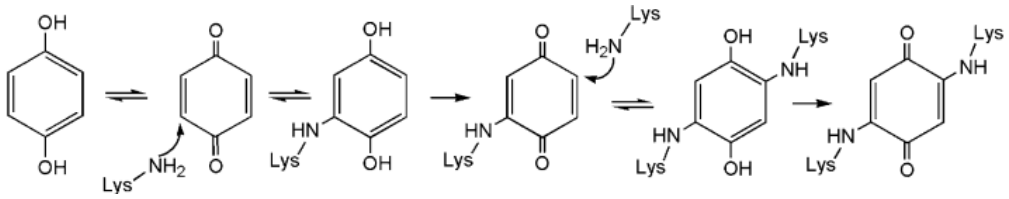

Figure 9. Possible interaction between Lys residue and quinone moiety (Li et al. 2005).

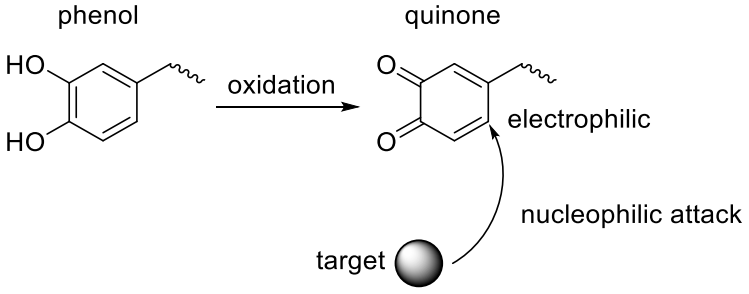

Figure 10. Schematic drawing of pathologically activated therapeutics design (modified based on Lipton 2007).

1.5.1.2. Other molecules as αSN aggregation modulators

In addition to the polyphenolic moiety, other molecules have also been studied on. A molecular tweezer, CLR01, has been developed to directly bind to the αSN monomer near the N terminus, which alters its charge distribution, swells the chain, and increases protein reconfiguration rate (**Figure 11b**) (Acharya et al. 2014). In addition, cyclic peptides (CPs), such as CP1 and CP2, and their derivatives have been reported as a new class of αSN aggregation modulators to prevent fibrillation and decrease the cytotoxicity of aggregates (**Figure 11a**) (Luo and Abrahams 2014). In another study, a class of binding proteins termed β-wrapins with affinity for αSN has been engineered and has been demonstrated to inhibits αSN aggregation and toxicity by interfering with the nucleation phase of aggregation (Mirecka et al. 2014).

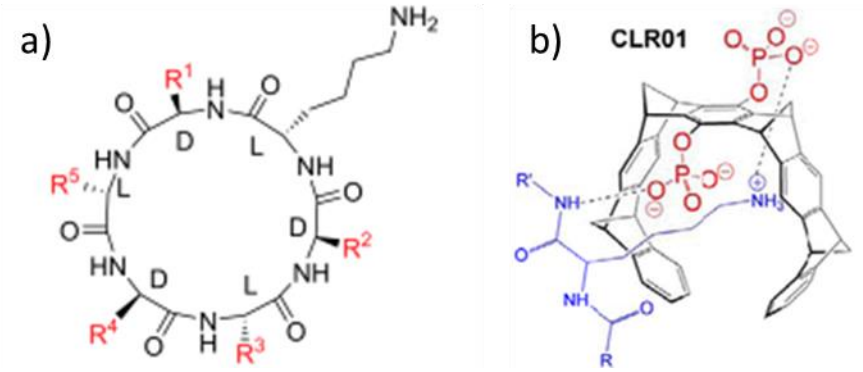

Figure 11. Examples of other type of αSN aggregation modulators **a)** scaffold of cyclic peptides (CPs) (Luo and Abrahams 2014); **b)** molecular tweezer, CLR01 (Acharya et al. 2014).

1.5.2. Therapeutic development targeting MAO-B

The two isoforms of MAO, which are the major neurotransmitter-degrading enzymes in the central nervous system (CNS), are tightly associated with the

mitochondrial outer membrane (Binda et al. 2002, Youdim, Edmondson, and Tipton 2006). Despite of approximately 70% identity of amino acid sequence, they differ in substrate specificities and tissue distribution (Youdim, Edmondson, and Tipton 2006). While neurotransmitters such as serotonin and norepinephrine are preferentially metabolized by the MAO-A isoform, phenylethylamine is mainly metabolized by the MAO-B isoform (Youdim and Riederer 2004). In addition, it has been suggested that the level of MAO-B is near 6-fold higher than the MAO-A in the human SNpc, and both isoforms appear to equally metabolize DA (Tong et al. 2013, O'Carroll et al. 1983).

As displayed in **Figure 12a**, the crystal structure of human MAO-B is dimeric with extensive monomer-monomer interactions, and the C-terminal tail region is responsible for the membrane attachment (Binda et al. 2002). The structure of a single monomer is shown in **Figure 12b**: the side chain of isoleucine199 functions as a gate separating the hydrophobic entrance cavity and substrate cavity, and the flavin adenine dinucleotide (FAD) coenzyme is covalently bound in an 8α-thioether linkage to cysteine397 at the distal end of the substrate cavity (Edmondson, Binda, and Mattevi 2007).

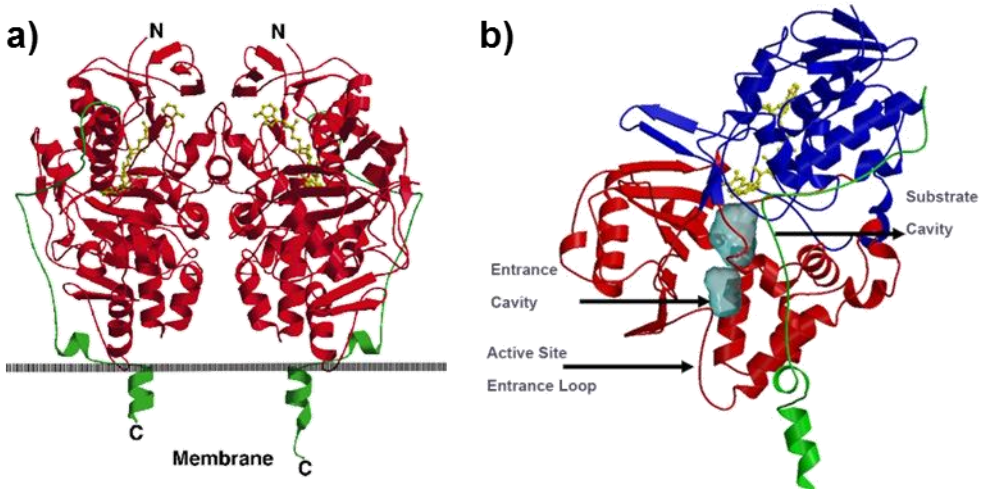

Figure 12. Structure of human MAO-B enzyme. **a)** Ribbon diagram of the MAO-B dimer, which has monomer A displayed on the right and monomer B on the left (Binda et al. 2002). The flavin moiety is shown in yellow in a ball and stick model. The flavin binding domain and the substrate domain are colored in red, and the C-terminal membrane binding domain is shown in green. **b)** Ribbon diagram of human MAO-B monomer (Edmondson, Binda, and Mattevi 2007). The flavin moiety is shown in yellow in a ball and stick model. The flavin binding domain is shown in blue, the substrate domain in red and the C-terminal membrane binding domain in green.

1.5.2.1. Rationale for targeting MAO-B

As mentioned previously, MAO-B catalyzes the deamination of DA and generates reactive aldehyde, hydrogen peroxide, and ammonia (**Figure 1**) (Meiser, Weindl, and Hiller 2013). While the reactive aldehyde derived from dopamine degradation does not appear to accumulate in the healthy brain, a great reduction in the level of aldehyde dehydrogenase observed in the PD brain may cause the aldehydes to adduct with amine groups and generate toxic species (Youdim, Edmondson, and Tipton 2006). In addition, neurotoxicity may

also derive from Fenton reaction that involves iron and hydrogen peroxide, another product from DA metabolism by MAO-B (Youdim and Bakhle 2006).

It has been reported that MAO-B level adopts a distinct developmental pattern: its activity remains constant during early childhood and rise during advanced age (Nicotra et al. 2004). Multiple studies have suggested that both the content and activity of MAO-B increase with aging in mammalian species, including humans (Nicotra et al. 2004). Moreover, increased level of MAO-B in PD subjects has been observed as a consequence of gliosis (Youdim, Edmondson, and Tipton 2006). Subsequently, increased level of the catalytic reaction products, DOPAL and hydrogen peroxide, which may promote apoptotic signaling events resulting in the dopaminergic cell loss, and reduced level of dopamine may take place (Edmondson et al. 2009). In addition to the age-related increase of brain MAO-B level, increase of brain iron with aging may further the Fenton reaction and hydroxyl radical generation (Youdim and Bakhle 2006).

Thus, when targeting the MAO-B with enzyme inhibitors, increased level of monoamine that is available to the membrane receptors and decreased level of toxic products may be achieved, which may have a beneficial effect on the treatment of PD (Youdim and Bakhle 2006). Although DA is also metabolized by MAO-A isoform, due to the “cheese effect”, which refers to a hypertensive crisis caused by the hindered metabolism of tyramine and other sympathomimetic amines by MAO-A, the use of non-selective MAO inhibitors requires dietary

restrictions (Youdim and Riederer 2004, Youdim, Edmondson, and Tipton 2006). Therefore, selective MAO-B inhibitors are preferred.

1.5.2.2. MAO-B inhibitors under development

The common molecular scaffolds of MAO-B inhibitors under development can be categorized into propargylamines and oxygen or nitrogen heterocycles (Finberg 2014, Helguera et al. 2012, Reis et al. 2012). These heterocyclic scaffolds are usually originated from privileged structures, including coumarins, chalcones, chromones, pyrazoles, xanthines, and isatins (Reis et al. 2012, Carradori and Silvestri 2015). Here, only the propargyl-based MAO-B inhibitors are briefly reviewed.

Following the development and clinical application of neuroprotective MAO-B inhibitors, selegiline and rasagiline, various compounds with propargyl functional moiety have been studied. One of the most well-known examples is compound M30, a multi-target drug functioning by iron chelation and MAO-B inhibition, and its analog, VAR10303, has also been studied in details (**Figure 13**) (Gal et al. 2006, Bar-Am et al. 2015). Furthermore, other highly potent and selective MAO-B inhibitors have also been developed through templates shown in **Figure 13** (Huleatt et al. 2015, Can et al. 2017).

In addition to the MAO-B inhibition, studies have revealed the neuroprotective effect of the propargylamine derivatives in cellular and animal models; however, this effect is independent from MAO-B inhibition but probably mediated through apoptosis signaling pathways (Tatton, Chalmers-Redman, and

Tatton 2003). Rasagiline, the FDA approved MAO-B inhibitor, for example, has been shown to maintain mitochondrial integrity and up-regulate neurotrophic factors (Weinreb et al. 2010). The multi-target compound M30 has shown neuroprotective effect in neuronal cell culture, and similar to rasagiline, its mechanism has been suggested to be by regulating the anti-apoptotic Bcl-family proteins and PKC activation (Gal et al. 2006). Moreover, both M30 and its analog VAR10303 have displayed neuroprotective effect in PD animal models (Gal et al. 2006, Bar-Am et al. 2015).

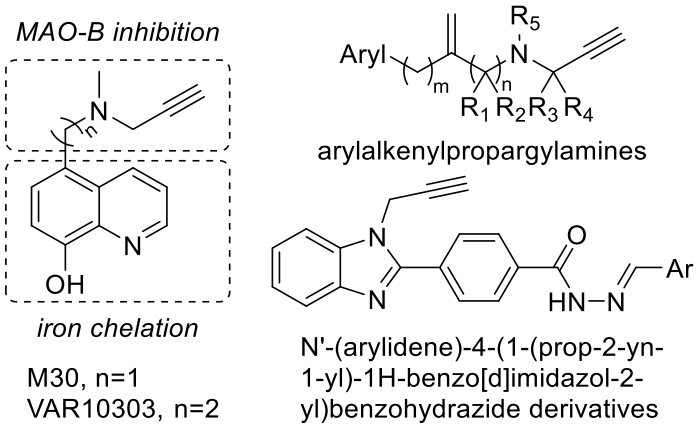

Figure 13. Examples of MAO-B inhibitors.

CHAPTER 2 HYPOTHESIS AND SPECIFIC AIMS

Parkinson's disease (PD), the second most common neurodegenerative disorder, gives rise to a wide array of clinical features ranging from motor to non-motor symptoms. In addition to levodopa, the gold standard treatment, various therapeutic treatments have been explored and developed over the years, including dopamine receptor agonists, monoamine oxidase (MAO) inhibitors, and catechol-*O*-methyltransferase (COMT) inhibitors (Factor 2008). However, these current available clinical treatments are only able to provide symptomatic relief and fail to delay the disease progression (Tarazi et al. 2014). Furthermore, the long-term use of levodopa leads to motor complications including dyskinesia (Jankovic and Aguilar 2008). Thus, there is still a great unmet need for effective PD treatment.

2.1. Hypothesis

PD is a chronic and progressive disease, and its pathogenesis has been identified to be multifactorial (Alves, Forsaa, Pedersen, Dreetz Gjerstad, et al. 2008). Due to the complexity observed in the disease pathogenesis, treatments that address the pathogenic factors involved in PD might offer an advantage in combating the disease by delaying the disease progression. The hypothesis of this project is that the incorporation of dopamine D_2/D_3 agonistic component with accessory moieties targeting α-synuclein (αSN) aggregation or MAO enzyme has the potential to provide both symptom relieving and disease modifying effects as a promising approach for new generation PD treatment.

2.2. General aim

The general aim of this work is to develop a library of compounds that link the dopamine D_2/D_3 agonistic moiety with additional functional moieties targeting either αSN aggregation or MAO enzyme based on the previously established hybrid structure approach to conduct a structure-activity relationship (SAR) study and discover possible lead compounds through both *in vitro* and *in vivo* evaluations.

2.3. Specific aims

2.3.1. Ligand design and synthesis

a) Design and synthesize of novel dopamine D_2/D_3 receptor agonists that can potentially modulate αSN aggregation by incorporating dihydroxy or hydroxyl-methoxy component with D_2/D_3 agonist fragment through a linker based on the hybrid molecular template. A SAR study has been carried out to assess the effect of linker and dihydroxy or monohydroxy phenolic structure modifications.

b) Design and synthesize of novel dopamine D_2/D_3 receptor agonists that can potentially inhibit MAO-B enzyme activity by incorporating the propargyl group with D_2/D_3 agonist fragment based on the hybrid molecular template. An initial SAR study has been conducted based on the generated compound library.

2.3.2. *In vitro* radioligand binding assay using [^{3}H]-spiperone

The synthesized compounds have been evaluated for their *in vitro* affinity towards the D_2 and D_3 dopamine receptors by using radioligand binding assays.

2.3.3. *In vitro* functional assay using [^{35}S]-GTPγS

Based on the binding affinity, compounds were selected and further evaluated for their functional activity through an *in vitro* functional assay.

2.3.4. *In vitro* neuroprotection study

In addition to the receptor assays, selected lead compounds have been assessed for their potential neuroprotective effect through the neurotoxin-based *in vitro* models, 6-hydroxydopamine (6-OHDA) or rotenone model in PC12 cells.

2.3.5. *In vitro* αSN aggregation study

Selected lead compounds containing the dihydroxy phenolic moiety has been tested for their ability to modulate αSN aggregation through *in vitro* studies, including shaking and seeding assays.

2.3.6. *In vitro* MAO inhibition assay

Selected lead compounds containing the propargyl group has been evaluated for their ability to inhibit MAO enzyme activity through *in vitro* enzymatic assay experiments.

2.3.7. *In vivo* assays with rat model of PD

Selected lead compounds have been examined further for their *in vivo* potency in a PD animal model, the reserpine-induced hypolocomotion rat model.

*** CHAPTER 3 & 4 CONTAIN MATERIAL FROM PUBLISHED WORK IN WHICH I WAS THE FIRST AUTHOR. THE CO-AUTHORS OF THESE PUBLICATIONS AGREE TO THE USE OF THE PUBLISHED DATA IN THIS DISSERTATION.**

CHAPTER 3 RESULTS AND DISCUSSION

3.1. Overview

The first main objective is to design and develop a series of novel dopamine D_2/D_3 receptor agonists that can potentially modulate α-synuclein (αSN) aggregation by combining the dihydroxy or hydroxy-methoxy component with D_2/D_3 agonist fragment through various linkers according to the hybrid molecular template. Based on the results of *in vitro* receptor assays, compounds were selected and further evaluated to determine their potential αSN aggregation modulatory properties and neuroprotective effect. Subsequently, lead compounds were identified by using a well-established Parkinson's disease (PD) animal model. The second main objective is to design and synthesize a series of novel dopamine D_2/D_3 receptor agonists that may potentially inhibit monoamine oxidase B (MAO-B) activity by introducing the propargyl group into the hybrid molecular template. An initial structure-activity relationship (SAR) study was conducted based on the generated compound library through *in vitro* receptor assays and enzymatic studies. Moreover, *in vitro* neuroprotection models and a PD animal model were also used to further evaluate potential candidates. Thus, this chapter will describe the following:

1) Chemistry involved in generating compound libraries

2) *In vitro* binding data for all the compounds and functional activity data for selected compounds
3) *In vitro* αSN aggregation modulation data for selected compounds
4) *In vitro* MAO inhibition data for selected compounds
5) *In vitro* neuroprotection data for selected compounds
6) *In vivo* efficacy data for selected compounds

All the experimental details, including synthesis procedures, spectral data, and protocols for *in vitro* and *in vivo* biological evaluations will be described in Chapter 4.

3.2. Design, synthesis, and the initial SAR study of novel multifunctional dopamine D_2/D_3 receptors agonists with potential neuroprotection and anti-αSN aggregation properties

In continuation of our work for the development of multifunctional dopamine D_2/D_3 receptor agonists for the symptom-relieving and disease-modifying treatment of PD based on the hybrid structure strategy, which has led to the successful identification of several potent and promising lead compounds including **D-520** and **D-512** (**Figure 14**) early on, a modified hybrid molecule template has been developed. This molecular template (**Figure 15**) joined the headgroups derived from the known dopamine D_2/D_3 receptor agonists, pramipexole and 5-hydroxy-*N,N*-dipropyl-2-aminotetralin (5-OH-DPAT), with the dihydroxy or hydroxy-methoxy component, which has been demonstrated to modulate αSN aggregation, through an alkyl linker, which replaced the piperazine

ring linker in the previous template design as seen in the lead compounds **D-520** and **D-512**. In the current study, the influence of various linkers along with the introduction of dihydroxy or hydroxy-methoxy functionalities has been explored to evaluate the effect of linker length, the saturation state of linker, and hydroxy or methoxy substitutions on D_2/D_3 agonist potencies. In addition to these alkyl linker compounds, a para-dihydroxy substituted analog of a previously developed lead compound **D-520**, (−)-**49** (**D-670**), was also designed and synthesized. In the previous studies, lead compound **D-520** has shown a great effect in the αSN aggregation inhibition and neuroprotection against 6-OHDA-induced toxicity in addition to its potent and efficacious D_2/D_3 receptor agonistic activities seen in both *in vitro* and *in vivo* studies (Modi et al. 2014). Thus, it is interesting to include its para-substituted analog (−)-**49** (**D-670**) in this study to briefly assess the effect of ortho- vs. para- dihydroxy substitution.

Following the initial characterization via *in vitro* binding assay and GTPγS binding functional assay, compounds were selected for further *in vitro* biological evaluation to assess their neuroprotective effect and their ability to modulate αSN aggregation. Finally, selected compounds were tested *in vivo* in a well-established PD animal model.

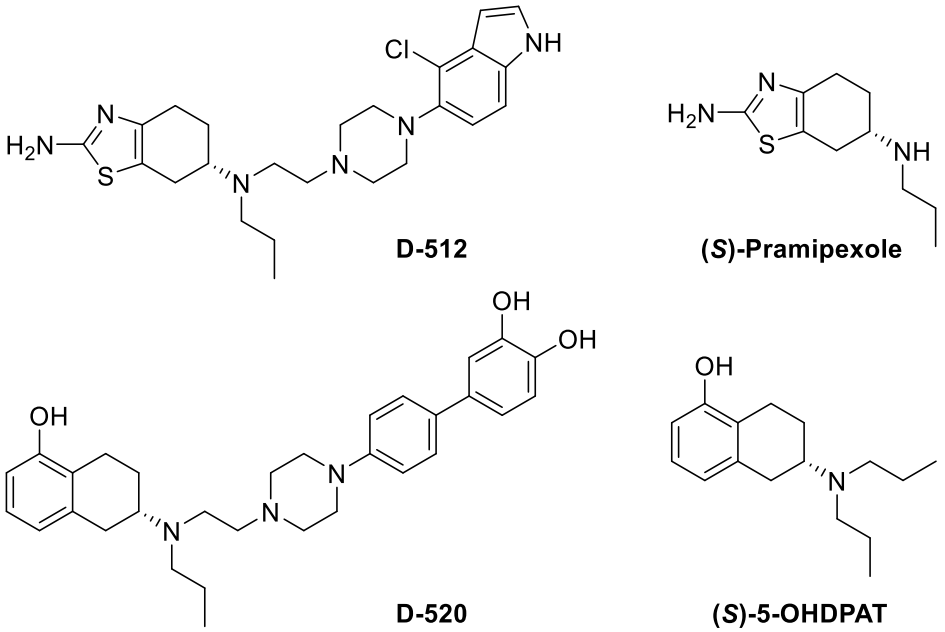

Figure 14. Molecular structures of dopamine D_2/D_3 receptor agonists.

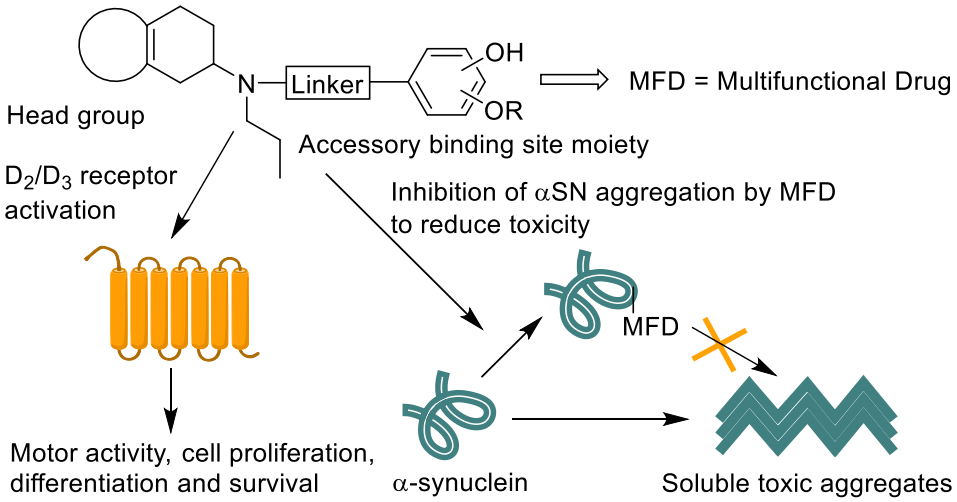

Figure 15. The hybrid molecule template for multifunctional dopamine D_2/D_3 receptor agonists that may potentially modulate αSN aggregation.

3.2.1. Synthesis of multifunctional αSN modulators

Scheme 1 describes the synthesis of a series of compounds where the 2-aminothiazole head group is attached to various diphenol- or methoxyphenol fragments via five-carbon alkyl linkers. One 5-hydroxy aminotetralin analog is also included in this scheme. Commercially available ethyl 4-bromobutyrate (**1**) was reacted with triphenylphosphine (TPP) to give phosphonium bromide **2**, which was subjected to the Wittig olefination with aldehydes **3a** or **3b** using sodium hexamethyldisilazide (NaHMDS) to obtain preferentially (*Z*:*E* > 20:1) (*Z*)-alkene products **4a** and **4b**, respectively. Their stereochemistry was confirmed by a smaller coupling constant (*J* = 11.2 Hz) observed for the *Z*-isomers as opposed to a larger vicinal coupling (*J* = 16 Hz) obtained for the corresponding (*E*)-isomers. Pd/C-catalyzed hydrogenation of **4a** and **4b** yielded corresponding saturated intermediates **5a** and **5b**. Then these esters were reduced to aldehydes **6a** and **6b** by using diisobutylaluminium hydride (DIBALH). Reductive amination with sodium triacetoxyborohydride was used to couple **6a** and **6b** with (±)- or (−)-pramipexole to give (±)-**7a** (**D-548**), (−)-**7a** (**D-591**), (±)-**7b**, and (−)-**7b**, respectively, which were then reacted with boron tribromide to yield corresponding dihydroxy-compounds (±)-**8a** (**D-575**), (−)-**8a** (**D-593**), (±)-**8b** (**D-584**), and (−)-**8b** (**D-601**). The (*Z*)-isomer of **4a** was separated by normal phase silica gel chromatography and used to synthesize target compound (±)-**12** (**D-567**). *tert*-Butyldimethylsilyl (TBS) protection of **4a** yielded intermediate **9**, which was reduced to alcohol **10** by DIBALH and then oxidized to aldehyde intermediate **11** by pyridinium chlorochromate (PCC) oxidation. Deprotection of

the TBS group and subsequent reductive amination gave the final compound (±)-**12** (**D-567**). Compound (−)-**14** (**D-644**), the aminotetralin analog of (−)-**8a** (**D-593**), was synthesized by coupling aldehyde **6a** with (−)-5-methoxy-*N*-propyl-2-aminotetralin through reductive amination followed by demethylation using hydrobromic acid.

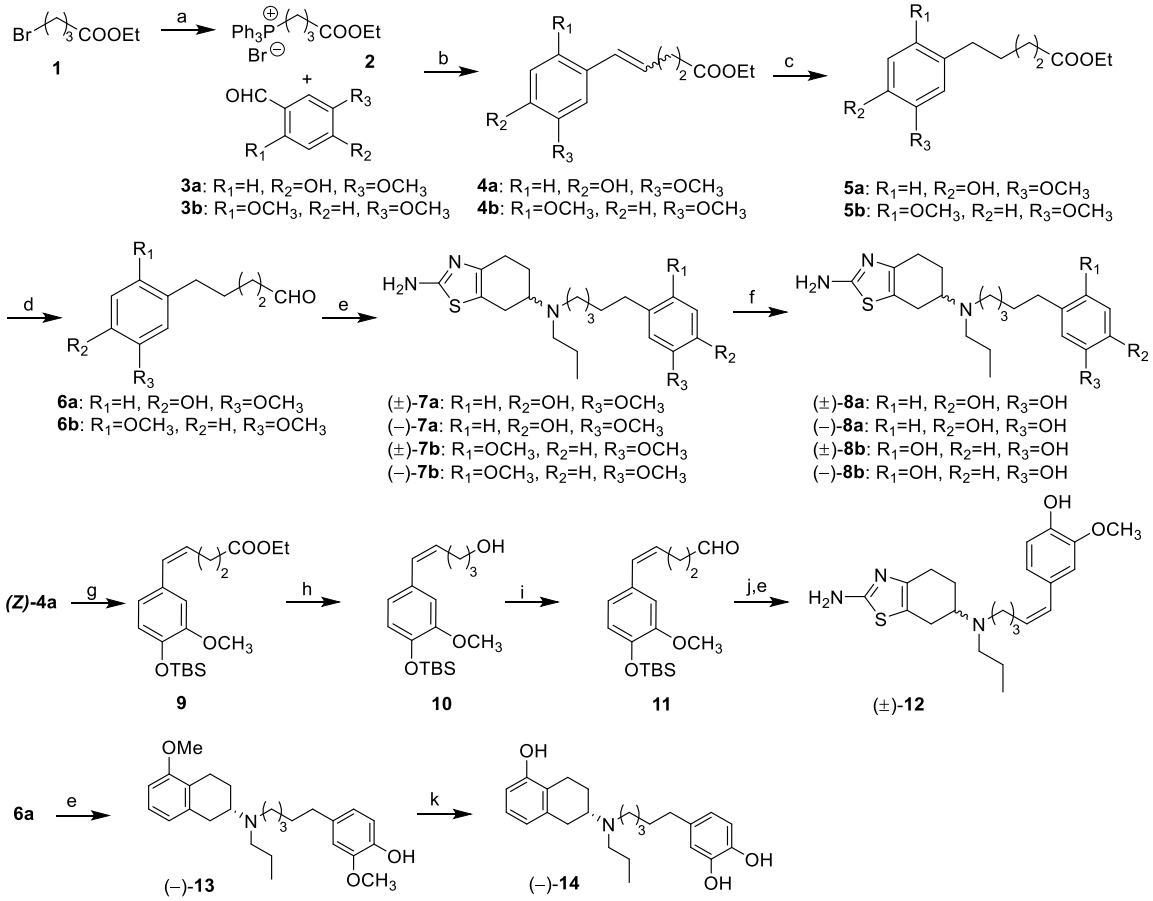

Scheme 1. Synthesis of compounds (±)-**7a** (**D-548**), (−)-**7a** (**D-591**), (±)-**8a** (**D-575**), (−)-**8a** (**D-593**), (±)-**8b** (**D-584**), (−)-**8b** (**D-601**), (±)-**12** (**D-567**), and (−)-**14** (**D-644**). Reaction and Conditions: (a) TPP, toluene, reflux, 16 h; (b) NaHMDS, THF, −78 °C to rt, 48 h; (c) 10% Pd/C, H_2, EtOH, rt, 2 h; (d) DIBALH, toluene, −78 °C, 2 h; (e) (±), (−)-pramipexole or (−)-5-methoxy-*N*-propyl-2-aminotetralin, $NaBH(OAc)_3$, CH_2Cl_2, rt, 36 h; (f) BBr_3, CH_2Cl_2, −78 °C to rt, 6 h; (g) TBDMSCl,

imidazole, DMF, rt, 2 h; (h) DIBALH, THF, −10 °C to rt, 6 h; (i) PCC, CH_2Cl_2, 0 °C to rt, 9h; (j) TBAF, THF, 0 °C, 1.5 h; (k) 48% HBr, reflux, 6 h.

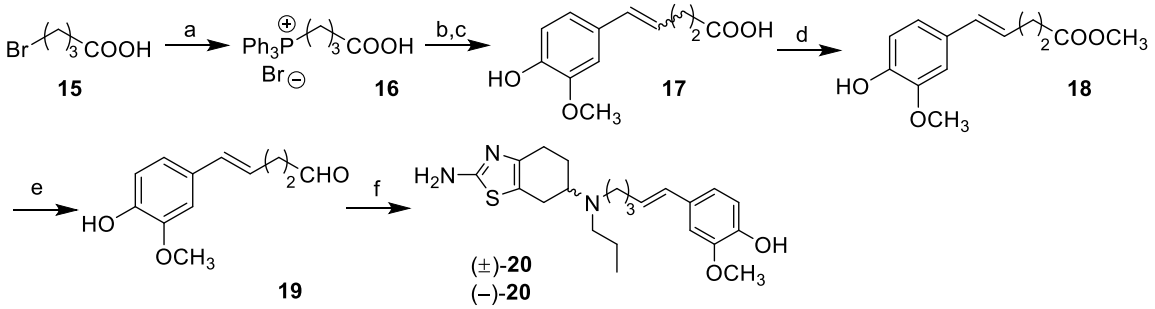

Scheme 2. Synthesis of compounds (±)-**20** (**D-604**) and (−)-**20** (**D-618**). Reaction and Conditions: (a) TPP, toluene, reflux, 16 h; (b) HMDS, *n*-BuLi, THF, 0 °C, 15 min; (c) vanillin, LiHMDS, THF, rt, 24 h; (d) CH_3COCl, MeOH, 0 °C to rt, 4 h; (e) DIBALH, toluene, −78 °C, 2 h; (f) (±) or (−)-pramipexole, $NaBH(OAc)_3$, CH_2Cl_2, rt, 36-48 h.

Scheme 2 depicts the synthesis of additional five-carbon linker containing compounds, (±)-**20** (**D-604**) and (−)-**20** (**D-618**), where the unsaturated linker fragment is in the (*E*)-conformation. Phosphonium salt **16** was first prepared by reacting 4-bromobutyric acid (**15**) with TPP. Then the Wittig olefination of **16** with vanillin (**3a**) using freshly prepared lithium hexamethyldisilazide (LiHMDS) gave preferentially (*E*:*Z* > 10:1) (*E*)-alkene intermediate **17**. **17** was converted to its corresponding methyl ester **18**, and its (*E*)-isomer (*J* = 15.6 Hz) was separated by column chromatography. Reduction to aldehyde followed by reductive amination with (±)- or (−)-pramipexole gave target compounds (±)-**20** (**D-604**) and (−)-**20** (**D-618**).

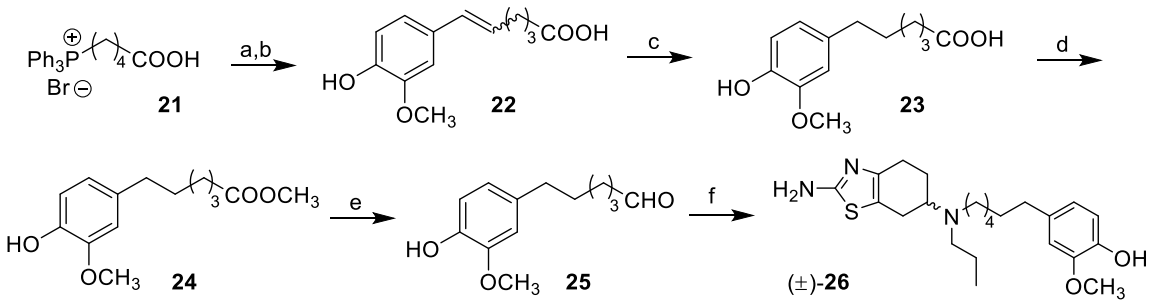

Scheme 3. Synthesis of compound (±)-**26** (**D-606**). Reaction and Conditions: (a) HMDS, *n*-BuLi, THF, 0 °C, 15 min; (b) vanillin, LiHMDS, THF, rt, 24 h; (c) 10% Pd/C, H_2, EtOH, rt, 2 h; (d) CH_3COCl, MeOH, 0 °C to rt, 4 h; (e) DIBALH, toluene, −78 °C, 2 h; (f) (±)-pramipexole, $NaBH(OAc)_3$, CH_2Cl_2, rt, 48 h.

Scheme 3 describes the synthesis of target compound (±)-**26** (**D-606**), which contains a saturated six-carbon linker. Commercially available phosphonium salt **21** was reacted with vanillin (**3a**) in the presence of freshly prepared LiHMDS resulting preferentially in (*E*)-alkene product **22**. This unsaturated carboxylic acid precursor was reduced through Pd/C-catalyzed hydrogenation and converted to corresponding methyl ester **24**. Final compound (±)-**26** (**D-606**) was obtained by the reduction of ester intermediate **24** to aldehyde **25** followed by the reductive amination of **25** with (±)-pramipexole.

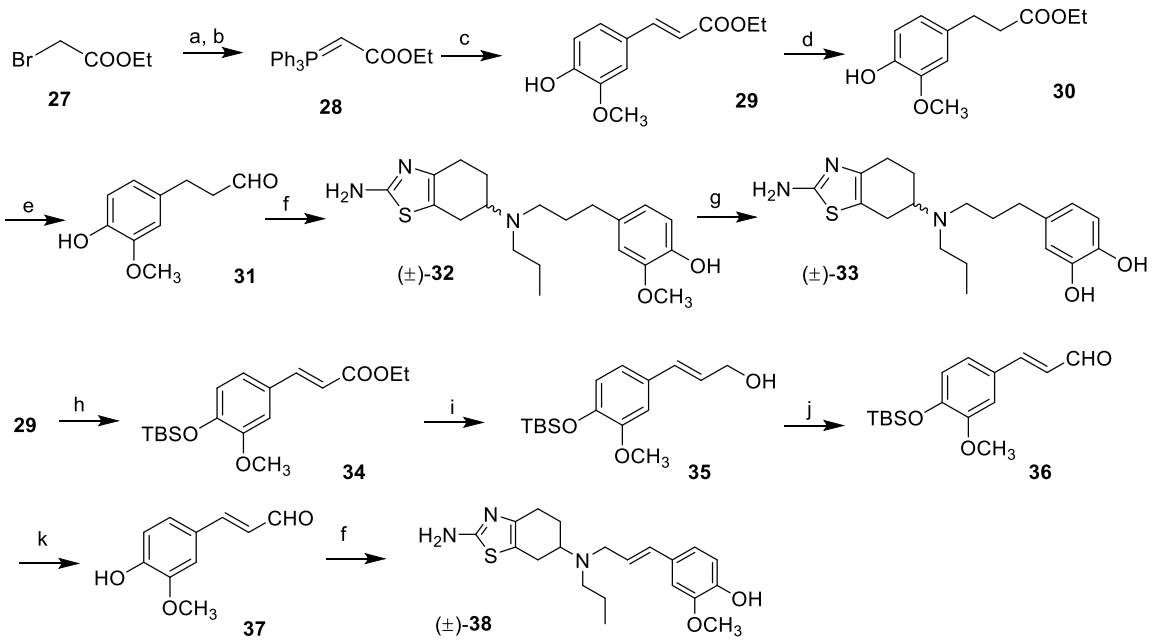

Scheme 4. Synthesis of compounds (±)-**32** (**D-547**), (±)-**33** (**D-573**), and (±)-**38** (**D-570**). Reaction and Conditions: (a) TPP, toluene, reflux, 16 h; (b) 1 M NaOH aq., 15 min; (c) vanillin, $CHCl_3$, reflux, 5 h; (d) 10% Pd/C, H_2, EtOH, rt, 2 h; (e) DIBALH, toluene, −78 °C, 2 h; (f) (±)-pramipexole, $NaBH(OAc)_3$, CH_2Cl_2, rt, 36-48 h; (g) BBr_3, CH_2Cl_2, −78 °C to rt, 6 h; (h) TBDMSCl, imidazole, DMF, rt, 2 h; (i) DIBALH, THF, −10 °C to rt, 6 h; (j) MnO_2, CH_2Cl_2, rt, 24h; (k) TBAF, THF, 0 °C, 1 h.

Scheme 4 shows the synthesis of another series of compounds with three-carbon linkers connecting the tetrahydrobenzo 2-aminothiazole head group to a diphenol- or methoxyphenol fragment. (*E*)-alkene intermediate **29** was prepared via the Wittig reaction. Pd/C-catalyzed hydrogenation was used to generate saturated ester precursor **30**, which was then converted to aldehyde **31** by DIBALH. Target compound (±)-**32** (**D-547**) was prepared by the reductive amination of aldehyde **31** with (±)-pramipexole. Demethylation was then achieved to obtain target compound (±)-**33** (**D-573**). To prepare compound (±)-**38**

(**D-570**), intermediate **29** was first protected and reduced to alcohol **35**. Then aldehyde **37** was synthesized by the oxidation of alcohol intermediate **35** using manganese dioxide followed by the deprotection of TBS group in intermediate **36**. The aldehyde intermediate **37** was then reacted with (±)-pramipexole to yield final compound (±)-**38** (**D-570**).

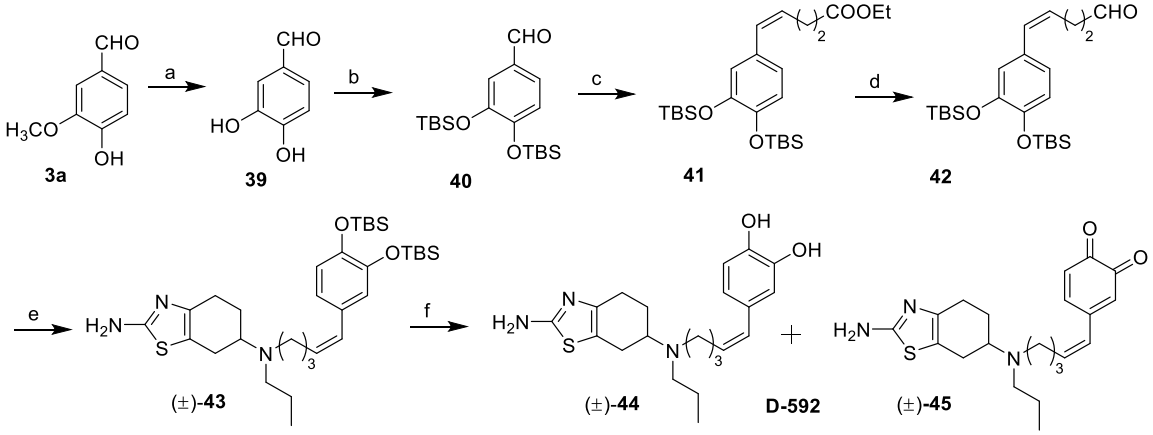

Scheme 5. Synthesis of compounds (±)-**44**&**45** (**D-592**). Reaction and Conditions: (a) BBr_3, CH_2Cl_2, −78 °C to rt, 6 h; (b) TBDMSCl, imidazole, DMF, rt, 2 h; (c) phosphonium bromide **2**, NaHMDS, THF, −78 °C to rt, 48 h; (d) DIBALH, toluene, −78 °C, 2 h; (e) (±)-pramipexole, $NaBH(OAc)_3$, CH_2Cl_2, rt, 36 h; (f) TBAF, THF, 0 °C, 1.5 h.

Scheme 5 outlines synthesis of **D-592**, a mixture of compounds (±)-**44, 45** as deduced from NMR and mass spectroscopy (*m/z* $[M + H]^+$: major 388.46, minor 386.44). Air oxidation of the catechol to the corresponding dione could be a result of stabilization from an extended conjugation in the dione state. Prior to coupling to the phosphonium salt through Wittig reaction, aldehyde **3a** was first demethylated and TBS-protected by tert-butyldimethylsilyl chloride (TBDMSCl) to

give intermediate **40**. After the Wittig olefination with phosphonium bromide **2**, reduction to aldehyde intermediate **42** was achieved by chemistry described above. Subsequent reductive amination of **42** with (±)-pramipexole resulted in intermediate (±)-**43**, which was deprotected to give **D-592** as a mixture of compounds (±)-**44** and **45**.

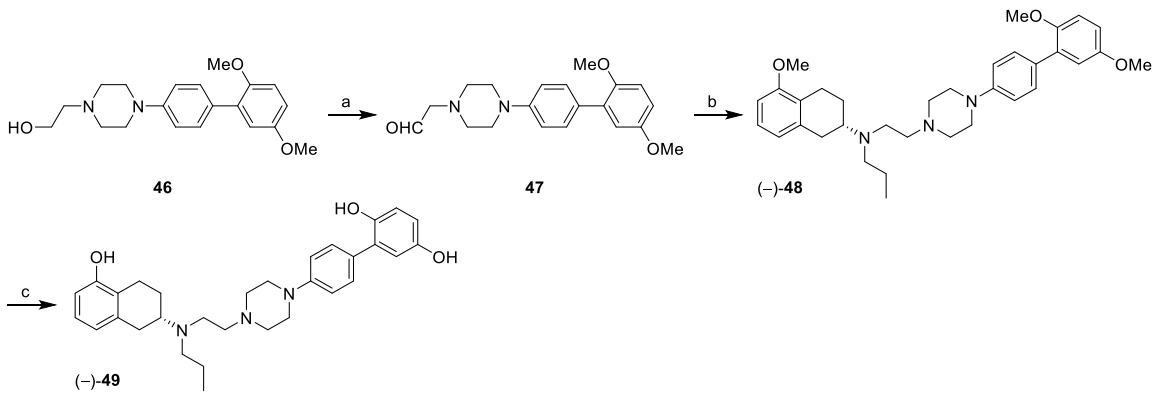

Scheme 6. Synthesis of compound (−)-**49** (**D-670**). Reaction and Conditions: (a) oxalyl chloride, DMSO, CH_2Cl_2, Et_3N, −78 °C to rt, 2 h; (b) (−)-5-methoxy-*N*-propyl-2-aminotetralin, $NaBH(OAc)_3$, CH_2Cl_2, rt, 40 h; (c) 48% HBr, reflux, 6.5 h.

Scheme 6 describes the synthesis of compound (−)-**49** (**D-670**), which is the analog of **D-520**. Alcohol intermediate **46** (Modi et al. 2014) was oxidized to its corresponding aldehyde **47** using the Swern oxidation, and the subsequent reductive amination with (−)-5-methoxy-*N*-propyl-2-aminotetralin was conducted in the presence of sodium triacetoxyborohydride. Then the demethylation by hydrobromic acid was used to produce the final compound (−)-**49** (**D-670**).

3.2.2. *In vitro* receptor assays with multifunctional αSN modulators

In the current SAR study to explore the effect of structural variations in the linker region that connects the D_2/D_3 agonistic head group with accessory binding site moiety, the replacement of the piperazine ring in the lead compounds, such as **D-520**, with saturated and unsaturated alkyl linkers was pursued. By varying the alkyl chain length, compounds with three to six carbon linkers were designed. The effect of linker length on the D_2/D_3 binding affinity can be inferred from compounds in the saturated series, which includes (±)-**32** (**D-547**)**,** (±)-**7a** (**D-548**)**,** and (±)-**26** (**D-606**). Among them, compound (±)-**26** (**D-606**) with a six-carbon linker exhibited the highest affinity for both D_2/D_3 receptors (K_i, D_2=58.5 nM, D_3=0.675 nM, **Table 1**). Compound (±)-**7a** (**D-548**)**,** which has a five-carbon linker, also displayed potent binding affinity at D_3 receptor (K_i, D_3=3.62 nM) and moderate affinity for D_2 receptor (K_i, D_2=175 nM)**.** However, the three-carbon linker compound (±)-**32** (**D-547**) gave much weaker binding, especially for D_2 receptor (K_i, D_2=2,404 nM, D_3=15.8 nM). These results suggest that linker length has a considerable effect on the binding affinity of these compounds: lengthening the linker chain from three-carbon to six-carbon greatly improves the affinity for both D_2 receptor (by 41-fold) and D_3 receptor (by 23-fold). The high activity of the six-carbon linker compound (±)-**26** (**D-606**) could be because of better accessibility and/or interactions of the tetrahydrobenzo 2-aminothiazole head group moiety at the D_2/D_3 receptors binding sites. The binding data of (±)-**32** (**D-547**) also suggests that a greater selectivity for D_3 receptor could be achieved by

connecting the head group and the accessory binding fragment through a linker with appropriate length.

The increasing trend of receptor binding affinity may indicate lesser steric hindrance occurred between the phenyl ring in the designed molecules and the binding pocket of receptors when extended linkers were incorporated. It may also be reasoned that a six- or a five-carbon linker could confer more flexibility; thus, (±)-**26** (**D-606**) and (±)-**7a** (**D-548**) may adopt different conformations than the corresponding three-carbon linker compound (±)-**32** (**D-547**). Towards this end, conformational restrictions were introduced in the linker portion through insertion of a double bond. Further, with an aim to impart potential neuroprotective property, a conjugated double bond, as in curcumin, was particularly envisaged resulting in substituted styrene accessory binding fragments. The effect of introducing a double bond in the linker portion is more complicated. For compounds containing three-carbon linkers, the incorporation of an (*E*)-double bond in compound (±)-**38** (**D-570**) greatly reduced the binding affinity for both D_2 and D_3 receptors in comparison to its corresponding saturated linker analog (±)-**32** (**D-547**) (K_i, D_2= 4,634 vs. 2,404 nM, D_3= 39.1 vs. 15.8 nM, **Table 1**). For a five-carbon linker saturated analog (±)-**7a** (**D-548**) (**Table 1**), the introduction of an (*E*)-double bond as in (±)-**20** (**D-604**) improved binding affinity at D_2 receptor (K_i, D_2=150 nM) and was also tolerated at D_3 receptor (K_i, D_3=4.24 nM). To determine the effect of stereochemistry, corresponding (*Z*)-isomer analog, compound (±)-**12** (**D-567**)**,** was also synthesized. As predicted, stereochemistry

did influence the binding affinity as the (*Z*)-isomer analog (±)-**12** (**D-567**) displayed reduced affinity at both D_2 and D_3 receptors (K_i, D_2=233 nM, D_3=23.3 nM) when compared to its saturated (±)-**7a** (**D-548**) and the (*E*)-isomer counterpart (±)-**20** (**D-604**). These results suggest that the length along with the stereochemistry of linkers influences the binding of compounds at both D_2 and D_3 receptors. Overall, this SAR study demonstrates that the piperazine ring present in the previous lead compounds could be replaced by an appropriate alkyl linker in the present series of compounds while maintaining affinity and potency.

Next, the focus was placed on the terminal accessory binding fragment that is designed to impart multifunctional properties to the designed compounds for combating neurodegeneration in PD. Structural motifs present in naturally-occurring compounds including polyphenols and curcumin, were substituted as the accessory binding fragments. Effects of various hydroxyl or methoxy substitutions on the phenyl ring were investigated through compounds (±)-**7a** (**D-548**)**,** (±)-**8a** (**D-575**)**,** (±)-**32** (**D-547**)**,** and (±)-**33** (**D-573**)**.** Compounds with either an *ortho*- or a *para*-substitution on the aromatic ring were explored, as such substitution has a potential of forming a quinone/semiquinone moiety for αSN aggregation. Compound (±)-**7a** (**D-548**), with a hydroxyl at the *p*-position and a methoxy at the *m*-position, exhibited potent binding affinity for D_3 receptor (K_i, D_3=3.62 nM) and moderate affinity for the D_2 receptor (K_i, D_2=175 nM). The replacement of *m*-methoxy group in (±)-**7a** (**D-548**) with a hydroxyl group resulting in (±)-**8a** (**D-575**) exhibited a moderate improvement for both D_2 and D_3

binding (K_i, D_2=116 nM, D_3=2.59 nM, **Table 1**). Among the three-carbon linker analogs, the dihydroxyl analog (±)-**33** (**D-573**) showed a significant increase in affinity for D_2 receptor (K_i, D_2=499 nM) as compared to the hydroxy-methoxy substituted analog (±)-**32** (**D-547**) (K_i, D_2= 2,404 nM); however, for D_3 binding, (±)-**33** (**D-573**) (K_i, D_3=11.9 nM) showed little or no enhancement over (±)-**32** (**D-547**) (K_i, D_3=15.8 nM). These results demonstrate that the dihydroxy-compounds (±)-**8a** (**D-575**) and (±)-**32** (**D-547**) exhibited better binding profiles. Next, to briefly assess the effect of substituent position, compound (±)-**8b** (**D-584**)**,** having hydroxyls at the 2′- and 5′-positions, was synthesized. This compound exhibited comparable binding affinity for D_2 receptor and a slightly improved binding for D_3 receptor compared to its counterpart (±)-**8a** (**D-575**) (K_i, D_2= 117 vs. 116 nM, D_3= 1.01 vs. 2.59 nM)**.** Thereafter, to investigate the effect of a dihydroxyl substituent in the presence of an unsaturated linker, compound (±)-**44** was designed and synthesized. However, probably as a result of air oxidation, the resulting compound was obtained as an inseparable mixture of (±)-**44** and dione (±)-**45** which showed moderate affinity for both D_2 and D_3 receptors (K_i, D_2=121 nM, D_3=25.0 nM).

Our previous studies have demonstrated that compounds with (−)-(*S*)-isomer of pramipexole as the head group generally resulted in greater binding affinity than their (+)-(*R*)- isomer counterparts (Das et al. 2015). Thus, (−)-isomers of selected compounds **7a, 8a, 8b, 20** were synthesized. Compounds (−)-**7a** (**D-591**) (K_i, D_2=68.3 nM, D_3=1.57 nM) and (−)-**8a** (**D-593**) (K_i, D_2=65.7 nM,

D_3=1.42 nM) demonstrated improved binding profile, particularly for the D_2 receptor, in comparison to their racemic counterparts (±)-**7a** (**D-548**) and (±)-**8a** (**D-575**), respectively**.** Compound (−)-**8b** (**D-601**) exhibited a binding K_i, for D_3 (0.78 nM) that was among the higher affinity values observed in this series of compounds. In general, (*S*)-isomers displayed somewhat higher binding affinities for both D_2/D_3 receptors than their racemic counterparts except for (−)-**20** (**D-618**) (K_i, D_2=123 nM, D_3=22.3 nM), where a decrease of D_3 binding and little or no change in D_2 binding were observed.

A bioisosteric replacement of the 2-aminothiazole head group in compound (−)-**8a** (**D-593**) with an aminotetralin moiety to give (−)-**14** (**D-644**) was performed. In consistence with our previous data, the aminotetralin analog (−)-**14** (**D-644**) (K_i, D_2=4.67 nM, D_3=0.493 nM) showed much better binding affinity at both D_2 and D_3 receptors compared to the 2-aminothiazole derivative (−)-**8a** (**D-593**) (K_i, D_2=65.7 nM, D_3=1.42 nM).

In addition to these alkyl linker compounds, (−)-**49** (**D-670**), the para-dihydroxy analog, was studied in pair with its ortho-substituted parent compound **D-520**. Comparing to **D-520**, the newly developed para-substituted analog exerted a visible reduction in affinity towards both D_2/D_3 receptors with a comparable D_2/D_3 receptor selectivity (K_i, D_2= 79.5 vs. 41.8 nM, D_3= 0.643 vs. 0.350 nM, D_2/D_3 = 124 vs. 119, for (−)-**49** (**D-670**) and **D-520**, respectively, **Table 1**), suggesting a modest effect of the ortho- to para- dihydroxy substitutions on receptor binding in the current scaffold.

Table 1. K_i values (nM) for inhibition of [^{3}H] spiroperidol binding (HEK - $D_{2,3}$ cells)[a] (cLogP and tPSA values are calculated using ChemDraw)

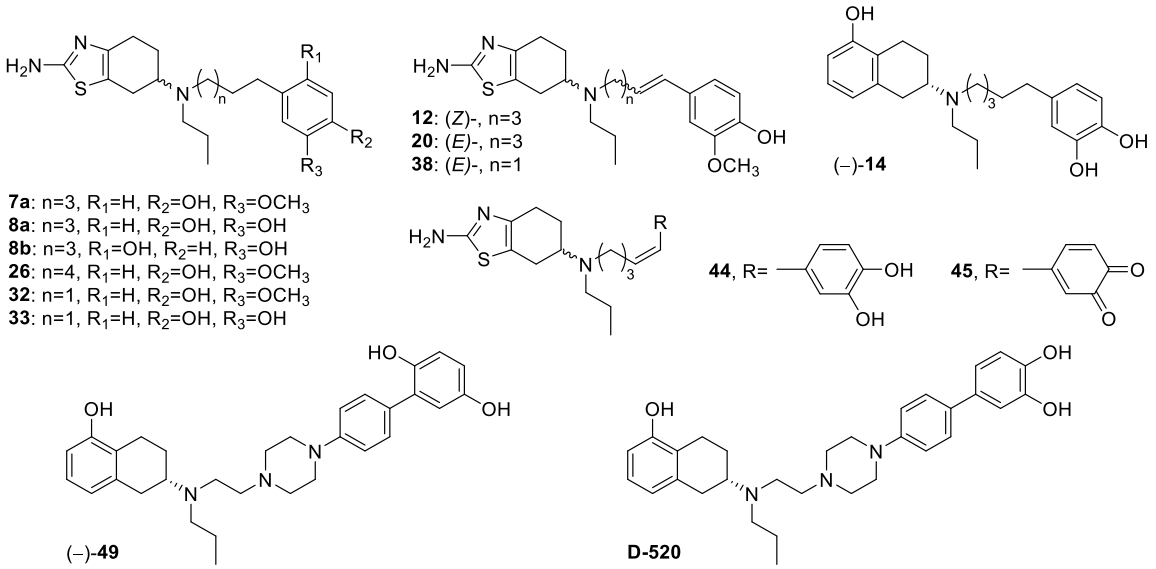

Compound	K_i (nM), [^{3}H]spiperone		D_{2L}/D_3	cLogP	tPSA
	D_{2L}	D_3			
dopamine[b]	990 ± 198	101 ± 14.9	10		
(−)-**5-OH-DPAT**	153 ± 32	2.07 ± 0.38	74		
(±)-**7a,** D-548	175 ± 8	3.62 ± 0.78	48	4.42	71.08
(−)-**7a,** D-591	68.3 ± 12.0	1.57 ± 0.41	43	4.42	71.08
(±)-**8a,** D-575	116 ± 8	2.59 ± 0.31	45	3.97	82.08
(−)-**8a,** D-593	65.7 ± 11.7	1.42 ± 0.14	46	3.97	82.08
(±)-**8b,** D-584	117 ± 17	1.01 ± 0.28	116	3.85	82.08
(−)-**8b,** D-601	112 ± 8	0.78 ± 0.20	143	3.85	82.08
(±)-**12,** D-567	233 ± 8	23.3 ± 4.0	10	4.12	71.08
(−)-**14,** D-644	4.67 ± 0.65	0.493 ± 0.067	9	5.22	63.93
(±)-**20,** D-604	150 ± 20	4.24 ± 0.74	35	4.12	71.08
(−)-**20,** D-618	123 ± 18	22.3 ± 2.2	6	4.12	71.08

(±)-**26,** D-606	58.5 ± 7.3	0.675 ± 0.178	87	4.95	71.08
(±)-**32,** D-547	2,404 ± 29	15.8 ± 2.0	153	3.36	71.08
(±)-**33,** D-573	499 ± 16	11.9 ± 1.9	42	2.92	80.08
(±)-**38,** D-570	4,634 ± 325	39.1 ± 5.4	119	3.26	71.08
(±)-**44&45,** D-592	121 ± 21	25.0 ± 1.96	5	N/A	N/A
(−)-**49**, D-670	79.5 ± 7.7	0.643 ± 0.089	124	5.72	70.41
D-520[b]	41.8 ± 11.2	0.350 ± 0.101	119	6.09	70.41

[a] Results are expressed as means ± SEM for three to four experiments, each performed in triplicate.
[b] Data was obtained under almost identical assay conditions (Zhen et al. 2015, Modi et al. 2014).

The optically active compounds **7a, 8a, 8b, 14** and **20** were also assessed by measuring the stimulation of [^{35}S]GTPγS binding in comparison to dopamine, the full agonist, to evaluate their ability of activating human dopamine hD_2 and hD_3 receptors expressed in CHO cells. Compounds (−)-**7a** (**D-591**), (−)-**8a** (**D-593**), (−)-**8b** (**D-601**), (−)-**14** (**D-644**), and (−)-**20** (**D-618**) exerted high functional potency and efficacy at both D_2/D_3 receptors (**Table 2**). In contrast to the more selective binding affinity observed for D_3 receptor, all tested compounds turned out to be comparably potent and full agonist at both D_2 and D_3 receptors. Compound (−)-**7a** (**D-591**) was the most potent among the 2-aminothiazole derivatives with a very high functional potency (EC_{50} (GTPγS); D_2 =2.09 nM and D_3 =0.78 nM) and full agonist activity (%*E*max, D_2=96.2, D_3=94.4) at both D_2 and D_3 receptors. Similarly, compound (−)-**8b** (**D-601**) also turned out to be an agonist with comparable potency (EC_{50} (GTPγS); D_2=9.3 nM and D_3=1.22 nM). On the other hand, the aminotetralin analog (−)-**14** (**D-644**), showed a non-

selective profile (D_2/D_3=0.82). When compared to its 2-aminothiazole derivative counterpart (−)-**8a** (**D-593**), a great improvement in potency at both D_2/D_3 receptors (EC_{50} (GTPγS); D_2 =0.27 vs. 22.9 nM and D_3 =0.33 vs. 2.62 nM for (−)-**14** (**D-644**) and (−)-**8a** (**D-593**), respectively) was observed. As for the efficacy, a decrease at D_2 receptor and an increase at the D_3 receptor were observed when comparing compound (−)-**14** (**D-644**) to (−)-**8a** (**D-593**) (%*E*max, D_2= 88.8 vs. 97.4, D_3=90.9 vs. 83.4) (Luo et al. 2016).

When comparing the para-dihydroxy substituted compound (−)-**49** (**D-670**) to its ortho-substituted counterpart **D-520**, it was interesting to notice a modest increase in the potency to both D_2/D_3 receptors in contrast to the decrease in the binding affinity from the aforementioned binding assay (EC_{50} (GTPγS); D_2 =2.75 vs. 4.73 nM and D_3 =0.0827 vs. 2.18 nM, for (−)-**49** (**D-670**) and **D-520**, respectively, **Table 2**). In addition, compound (−)-**49** (**D-670**) became more selective for D_3 receptor (D_2/D_3 = 33.25 vs. 2.17, **Table 2**). On the other hand, while the efficacy of compound (−)-**49** (**D-670**) to the D_2 receptor remained the same when compared to **D-520**, it was found to be enhanced for **D-670** in the case of the D_3 receptor (%*E*max, D_2= 81.8 vs. 80.9, D_3=86.4 vs. 58.3, for (−)-**49** (**D-670**) and **D-520**, respectively, **Table 2**).

Table 2. Stimulation of [^{35}S]GTPγS Binding to hD_2 and hD_3 receptors expressed in CHO cells[a]

Compound	CHO-D_2	CHO-D_3	D_2/D_3

	[^{35}S]GTPγS EC_{50} (nM)	%Emax	[^{35}S]GTPγS EC_{50} (nM)	%Emax	
Dopamine	376 ± 39	100	7.26 ± 0.21	100	51.79
(−)-**7a,** D-591	2.09 ± 0.22	96.2 ± 2.3	0.78 ± 0.10	94.4 ± 4.2	2.68
(−)-**8a,** D-593	22.9 ± 1.6	97.4 ± 3.6	2.62 ± 0.49	83.4 ± 8.2	8.74
(−)-**8b,** D-601	9.3 ± 2.49	88.0 ± 3.6	1.22 ± 0.30	90.9 ± 5.5	7.62
(−)-**14,** D-644	0.27 ± 0.62	88.8 ± 3.5	0.33 ± 0.09	90.9 ± 2.6	0.82
(−)-**20,** D-618	37.7 ± 5.6	84.3 ± 3.6	20.4 ± 5.8	87.5 ± 6.2	1.85
(−)-**49**, D-670	2.75 ± 0.10	81.8 ± 7.2	0.0827 ± 0.0048	86.4 ± 4.5	33.25
D-520[b]	4.73 ± 0.44	80.9 ± 6.6	2.18 ± 0.30	58.3 ± 9.6	2.17

[a] Results are expressed as means ± SEM for three to five experiments, each performed in triplicate.
[b] Data was obtained under almost identical assay conditions (Modi et al. 2014)

3.2.3. *In vitro* anti-aggregation study

So far the effects of structural variations in the designed compounds on the receptor activities have been studied and discussed. In this section, focus will be cast on the ability of selected compounds to modulate αSN aggregation, which was tested through both the shaking and seeding studies.

3.2.3.1. Shaking study

In this experiment, αSN was continuously shaken at aggregation-prone conditions for six days to produce β-sheet-positive fibrillar structures, which can be detected by thioflavin T (ThT). Aliquots were taken in the beginning (day 0) and the end (day 6) of this experiment, and they were characterized through both transmission electron microscope (TEM) and circular dichroism (CD) spectroscopy. As shown in **Figure 16**, the morphology of αSN transferred from

the initial spherical look (day 0) to fibrillar structure at the endpoint of the study (day 6). Further protein secondary structure analysis through far-UV CD spectra revealed a significant reduction in the intensity of the negative shoulder around 203 nm, suggesting a more structured state (**Figure 17**).

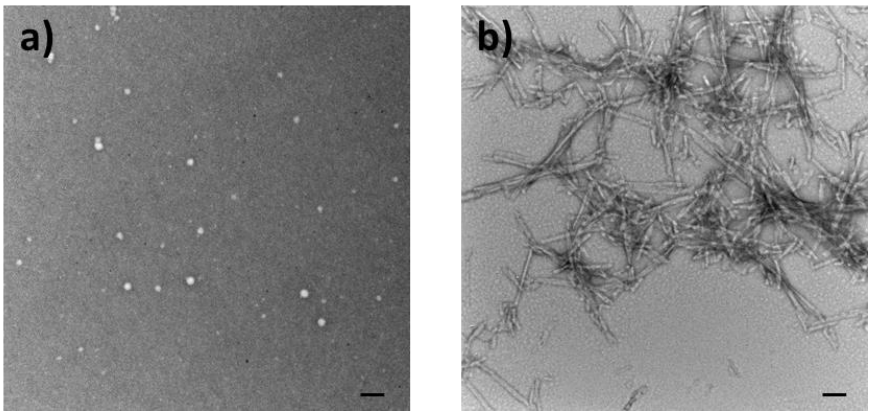

Figure 16. TEM analysis of samples collected in the αSN (60 μM) shaking experiment. (**a**) aliquot at day 0, (**b**) aliquot at day 6; Scale bar = 100 nm.

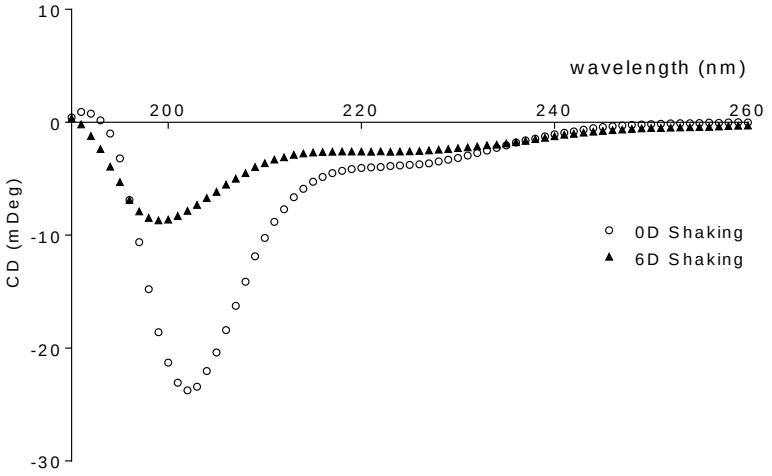

Figure 17. Circular dichroism spectra analysis of samples collected in the αSN (60 μM) shaking experiment.

The potential candidate compound (−)-**8a** (**D-593**) was first evaluated through this shaking experiment in comparison to the reference compound **D-520**: αSN was shaken in the presence or absence of the tested compound (1:2 ratio) at aggregation-prone conditions for six days. Aliquots collected at day 0 and day 6 were analyzed by both ThT and cell viability assay. When tested for cell viability, the collected aliquots were diluted with cell medium for the treatment with the PC12 cells. The final concentrations resulted from the dilution were 10 μM for αSN and 20 μM for the compounds.

A significant inhibition of ThT activity was observed at day 6 in the presence of the test compound (−)-**8a** (**D-593**) or reference compound **D-520** compared to αSN alone, indicating alteration of the aggregation process in the presence of these drugs (**Figure 18a**). However, while **D-520** increased the cell viability by 24%, this new compound failed to generated a similar effect to reduce the cytotoxicity induced by αSN in the current assay condition: only a statistically non-significant 9% increase in cell viability was detected (**Figure 18b**).

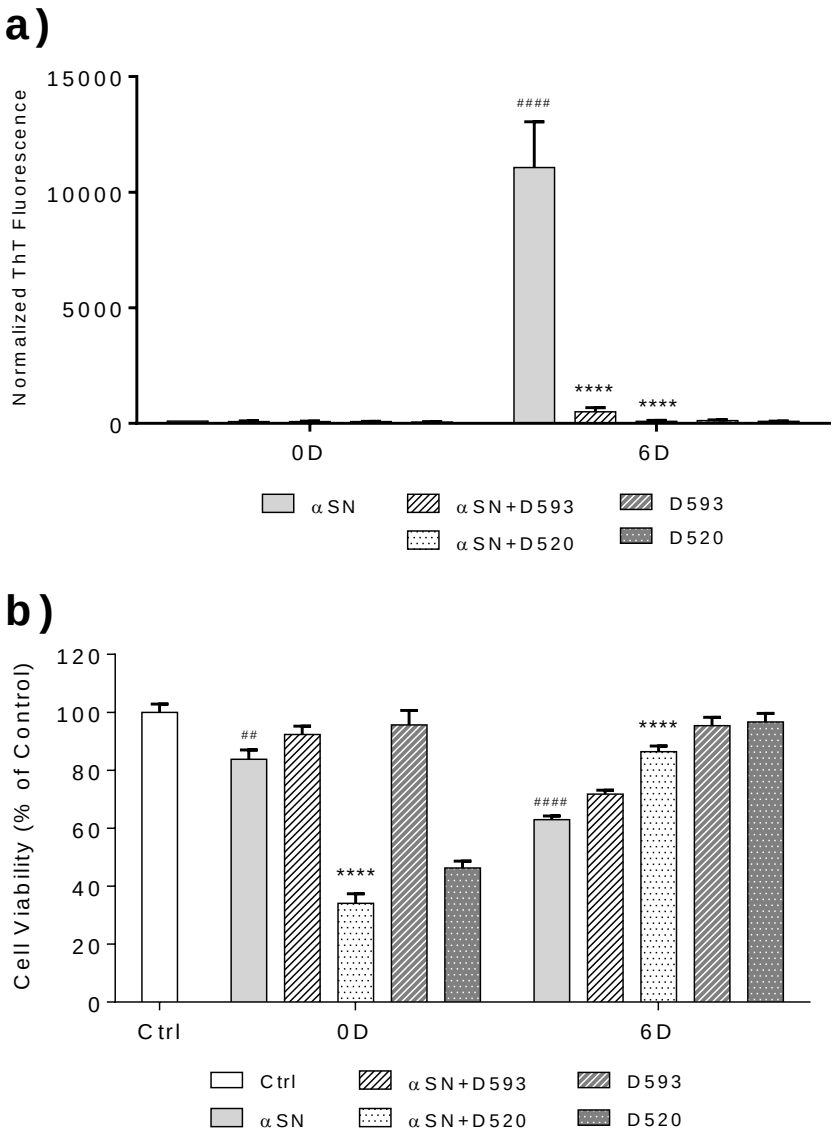

Figure 18. Modulation of compound (−)-**8a** (**D-593**) on the aggregation of αSN induced by shaking. Tested compound (−)-**8a** (**D-593**) and reference compound **D-520** (120 μM) were incubated with αSN (60 μM) over a period of 6 days. Drugs were also tested alone to show any direct effect on assays. **a)** Fibrillation was measured by ThT assay. Readings from ThT assay were normalized by assigning the reading of αSN alone day 0 sample as 100%. The data are shown as means ± SEM of three independent experiments. One-way ANOVA followed by Tukey's multiple comparison post hoc test was performed (#### $p \leq 0.0001$ compared to the αSN-0D, **** $p \leq 0.0001$ compared to the αSN sample at corresponding time points). **b)** Cell viability was measured by MTT assay.

Readings were normalized to the untreated control. The data are shown as means ± SEM of three independent experiments. One-way ANOVA followed by Tukey's multiple comparison post hoc test was performed (## $p \leq 0.01$, #### $p \leq 0.0001$ compared to the untreated control, **** $p \leq 0.0001$ compared to the αSN sample at corresponding time points).

3.2.3.2. Seeding study

The shaking assay has been widely accepted and applied in the screening for αSN aggregation modulators, and the continuous agitation considerably shorten the experimental time span. However, the fact that it was done in aggressive agitation conditions renders it relatively artificial in terms of mimicking the actual αSN aggregation process in the PD brain. An *in vitro* seeding assay without any shaking has been developed recently to overcome this drawback while trying to maintain a relatively short experimental time span (Yedlapudi et al. 2016).

In this experiment, ThT-positive preformed fibrils (PFF), the αSN seeds, were first generated by shaking at aggregation-prone condition, which were subsequently added to and incubated with αSN monomers over the time. Aliquots were taken in the beginning (day 0) and every 10 days throughout this assay, and they were characterized via both transmission electron microscope (TEM) and circular dichroism (CD) spectroscopy. As shown in **Figure 19a**, the seeds generated through a shaking procedure adopted the morphology similar to what was observed in the shaking day 6 sample. When the seeding reaction was initiated (day 0) by the addition of PFF to the αSN monomers pool, the PFF served as a template or scaffold to recruit adjacent monomers (**Figure 19b**) and

αSN aggregation continued (**Figure 19c**). Unlike the relatively uniformed mixture of fibrils observed in the shaking day 6 samples (**Figure 16b**), the product of the seeding reaction is rather heterogenous: a considerable amount of monomers or small order aggregates were still visible in the same view with the meshed fibrils (**Figure 19d**).

Furthermore, the far-UV CD spectra revealed an incubation time-dependent patent. A clear reduction in the intensity of the negative shoulder around 203 nm and an increase in the intensity of the negative shoulder around 220 nm suggest a gradual conversion to more structured states over the time (**Figure 20**). However, the extent of these alterations was much less comparing to the observation made in the shaking assay, which could be due to the heterogenicity of the finial protein mixture obtained from the seeding process.

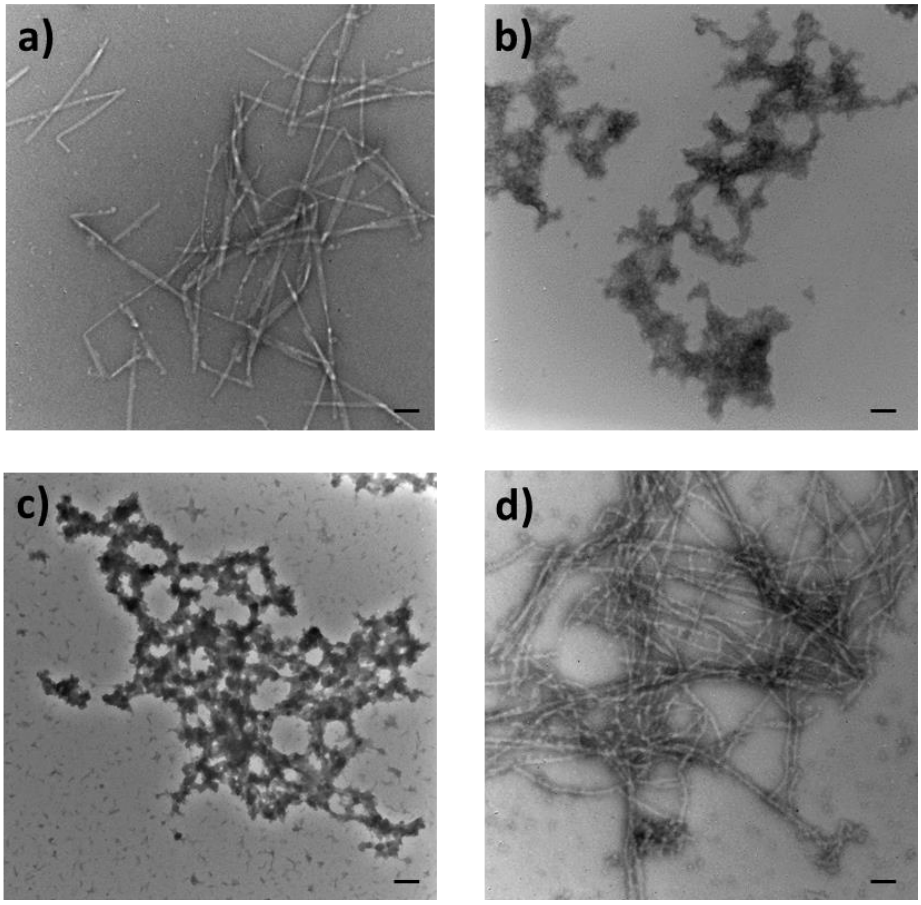

Figure 19. TEM analysis of samples collected in the αSN (1.25 mg/mL = 86.45 µM) 0.5% seeding experiment. (**a**) PFF, (**b**) seeding aliquot at day 0, (**c**) seeding aliquot at day 10, (d) seeding aliquot at day 30; Scale bar = 100 nm.

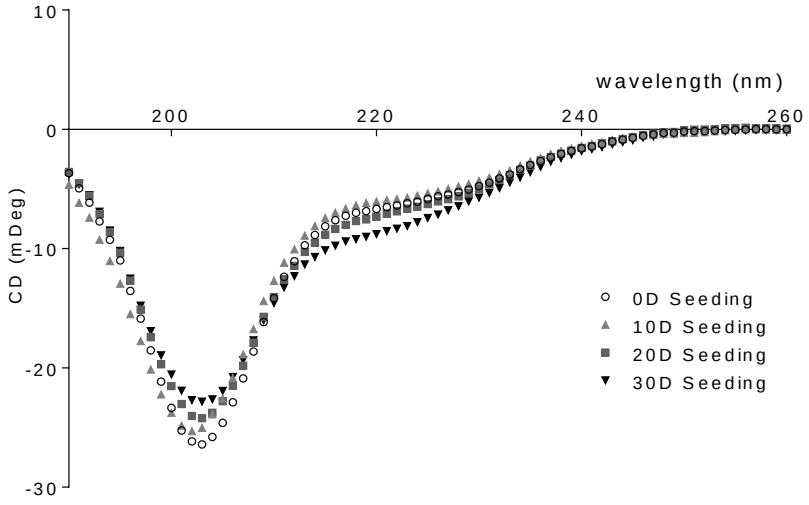

Figure 20. Circular dichroism spectra analysis of samples collected in the αSN (86.45 μM) 0.5% seeding experiment.

Three representative compounds (−)-**8a** (**D-593**), (−)-**20** (**D-618**), and (−)-**14** (**D-644**) were selected and tested in this assay in comparison to the reference compound **D-520**. αSN was seeded with 0.5% (v/v) PFF and incubated in the presence or absence of the tested compound (1:2 ratio) for 10 days, while αSN alone and compounds alone were also included. Aliquots collected at day 0 and day 10 were analyzed by both ThT and cell viability assay. When tested for cell viability, the collected aliquots were diluted with cell medium and treated to the PC12 cells, resulting a final concentration of 10 μM for αSN and 20 μM for compounds.

As seen in **Figure 21a**, the reference compound **D-520** and compound (−)-**14** (**D-644**) significantly reduced the ThT activity by either 289% or 303% at day 10 comparing to the 10 day αSN seeding sample. However, only 105% and

185% decrease of ThT signals were observed for compound (−)-**8a** (**D-593**) and (−)-**20** (**D-618**), respectively. The less extent of ThT signal reduction by (−)-**8a** (**D-593**) in this assay could result from the autofluorescence generated through the incubation of compound itself.

When the PC12 cells were exposed to the 10 day αSN seeding sample, a 43% cell death was observed. While the reference compound **D-520** was able to enhance the cell viability tremendously by 27%, compounds (−)-**8a** (**D-593**) and (−)-**14** (**D-644**) moderately raised the viability by 16% and 18%, respectively (**Figure 21b**). As for compound (−)-**20** (**D-618**), the increase in cell viability was limited to only 9% (**Figure 21b**). This cell viability data as well as the ThT data suggest that the methoxy-hydroxy compound is less potent in modulating seeded αSN aggregation.

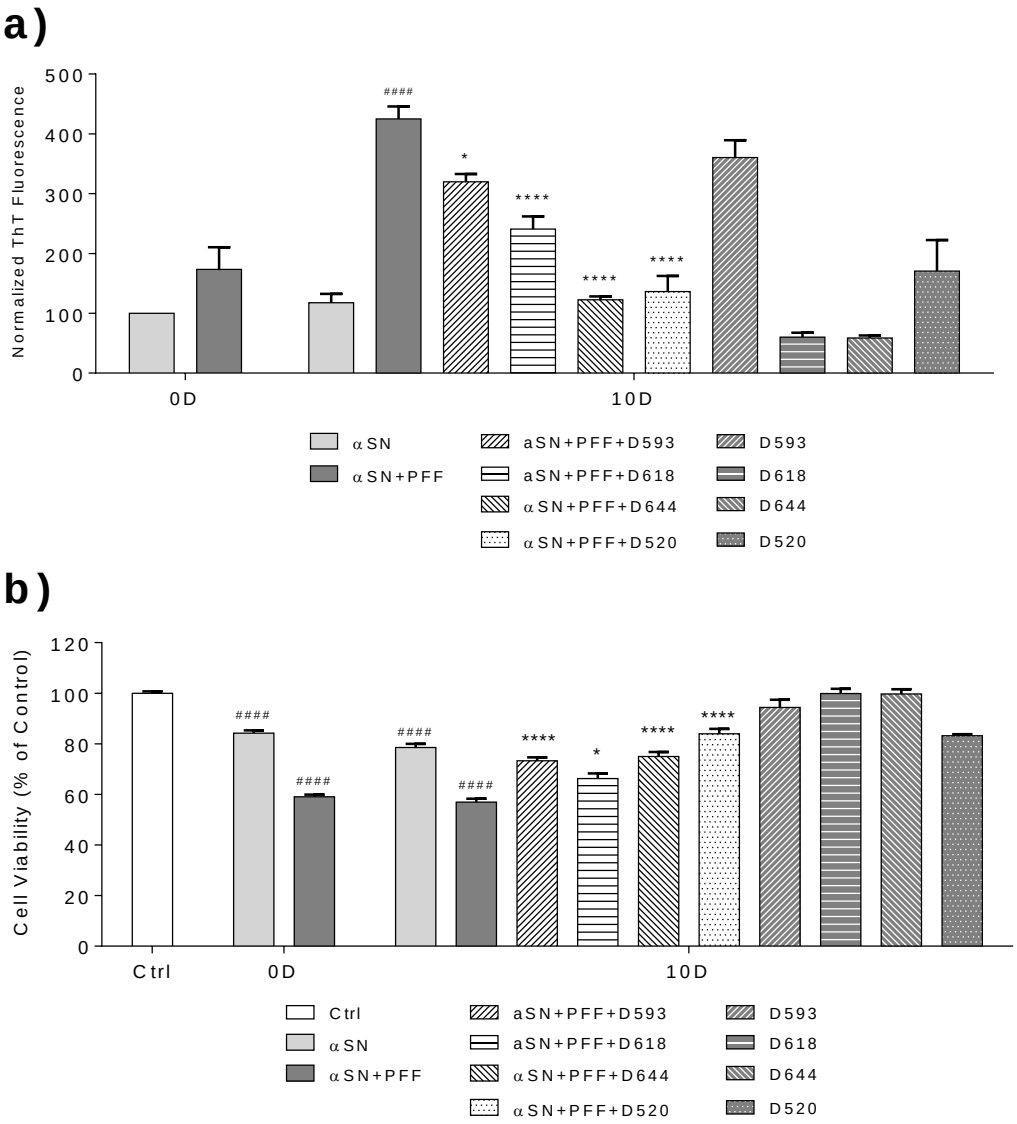

Figure 21. Modulation of the aggregation of αSN induced by 0.5% (v/v) seeding by compounds (−)-**8a** (**D-593**), (−)-**20** (**D-618**), and (−)-**14** (**D-644**). Test compounds (−)-**8a** (**D-593**), (−)-**20** (**D-618**), and (−)-**14** (**D-644**) and the reference compound **D-520** (172.9 μM) were incubated with αSN (86.45 μM) for 10 days. Drugs were also tested alone as controls to show any direct effect on assays. **a)** Fibrillation was measured by ThT assay. Readings from ThT assays were normalized by assigning the data of αSN alone from day 0 sample as 100%. The data are shown as means ± SEM of three independent experiments. Data and statistics of **D-520** were taken from Yedlapudi et al. 2016. One-way ANOVA followed by Tukey's multiple comparison post hoc test was performed (#### $p \leq$

0.0001 compared to the αSN-0D, * $p \leq 0.05$, **** $p \leq 0.0001$ compared to the seeded αSN sample at day 10). **b)** Cell viability was measured by MTT assay. Readings were normalized to the untreated control. The data are shown as means ± SEM of three independent experiments. Data and statistics of **D-520** were taken from Yedlapudi et al. 2016. One-way ANOVA followed by Tukey's multiple comparison post hoc test was performed (#### $p \leq 0.0001$ compared to the untreated control, * $p \leq 0.05$, **** $p \leq 0.0001$ compared to the seeded αSN sample at day 10).

To gain more information on the effect of para- and ortho-dihydroxy substitution on seeded αSN aggregation, compound (−)-**49** (**D-670**) was studied along with its ortho-substituted analog **D-520** for a prolonged period of 30 days. As seen in **Figure 22a**, a gradual increased ThT signal as an indication of fibrilization was found throughout the seeding process, and both pare- and ortho-compounds significantly reduced this signal, which suggests a significant inhibition to the PFF induced aggregation. When the PC12 cells were treated with 10 day to 30 day αSN PFF seeded samples, about 48% cell death were induced. However, when the seeded samples were incubated with either compound (−)-**49** (**D-670**) or **D-520**, the samples became much less toxic to the cells in contrast to PFF induced untreated seeded samples at the corresponding time points. Both compounds were able to improve the cell viability considerably by approximately 30-40% (**Figure 22b**). Thus, both para- and ortho-dihydroxy substitutions exerted comparable anti-aggregation activity.

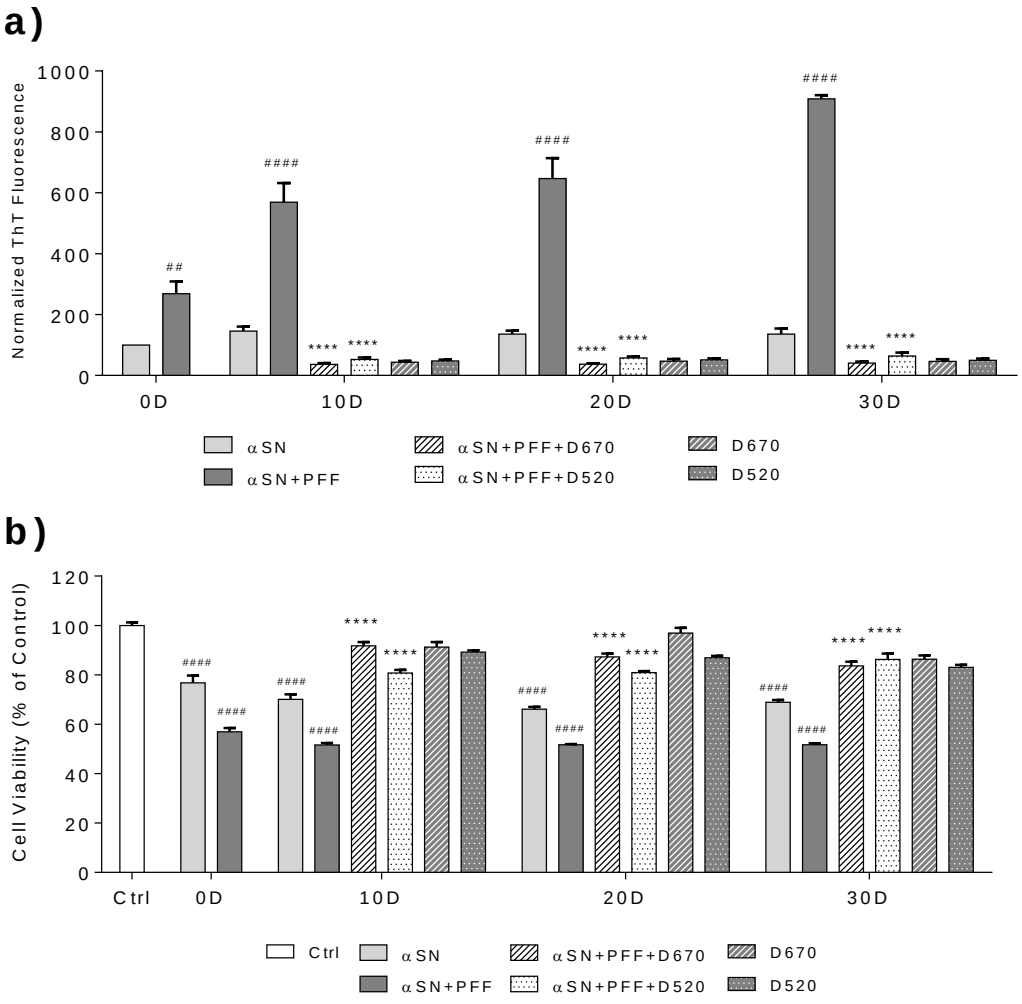

Figure 22. Modulation of compound (−)-**49** (**D-670**) on the aggregation of αSN induced by 0.5% (v/v) PFF seeding. Test compound (−)-**49** (**D-670**) and the reference compound **D-520** (172.9 μM) were incubated with αSN (86.45 μM) in presence of 0.5% PFF for 30 days. Drugs were also tested alone to show any direct effect on assays. **a)** Fibrillation was measured by ThT assay. Readings from ThT assay were normalized by assigning the reading of αSN alone at day 0 sample as 100%. The data are shown as means ± SEM of three independent experiments. One-way ANOVA followed by Tukey's multiple comparison post hoc test was performed (## $p \leq 0.01$, #### $p \leq 0.0001$ compared to the αSN-0D, **** $p \leq 0.0001$ compared to the seeded αSN sample at corresponding time points). **b)** Cell viability was measured by MTT assay. Readings were normalized to the untreated control. The data are shown as means ± SEM of three independent experiments. One-way ANOVA followed by Tukey's multiple comparison post hoc test was performed (#### $p \leq 0.0001$ compared to the

untreated control, **** $p \leq 0.0001$ compared to the seeded αSN sample at corresponding time points).

3.2.4. Neuroprotection against 6-OHDA induced toxicity in PC12 cell line with multifunctional αSN modulators

Following the screening through the *in vitro* receptor assays and αSN anti-aggregation study, three representative alkyl linker compounds (−)-**8a** (**D-593**), (−)-**20** (**D-618**), and (−)-**14** (**D-644**) were selected based on their structural diversity on the terminal aromatic substitutions and the agonist head groups to evaluate their protective effect in reversing toxicity induced by 6-hydroxydopamine (6-OHDA). This dopaminergic neurotoxin is widely used in PD study because of its known effect in causing cell death via the production of reactive oxygen species in a dose dependent manner (Blum et al. 2000, Soto-Otero et al. 2000).

First, these selected compounds were assessed for toxicity to the PC12 cells, for which the cells received treatments with the compounds at various doses for 24 h. As shown in **Figure 23 a)** and **b)**, compounds (−)-**8a** (**D-593**), (0.1-30 μM) and (−)-**20** (**D-618**) (1-50 μM) had no noticeable effect on cell viability compared to the untreated control. In contrast, compound (−)-**14** (**D-644**) (0.1-30 μM) slightly induced cell proliferation at higher concentrations (**Figure 23c**).

Then, the effect of compounds on 6-OHDA induced toxicity was examined. PC12 cells were first pretreated 24 h with increasing doses of compounds (−)-**8a**

(**D-593**) (0.1-30 µM)**,** (−)-**14** (**D-644**) (0.1-30 µM), or (−)-**20** (**D-618**) (1-50 µM), followed by the single treatment of 6-OHDA for additional 24 h. The dose of toxin was set to 75 µM to produce a significant reduction of cell viability based on the previously published data (Das et al. 2015). Cell viability was assessed by MTT assay. As shown in **Figure 23 d-f)**, compounds (−)-**8a** (**D-593**)**,** (−)-**20** (**D-618**), and (−)-**14** (**D-644**) were able to protect cells against 6-OHDA-induced toxicity in a dose-dependent manner. The greatest protection (18-25%) was seen at 30 µM dose point for all the three compounds (**Figure 23**).

In addition, compound (−)-**49** (**D-670**) was also tested in the same fashion for its ability to reverse the cytotoxicity induced by 6-OHDA. Unlike those alkyl linker compounds, compound (−)-**49** (**D-670**) demonstrated toxicity at higher doses and caused up to 38% cell death at the highest dose tested (**Figure 24a**). Due to the inherent toxicity of compound (−)-**49** (**D-670**) in the current assay conditions, the greatest protection (16%) was seen at 5 µM dose point (**Figure 24b**).

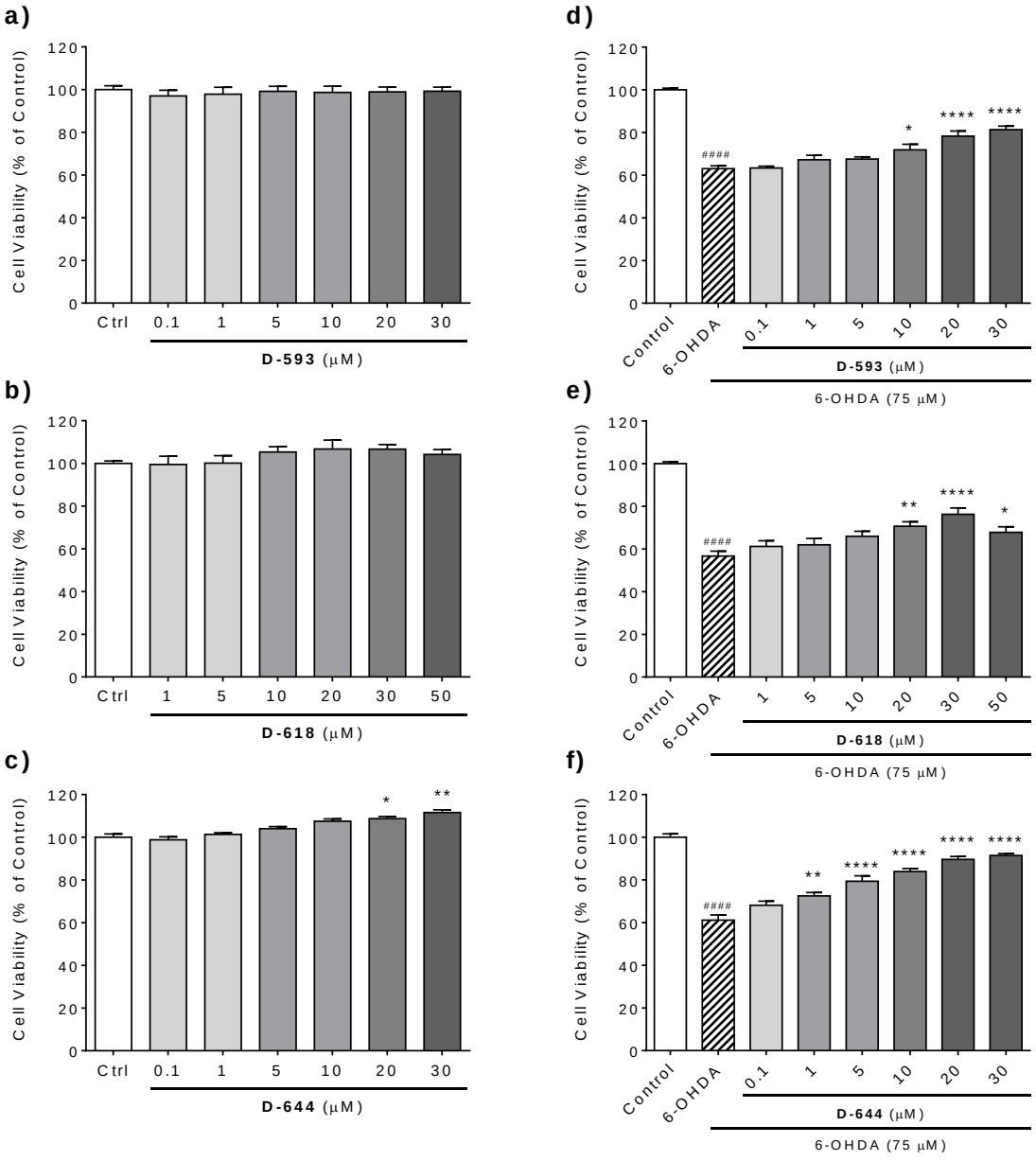

Figure 23. a-c) Dose-dependent effect of compounds (−)-**8a** (**D-593**) (**a**), (−)-**20** (**D-618**) (**b**), and (−)-**14** (**D-644**) (**c**) on the viability of PC12 cells in 24 h treatment. The results shown are mean ± SEM of three independent experiments performed in six to eight replicates. One-way ANOVA followed by Tukey's multiple comparison post hoc test was performed (* $p \leq 0.05$, ** $p \leq 0.01$ compared to the control). **d-e)** Dose-dependent effect on the viability of PC12 cells by 24 h pretreatment with compounds (−)-**8a** (**D-593**) (**d**), (−)-**20** (**D-618**) (**e**), and (−)-**14** (**D-644**) (**f**) followed by single treatment with 75 μM 6-OHDA for another 24 h.

The results shown are mean ± SEM of three independent experiments performed in six to eight replicates. One-way ANOVA followed by Tukey's multiple comparison post hoc test was performed (#### $p \leq 0.0001$ compared to the control; * $p \leq 0.05$, ** $p \leq 0.01$, **** $p \leq 0.0001$ compared to the 6-OHDA control).

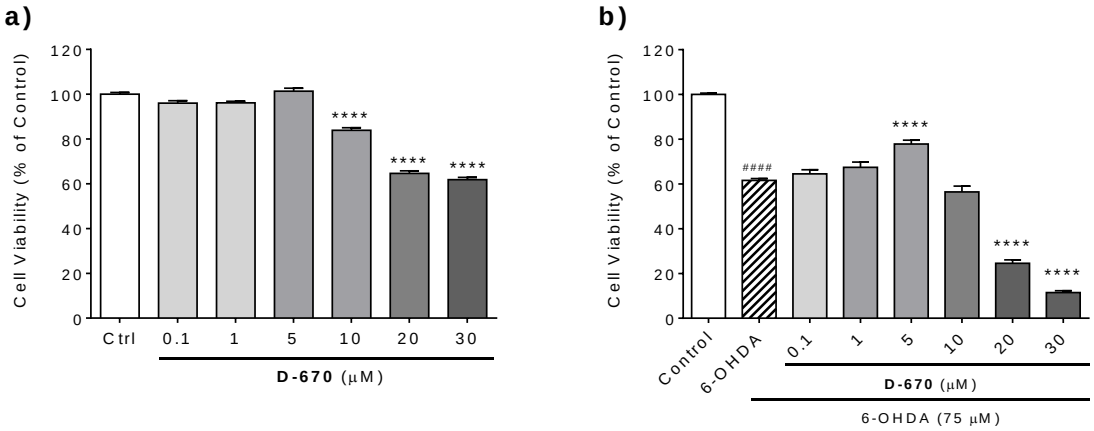

Figure 24. a) Dose-dependent effect of compound (−)-**49** (**D-670**) on the viability of PC12 cells by 24 h treatment. The results shown are mean ± SEM of three independent experiments performed in six to eight replicates. One-way ANOVA followed by Tukey's multiple comparison post hoc test was performed (**** $p \leq 0.0001$ compared to the control). **b)** Dose-dependent effect on the viability of PC12 cells by 24 h pretreatment with compound (−)-**49** (**D-670**) at various concentrations (0.1-30 µM) followed by single treatment with 75 µM 6-OHDA for another 24 h. The results shown are mean ± SEM of three independent experiments performed in six to eight replicates. One-way ANOVA followed by Tukey's multiple comparison post hoc test was performed (#### $p \leq 0.0001$ compared to the control; **** $p \leq 0.0001$ compared to the 6-OHDA control).

3.2.5. Reversal of reserpine-induced hypolocomotion in rats with multifunctional αSN modulators

Catalepsy was induced in rats by administrating reserpine, which can block the vesicular monoamine transporter (VMAT) and subsequently lead to the depletion of monoamines in the synapse of the peripheral sympathetic nerve terminals (Fernandes et al. 2012, Duty and Jenner 2011, Leao et al. 2015). In

this well-established PD model, significant inhibition of locomotion of rats, which indicates the development of akinesia, was observed 18 h after administrating reserpine (5 mg/kg, s.c.) (**Figure 25**). The ability of compounds (−)-**8a** (**D-593**) and (−)-**20** (**D-618**) to reverse the reserpine-induced hypolocomotion was investigated in this assay because of their high affinity and efficacy at D_2 and D_3 receptors in the *in vitro* receptor assays. At the dose of 10 μmol/kg i.p., compound (−)-**8a** (**D-593**) effectively reversed akinesia induced by reserpine treatment and displayed a steady continuous effect in comparison to the peak effect from reference drug ropinirole (**Figure 25**). This significant locomotor stimulation is likely to be mediated by postsynaptic D_2/D_3 receptor activation, which suggested that compound (−)-**8a** (**D-593**) can cross the blood-brain barrier effectively and function as a potent agonist. However, despite the similarity between the compounds (−)-**8a** (**D-593**) and (−)-**20** (**D-618**) in structure, predicted chemical properties, and *in vitro* receptor activities, the latter displayed only a slight activity in reversing the induced hypolocomotion (**Figure 25**). The reduced agonist efficacy may be due to a potential difference in compound metabolism.

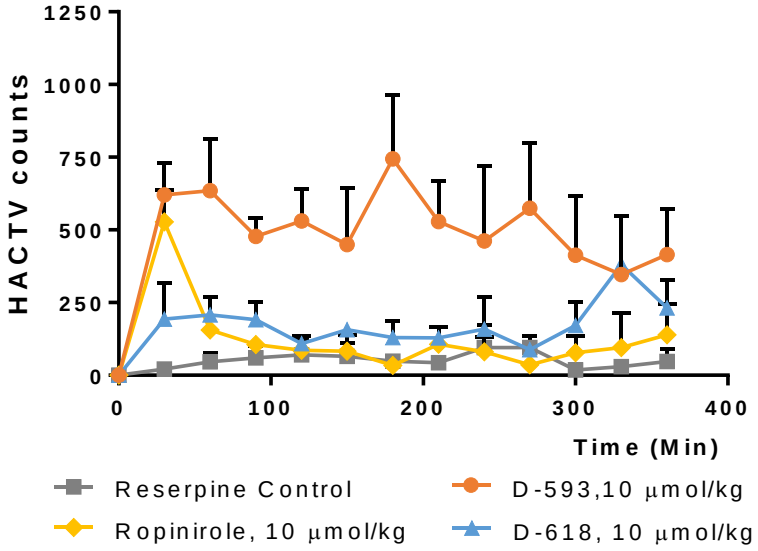

Figure 25. Effect of compounds (−)-**8a** (**D-593**), (−)-**20** (**D-618**), and ropinirole on reserpine-induced (5.0 mg/kg, s.c.) hypolocomotion in rats. Results are expressed as means ± SEM; n=2-3 rats per value. Horizontal activity (HACTV), which is the total number of beam interruptions that occurred in the horizontal sensor during a given sample period, was measured as described in Chapter 4. Locomotor data during each 30-min interval after the administration of compounds (−)-**8a** (**D-593**) (i.p.), (−)-**20** (**D-618**) (i.p.) or ropinirole (i.p.) at the dose of 10 µmol/kg compared to control reserpine treated rats in 18 h post reserpine treatment was plotted. Differences among treatments were significant by one-way ANOVA analysis (F (3, 48) = 32.27; $p< 0.0001$). Dunnett's analysis following ANOVA revealed that the effects of compounds (−)-**8a** (**D-593**) ($p< 0.0001$) and (−)-**20** (**D-618**) ($p< 0.05$) were significantly different when compared to reserpine control.

Besides these alkyl linker compounds, (−)-**49** (**D-670**), the para-dihydroxy analog of a highly potent and efficacious D_2/D_3 receptor agonist **D-520**, was also evaluated in the same PD animal model. However, this newly developed analog exhibited no *in vivo* agonistic activity when compared to the reserpine model (**Figure 26**). The loss of agonistic activity could be due to a faster phenol-

quinone conversion of the para-dihydroxy substitution or the interference of unpredicted compound metabolism.

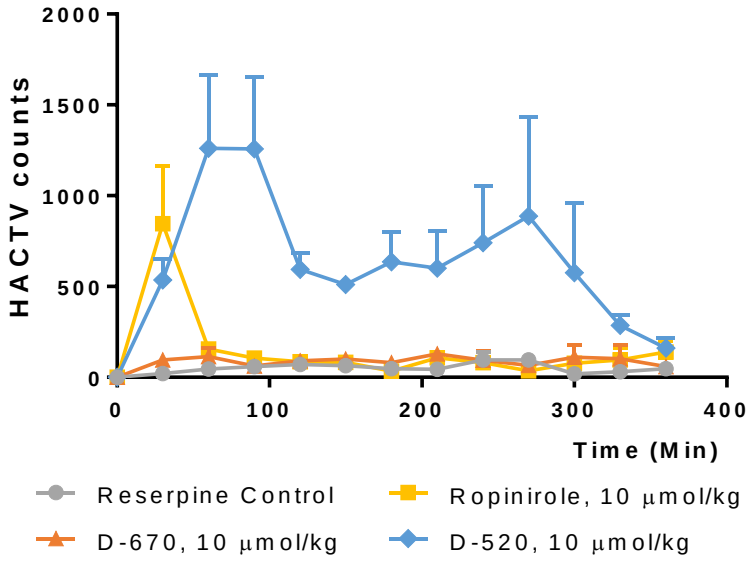

Figure 26. Effect of compounds (−)-**49** (**D-670**), **D-520**, and ropinirole on reserpine-induced (5.0 mg/kg, s.c.) hypolocomotion in rats. Results are expressed as means ± SEM; n=3-5 rats per value. Horizontal activity (HACTV), which is the total number of beam interruptions that occurred in the horizontal sensor during a given sample period, was measured as described in Chapter 4. Locomotor data during each 30-min interval after the administration of compounds (−)-**49** (**D-670**) (i.p.), **D-520** (i.p.), or ropinirole (i.p.) at the dose of 10 µmol/kg compared to control reserpine treated rats in 18 h post reserpine treatment was plotted. Differences among treatments were significant by one-way ANOVA analysis ($F(3, 48) = 19.99$; $p < 0.0001$). Dunnett's analysis following ANOVA revealed that the effects of compound (−)-**49** (**D-670**) was not significant when compared to reserpine control.

3.3. Design, synthesis, and the initial SAR study of novel multifunctional dopamine D_2/D_3 receptors agonists containing an propargyl moiety for potential MAO-B inhibitory activity

In this section, results from the initial SAR study on a group of novel dopamine D_2/D_3 receptor agonists that incorporates the *N*-propargylamine moiety, which has been reported to exert MAO-B inhibitory activity, will be shown and discussed. The hybrid molecule template (**Figure 27**) was modified from the previously established model that had resulted in the discovery of multiple promising lead compounds including **D-512** and **D-616** (**Figure 28**). In the current template, the propyl group was replaced by the propargyl group in the head group derived from pramipexole or 5-OH-DPAT. The dopamine D_2/D_3 receptors targeting head group was attached with various accessory binding site moieties, which originated from previously published lead compounds, through a linker, usually a piperazine ring. In addition, a pentynyl analog was also included in this series of compounds to provide further information of the effect of propargyl group replacement.

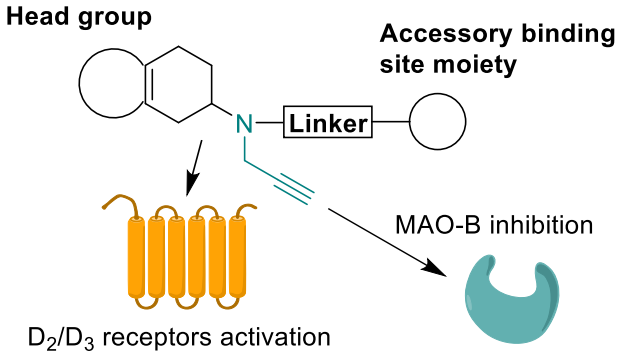

Figure 27. The hybrid molecule template for multifunctional dopamine D_2/D_3 receptor agonists that may potentially inhibit the MAO-B activity.

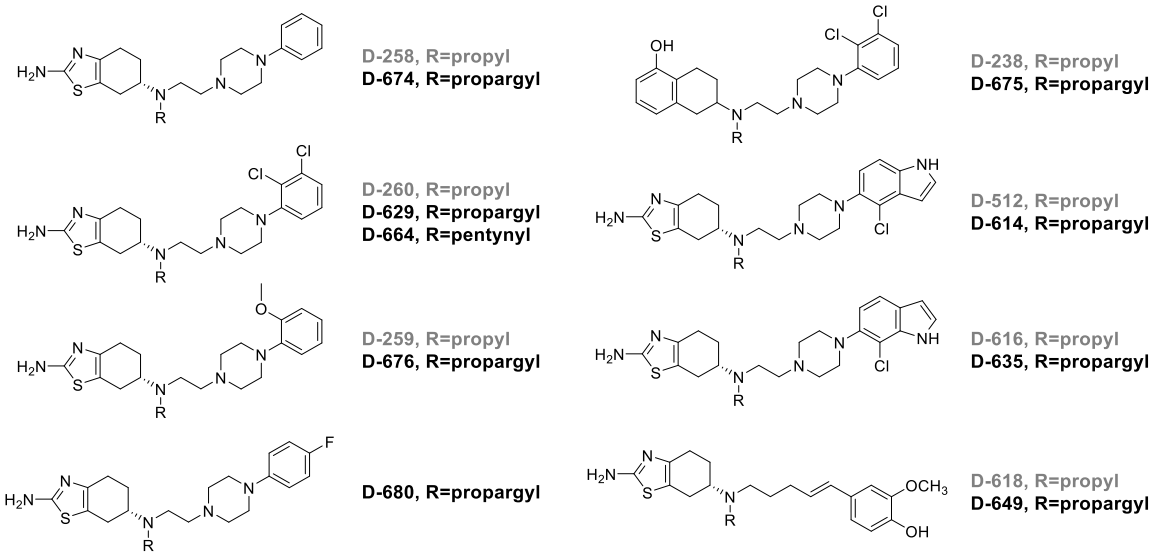

Figure 28. Structure of compounds in the initial brief SAR study. Compounds labeled as black were designed and synthesized, whose corresponding propyl containing parent molecules are labeled as grey.

3.3.1. Synthesis of multifunctional MAO-B inhibitors

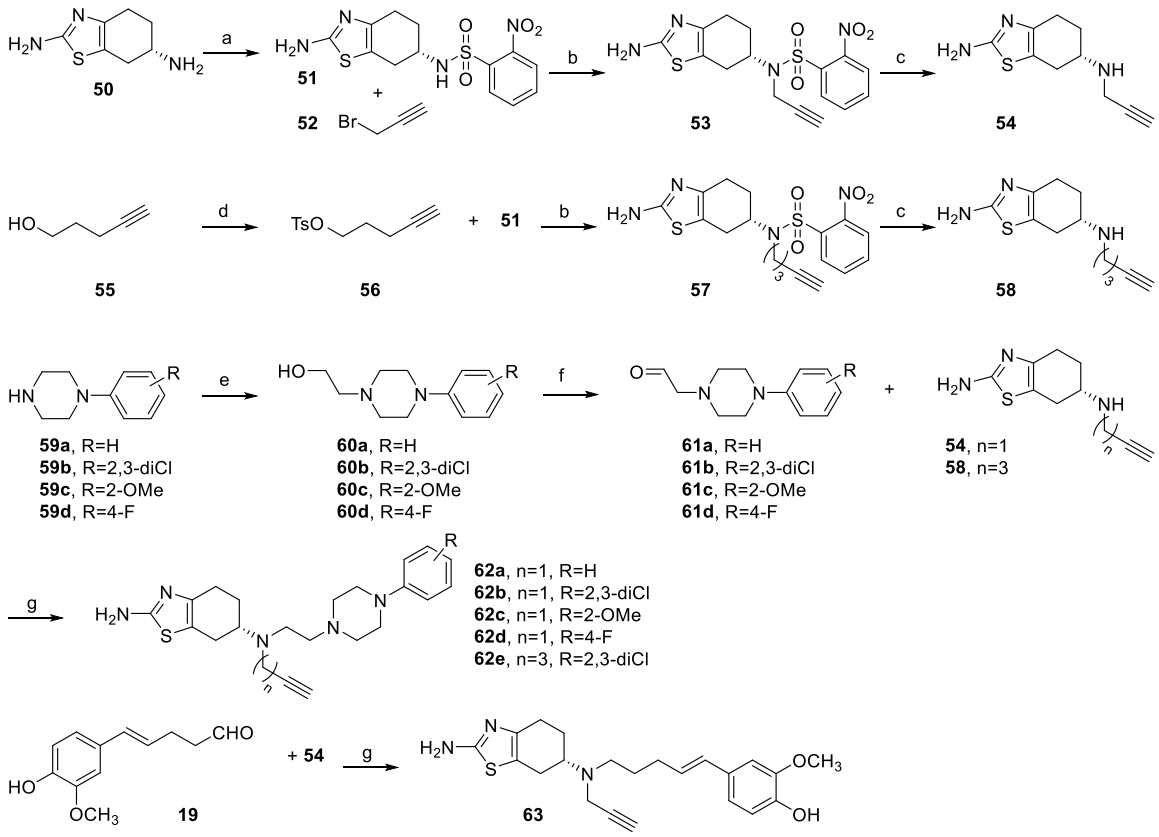

Scheme 7. Synthesis of compounds **62a** (**D-674**), **62b** (**D-629**), **62c** (**D-676**), **62d** (**D-680**), **62e** (**D-664**), and **63** (**D-649**). Reaction and Conditions: (a) 2-nitrobenzenesulfonyl chloride, Et_3N, THF, −10 °C to rt, 1.5 h; (b) K_2CO_3, CH_3CN, 50 °C, 24h or 85 °C, 36 h; (c) thioglycolic acid, K_2CO_3, DMF, 0 °C to rt to 55 °C, 18-21 h; (d) Et_3N, 4-DMAP, TsCl, CH_2Cl_2, 0°C to rt, overnight; (e) 2-bromoethanol, K_2CO_3, CH_3CN or EtOH, reflux, 4-20 h; (f) SO_3·Py or oxalyl chloride, DMSO, Et_3N, CH_2Cl_2, 0 or −78 °C to rt, 2 h; (g) $Na(OAc)_3BH$, CH_2Cl_2, rt, 40-48 h.

Scheme 7 describes the synthesis of four *N*-propargyl compounds and one *N*-pentynyl analog, all of which have a piperazine ring as the linker connecting a phenyl ring to the head group. Another propargyl containing compound that derived from (−)-**20** (**D-618**) mentioned in section 3.2 is also included. The common *N*-propargyl intermediate **54** and the *N*-pentynyl

intermediate **58** were synthesized by using the Fukuyama nosyl strategy adapted based on literature (Zivec, Anzic, and Gobec 2010). The starting diamine **50** (Brown et al. 2009) was first selectively protected by 2-nitrobenzenesulfonyl chloride to give the common sulfonamide intermediate **51**. For the *N*-propargyl intermediate **53**, commercially available propargyl bromide (**52**) was used to react with nitrobenzenesulfonamide **51**. And for the *N*-pentynyl intermediate **57**, commercially available pent-4-yn-1-ol (**55**) was first converted to corresponding tosylate **56,** which was then reacted with nitrobenzenesulfonamide **51** to produce tertiary amine **57**. Thioglycolic acid was used to deprotect tertiary amine **53** or **57** to generate secondary amine **54** or **58**, respectively. Amine intermediates **59a**, **59b**, **59c**, and **59d** were coupled with 2-bromoethanol to form the alcohol intermediates **60a**, **60b**, **60c**, and **60d,** respectively, which were subsequently oxidized by either the Parikh–Doering oxidation or the Swern oxidation to give corresponding aldehyde intermediates **61a**, **61b**, **61c**, and **61d**. These aldehyde intermediates were then coupled with either amine **54** or **58** to yield the final compounds **62a** (**D-674**), **62b** (**D-629**), **62c** (**D-676**), **62d** (**D-680**) and **62e** (**D-664**). The final compound **63** (**D-649**) was synthesized by reacting the (*E*)-alkene intermediate **19** described in section 3.2 with the common intermediate **53** in the presence of sodium triacetoxyborohydride.

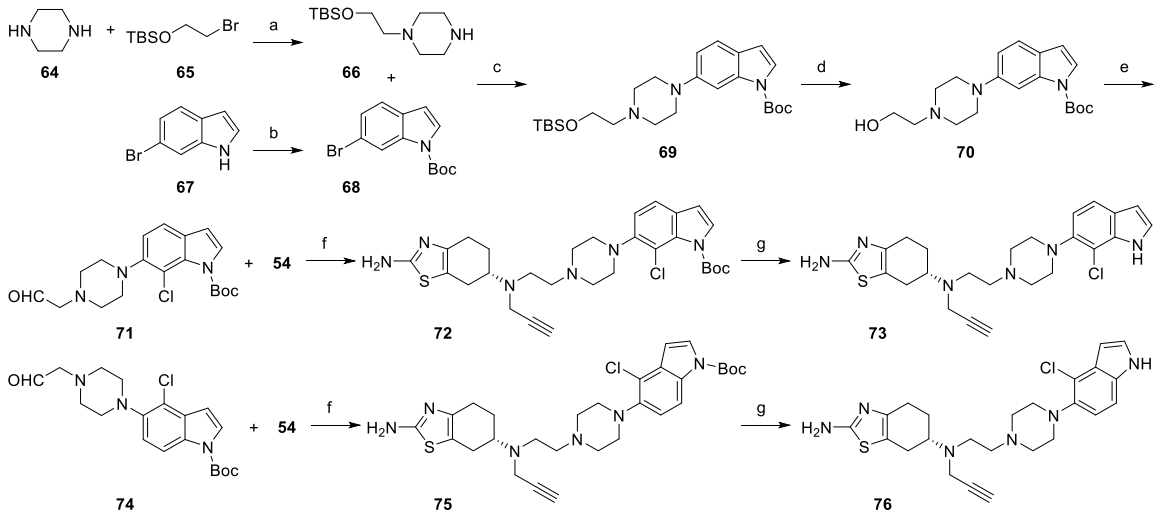

Scheme 8. Synthesis of compounds **73** (**D-635**) and **76** (**D-614**). Reaction and Conditions: (a) K_2CO_3, CH_3CN, reflux, 15 h; (b) $(Boc)_2O$, 4-DMAP, THF, rt, 12 h; (c) $Pd(OAc)_2$, BINAP, Cs_2CO_3, toluene, reflux, 24 h; (d) TBAF, THF, 0 °C to rt, 2 h; (e) oxalyl chloride, DMSO, Et_3N, CH_2Cl_2, −78 °C to rt, 2 h; (f) $Na(OAc)_3BH$, CH_2Cl_2, rt, 40-65 h; (g) CF_3COOH, CH_2Cl_2,0 °C to rt, 2 h.

Scheme 8 depicts the synthesis of a pair of compounds, **73** (**D-635**) and **76** (**D-614**), which have the indole rings as the accessory binding site moiety. The linker is synthesized by refluxing piperazine (**64**) with (2-bromoethoxy)-tert-butyl-dimethylsilane (**65**) in the presence of K_2CO_3. Following the *N*-protection of 6-bromoindole (**67**) with di-tert-butyl decarbonate, palladium-catalyzed cross coupling was used to combine the protected intermediate **68** with the linker fragment **66** in the presence of Cs_2CO_3 and BINAP to generate intermediate **69**, which was subsequently deprotected by tetra-n-butylammonium fluoride (TBAF) to produce alcohol intermediate **70**. Through the Swern oxidation, alcohol **70** was converted to its corresponding aldehyde **71** and further reacted with the common intermediate **54** in the presence of sodium triacetoxyborohydride to give the

intermediate **72**. In the same fashion, the aldehyde intermediate **74**, which was obtained following the procedure reported in literature (Johnson et al. 2012, 2013), was used first to couple with the common intermediate **54** to yield intermediate **75**. Finally, the deprotection of the Boc group was achieved by using trifluoroacetic acid to generate the final compound **73** (**D-635**) and **76** (**D-614**), respectively.

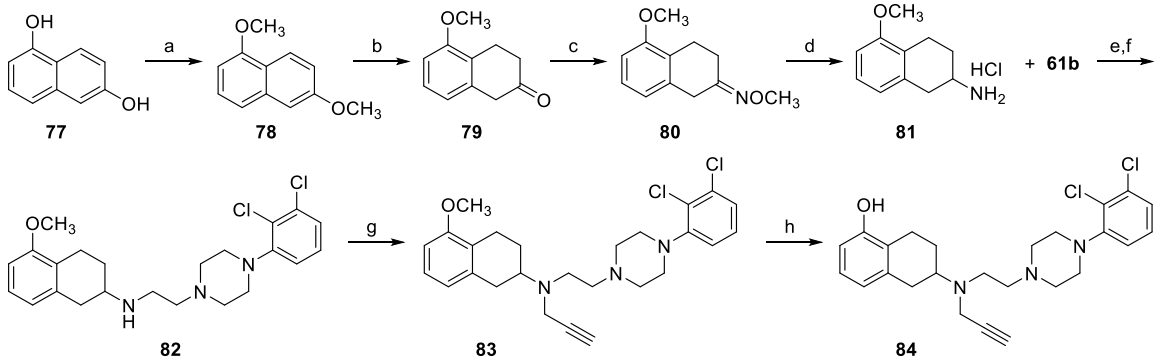

Scheme 9. Synthesis of compound **84** (**D-675**). Reaction and Conditions: (a) Me_2SO_4, K_2CO_3, acetone, reflux, 4 h; (b) Na, EtOH, reflux, 2 h; aqueous HCl, reflux, 1 h; (c) $MeONH_2{\cdot}HCl$, AcONa, 60% MeOH/H_2O, rt, 2 h; (d) H_2 (2 bar), 10% Pd/C, HCl, MeOH, rt, 2.5 h; (e) 2N NaOH aq; (f) $Na(OAc)_3BH$, CH_2Cl_2, rt, 40 h; (g) propargyl bromide, K_2CO_3, CH_3CN, 50-60 °C, 4 h; (h) BBr_3, CH_2Cl_2, −40 °C to rt, 4 h.

Scheme 9 shows the synthesis of final compound **84** (**D-675**), which is a racemic DPAT analog of compound **62b** (**D-629**). The amine intermediate **81** was synthesized following a published procedure (Hirayama, Ikunaka, and Matsumoto 2005). The starting material 1,6-dihydroxynaphthalene (**77**) went through bis-*O*-methylation and the Birch reduction to give tetralone intermediate **79**. Then it was converted to its corresponding oxime *O*-methyl ether **80**, and

further hydrogenation was used to produce the HCl salt of intermediate **81**. The free base of **81** was liberated by 2N NaOH aqueous solution and extracted with ethyl acetate. After coupling it to aldehyde **61b** through reductive amination, *N*-propargylation was applied to yield intermediate **83**, which was further demethylated by boron tribromide to produce the final compound **84** (**D-675**).

3.3.2. *In vitro* receptor assays with multifunctional MAO-B inhibitors

In this study, a small library of nine compounds was generated according to the hybrid molecule template, and *in vitro* binding and functional assays were conducted to gain information for the initial SAR study.

A radioligand competition assay was carried out with the rat D_{2L} and D_3 receptors expressed in HEK-293 cells to evaluate the receptor binding properties of the synthesized compounds. The newly synthesized compounds were first studied in pairs with their corresponding propyl containing parent compounds that had been developed and analyzed previously.

In general, a noticeable decrease in D_2 binding affinity due to the replacement of the propyl group with the propargyl group was observed. The D_2 binding affinity of compounds **76** (**D-614**) and **84** (**D-675**) decreased moderately compared to their propyl parent molecules, **D-512** and **D-238** (*K*i, D_2= 86.5 vs. 39 nM; 89.4 vs. 14.6 nM, **Table 3**). Moreover, compounds **62a** (**D-674**) and **73** (**D-635**) have exhibited great reduction in D_2 binding affinity when compared to their propyl counterparts **D-258** and **D-616**, respectively (*K*i, D_2= 661 vs. 243 nM; 172 vs. 16.4 nM, **Table 3**). This trend reached an extreme in the case of compound

63 (**D-649**), which exerted no binding affinity for D_2 receptor while the propyl containing molecule (−)-**20** (**D-618**) exhibited a good binding affinity (*K*i, D_2= 123 nM, **Table 3**). However, there was only a slight to no effect of the propargyl replacement in D_2 binding affinity for compound **62b** (**D-629**) in comparison to **D-260** (*K*i, D_2= 75 vs. 56.8 nM, **Table 3**). And in the case of compound **62c (D-676)**, an exception was found, which showed an increase in D_2 binding when compared to its corresponding propyl analog **D-259** (*K*i, D_2= 160 vs. 288 nM, **Table 3**).

A similar trend caused by the propargyl replacement has also been noticed in the change of D_3 binding affinity. As shown in **Table 3**, the D_3 binding affinity of compounds **62a** (**D-674**), **62b** (**D-629**), **62c** (**D-676**), **64** (**D-649**), **76** (**D-614**), and **84** (**D-675**) was reduced moderately to largely when compared to their propyl parent compounds **D-258**, **D-260**, **D-259**, (−)-**20** (**D-618**), **D-512**, and **D-238**, respectively (*K*i, D_3= 171 vs. 4.15 nM; 11.8 vs. 1.8 nM; 81.6 vs. 7.01 nM; 141 vs. 22.3 nM; 14.4 vs. 2.19 nM; 32.3 vs. 0.45 nM, **Table 3**). Nevertheless, compound **73** (**D-635**) has displayed a near 8-fold enhancement in D_3 binding affinity in comparison to its propyl counterpart **D-616** (*K*i, D_3= 0.145 vs. 1.15 nM, **Table 3**).

These trends suggest a generally reduced binding interaction between the propargyl group and the “propyl cleft” in the D_2 and D_3 receptors, which could be a result of either an increased rigidity or a slight change of conformation in the headgroup fragment induced by the propargyl replacement. In addition, the

abolishment of the D_2 receptor binding of compound **63** (**D-649**), which possesses a linear linker and a styrene moiety in the accessory binding site, could result from the induced conformational change of this compound that is not tolerated by receptor binding pocket.

Furthermore, it is interesting to notice in **Table 3** that in general these newly synthesized propargyl compounds **62a** (**D-674**), **62b** (**D-629**), **62c** (**D-676**), **76** (**D-614**), and **84** (**D-675**) are much less selective (D_2/D_3 ratio ranging from 2 to 6) for the dopamine D_2/D_3 receptors in contrast to their propyl parent molecules **D-258**, **D-260**, **D-259, D-512**, and **D-238** (D_2/D_3 ratio ranging from 18 to 59). However, the exceptions took place in the case of compounds **73** (**D-635**) and **63** (**D-649**) when compared to their propyl analogs **D-616** and (−)-**20** (**D-618**), which is due to either the uneven change between D_2/D_3 receptors binding or the complete loss of D_2 binding affinity, respectively (D_2/D_3, 1186 vs. 14; N/A vs. 6, **Table 3**). This suggests an important role of the interaction to propyl cleft in tuning the dopamine D_2/D_3 receptors selectivity.

To gain more insight into the role of the propargyl group in receptor binding, a 4-pentynyl analog **62e** (**D-664**), which has a more extended substituent in the headgroup fragment, was synthesized and tested. Comparing to the original propargyl compound **62b** (**D-629**), this analog exhibited a slight decrease in D_2 binding and a moderate decrease in D_3 binding (Ki, D_2 = 91.3 vs. 75.0 nM, D_3 = 24.2 vs. 11.8 nM, **Table 3**). The D_2/D_3 selectivity also showed a slight reduction accordingly (D_2/D_3, 3.8 vs. 6.3, **Table 3**). This suggests that the

size of *N*-substituents in the headgroup may have a limited effect on the binding to the propyl cleft of dopamine D_2/D_3 receptors.

Moreover, additional information on the effect of accessory binding site moieties can be gained from analyzing the D_2/D_3 receptors binding profile of the synthesized compounds. By introducing 2,3-dichloro or 2-methoxy group to the phenyl ring in the accessory binding site moiety, compounds **62b** (**D-629**) and **62c** (**D-676**) showed a great increase in the binding affinity for both D_2 and D_3 receptors when compared to the non-substituted compound **62a** (**D-674**) (*K*i, D_2 = 75.0 or 160 vs. 661 nM, D_3 = 11.8 or 81.6 vs. 171 nM, **Table 3**). However, the 4-fluoro substitution in compound **62d** (**D-680**) led to a reduction in the binding affinity for D_2 receptor and an improvement for D_3 receptor (*K*i, D_2 = 1,014 nM, D_3 = 93.9 nM, **Table 3**). In the case of **73** (**D-635**) and **76** (**D-614**), which only differ at the indole substituents, a great difference in both D_2/D_3 receptors binding especially the D_2/D_3 selectivity was found (*K*i, D_2 = 172 vs. 86.5 nM, D_3 = 0.145 vs. 14.4 nM, D_2/D_3, 1186 vs. 6, **Table 3**). This indicates that a proper modification at the accessory binding site may largely improve the binding property.

Table 3. K_i values (nM) for inhibition of [^{3}H] spiroperidol binding (HEK - $D_{2,3}$ cells)[a] (cLogP and tPSA values are calculated using ChemDraw)

Compound	K_i (nM), [^{3}H]spiperone		D_{2L}/D_3	cLogP	tPSA
	D_{2L}	D_3			
dopamine[b]	990 ± 198	101 ± 14.9	10		
(−)-**5-OH-DPAT**	153 ± 32	2.07 ± 0.38	74		

62a, D-674	661 ± 51	171 ± 8	4	3.58	48.1
62b, D-629	75 ± 10.3	11.8 ± 2.0	6	5.12	48.1
62c, D-676	160 ± 22	81.6 ± 5.8	2	3.52	57.33
62d, D-680	1,014 ± 92	93.9 ± 14.2	11	3.90	48.1
62e, D-664	91.3 ± 6.4	24.6 ± 2.6	4	6.05	48.1
63, D-649	no binding	141 ± 32	N/A	3.92	71.08
73, D-635	172 ± 16	0.145 ± 0.035	1186	4.51	60.13
76, D-614	86.5 ± 15	14.4 ± 1.0	6	4.51	60.13
84, D-675	89.4 ± 14.7	32.3 ± 2.0	3	6.36	29.95
D-258[b]	243 ± 65	4.15 ± 0.76	59	4.22	48.1
D-260[b]	56.8 ± 15.4	1.80 ± 0.32	32	5.76	48.1
D-259[b]	288 ± 86	7.01 ± 1.16	41	4.24	57.33
(−)-**20,** D-618	123 ± 18	22.3 ± 2.2	6	4.56	71.08
D-616[b]	16.4 ± 2.8	1.15 ± 0.19	14	5.14	60.13
D-512[b]	39 ± 5	2.19 ± 0.39	18	5.14	60.13
D-238[b]	14.6 ± 1.7	0.45 ± 0.16	32	7.00	29.95

[a] Results are expressed as means ± SEM for three to four experiments, each performed in triplicate.
[b] Data was obtained under almost identical assay conditions (Zhen et al. 2015, Biswas, Hazeldine, et al. 2008, Biswas, Zhang, et al. 2008, Das et al. 2015, Johnson et al. 2012).

Based on the binding results, compounds were selected and further assessed for their ability to activate human dopamine hD2 and hD3 receptors expressed in CHO cells by measuring the stimulation of [^{35}S]GTPγS binding. Dopamine (DA), the endogenous full agonist, was included for comparison. It is easy to notice that the propargyl replacement in compounds (−)-**62b** (**D-629**), (−)-**73** (**D-635**), and (−)-**76** (**D-614**) resulted in a moderate to large decrease in the potency at the D_2 receptor in comparison to their propyl counterparts **D-260**, **D-**

616, and **D-512** (EC_{50} (GTPγS); D_2 = 62.8 vs. 13.4 nM; 39.4 vs. 3.23 nM; 21.6 vs. 2.96 nM, **Table 4**). As for the efficacy, the propargyl replacement rendered both **62b** (**D-629**) and **76** (**D-614**) into partial agonists category for the D_2 receptor (E_{max}=17.4% and 26.7%, **Table 4**). However, compound **73** (**D-635**) still retained nearly full agonistic activity at D_2 receptor (E_{max}=86.8%, **Table 4**). On the other hand, while the propargyl replacement caused a noticeable reduction of potency to the D_3 receptor for compounds **62b** (**D-629**) and **76** (**D-614**) comparing to the propyl parent molecules **D-260** and **D-512** (EC_{50} (GTPγS); D_3 = 1.40 vs. 0.06 nM; 10.9 vs.1.26 nM, **Table 4**), compound **73** (**D-635**) exhibited a slight improvement in the potency at the D_3 receptor when compared to **D-616** (EC_{50} (GTPγS); D_3 = 0.84 vs.1.41 nM, **Table 4**). It is interesting to find that all these propargyl compounds **62b** (**D-629**), **74** (**D-635**), and **76** (**D-614**) remained full agonists at the D_3 receptor (E_{max}=106%; 93.0%; 94%, **Table 4**). These findings indicate that the propargyl replacement in the head group moiety may not be well-tolerated for the D_2 receptor activity; however, its effect on D_3 receptor activity is much less.

In addition, the pentynyl analog **62e** (**D-664**) was tested and compared with its propargyl version **62b** (**D-629**) to understand the effect of propargyl group. Unlike what was found in the binding assay, the extended pentynyl chain totally lost the agonistic activity at both D_2 and D_3 receptors. This could result from the steric interference of the head group interact with the D_2 and D_3 receptors, and it also suggests a great significance of the interaction between the head group to the propyl cleft.

Table 4. Stimulation of [^{35}S]GTPγS Binding to hD_2 and hD_3 receptors expressed in CHO cells[a]

Compound	CHO-D_2		CHO-D_3		D_2/D_3
	[^{35}S]GTPγS EC_{50} (nM)	%Emax	[^{35}S]GTPγS EC_{50} (nM)	%Emax	
dopamine	376 ± 39	100	7.26 ± 0.21	100	51.8
62b, D-629	62.8 ± 15.0	17.4 ± 2.3	1.40 ± 0.50	106 ± 4	44.8
62e, D-664	no stimulation		no stimulation		N/A
74, D-635	39.4 ± 6.31	86.8 ± 3.8	0.84 ± 0.05	93.9 ± 3.6	46.9
77, D-614	21.6 ± 9.6	26.7 ± 6.4	10.9 ± 2.4	94 ± 3.5	2.0
D-260[b]	13.4 ± 2.4	78.8 ± 0.8	0.06 ± 0.02	95.7 ± 10.7	223.3
D-616[c]	3.23 ± 0.78	101 ± 4	1.41 ± 0.08	113 ± 7	2.3
D-512[c]	2.96 ± 0.3	107 ± 3	1.26 ± 0.2	93.1 ± 4.4	2.4

[a] Results are expressed as means ± SEM for three to five experiments, each performed in triplicate.
[b] Data was obtained under similar assay conditions (Biswas, Hazeldine, et al. 2008).
[c] Data was obtained under almost identical assay conditions (Das et al. 2015, Johnson et al. 2012).

3.3.3. MAO inhibition assay with multifunctional MAO-B inhibitors

To further evaluate the effect of structural changes on the inhibition of MAO-B activity by selected compounds, a fluorescence-based enzymatic assay was carried out. Test compounds (25 μM) were incubated with the MAO-B enzyme (15 μg/mL) along with its substrate, kynuramine (25 μM), and the fluorescence of the product, 4-hydroxyquinoline (4-HQ), was measured. Pargyline, a potent and selective MAO-B inhibitor, was included as the reference compound, and it induced a 98.6% reduction of the MAO-B activity in the assay

conditions (**Figure 29**). Among all the test molecules, compounds **62b** (**D-629**), **63** (**D-649**), and **76** (**D-614**) were the most active and reduced the MAO-B activity by 53.5, 49.1%, and 43.1%, respectively (**Figure 29**). However, the inhibitory activity (100% - Activity%) was much less for the rest of test compounds. Comparisons could be drawn from compounds **62a** (**D-674**), **62b** (**D-629**), **62c** (**D-676**), and **62d** (**D-680**) to briefly assess the effect of substituents on the phenyl ring in the accessory binding site moiety on MAO-B inhibition. It seems while the non-substituted compound **62a** (**D-674**) and its electron donating 2-methoxy substituted counterpart **62c** (**D-676**) shared similar inhibitory activity, the electron withdrawing 2,3-dichloro substitution in compound **62b** (**D-629**) largely increased its MAO-B inhibitory effect (MAO-B inhibition% = 12.6%, 14.1% vs. 53.5%, **Figure 29**). Similarly, the electron withdrawing 4-fluoro substitution in compound **62d** (**D-680**) resulted in a moderate improvement in MAO-B inhibition when compared to the non-substituted parent molecule **62a** (**D-674**) (MAO-B inhibition% = 29.5% vs. 12.6%, **Figure 29**). These findings suggest that electron withdrawing substitutions in the phenyl ring may potentially enhance the MAO-B enzyme inhibitory activity; however, the position of the substitutions may also play a role in altering this effect.

In addition to the accessory binding site, alterations at the head group have also been briefly explored. Compound **84** (**D-675**), the racemic 5-OH-DPAT analog of compound **62b** (**D-629**), showed a reduced inhibitory activity (MAO-B inhibition% = 17% vs. 55%, **Figure 29**). Furthermore, the extension of the *N*-

substituent in the headgroup fragment rendered the *N*-pentynyl analog **62e** (**D-664**) much less effective in comparison to its parent compound **62b** (**D-629**) (MAO-B inhibition% = 26.9% vs. 53.5%, **Figure 29**). This reduced inhibition could be a result from a change of electron distribution or an increase in the steric hindrance.

Interestingly, although compound **63** (**D-649**) has an undesirable receptor binding profile, it showed a comparable enzyme inhibition to **62b** (**D-629**) (MAO-B inhibition% = 53.5% vs. 49.1%, **Figure 29**). In contrast, compound **73** (**D-635**) displayed promising D_2/D_3 receptor activities in the receptor assays, but its inhibitory effect is less potent (MAO-B inhibition% = 17.4%, **Figure 29**). This data suggests that there is no direct correlation between the D_2/D_3 receptor activities and enzyme inhibitory activity. This also indicates that the structural preference and conformational requirement for dopamine D_2/D_3 receptors binding and MAO-B enzyme interaction may have a relatively low compatibility in the current molecular template that requires further modifications.

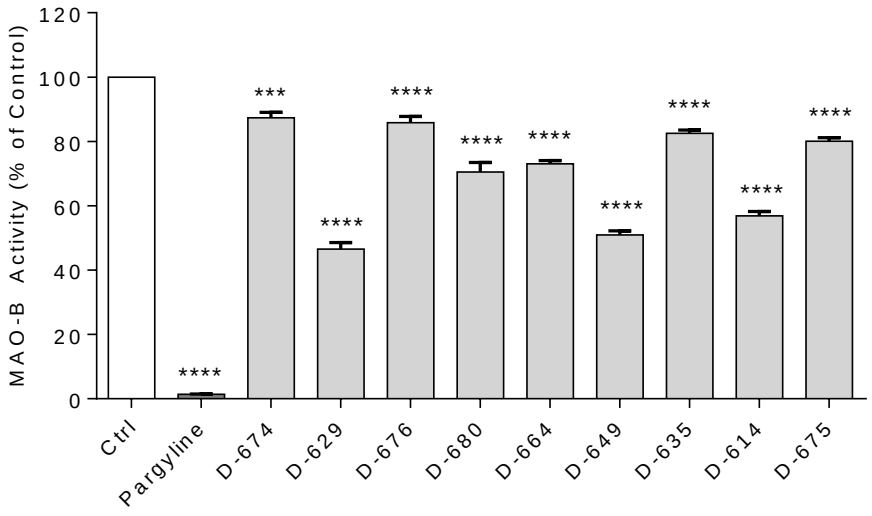

Figure 29. Initial screening of the synthesized compounds through MAO-B inhibition assay. All the compounds were tested at 25 µM. The results shown are means ± SEM from three independent experiments performed in triplicates. One-way ANOVA followed by Tukey's analysis was performed (*** $p \leq 0.001$, **** $p \leq 0.0001$ compared to the control).

Based on the data obtained from MAO-B inhibition assay, compounds **62b** (**D-629**) and **76** (**D-614**) were selected to be tested further. To gain additional information on the selectivity of compounds towards two isoforms of MAO, IC_{50} values for both MAO-A and MAO-B were determined by constructing dose-response curve with seven dose points. As displayed in **Table 5**, while compound **62b** (**D-629**) has only a slight selectivity for MAO-B (SI = 2.2), compound **76** (**D-614**) is non-selective towards both MAO isoforms (SI = 1.2). These results suggest further expanded SAR study with more structural modifications is required to gain a better MAO-B inhibitory profile.

Table 5. The IC_{50} values for the inhibition of recombinant human MAO-A and MAO-B by compounds[a]

Compound	MAO-B	MAO-A	SI[b]
	IC_{50} (μM)	IC_{50} (μM)	
Pargyline	0.28 ± 0.02	10.54 ± 0.79	37.6
62b (**D-629**)	31.67 ± 1.61	71.04 ± 10.30	2.2
76 (**D-614**)	32.34 ± 2.41	39.71 ± 3.95	1.2

[a] Results are expressed as means ± SEM for three experiments, each performed in triplicate.
[b] Selectivity index = IC_{50} (MAO-A)/IC_{50} (MAO-B)

3.3.4. Neuroprotection against neurotoxin-induced toxicity in PC12 cell line with multifunctional MAO-B inhibitors

Based on the results obtained from the *in vitro* receptor assays and enzymatic assay, compounds **76** (**D-614**) and **62b** (**D-629**) were selected for further testing.

These two compounds were first tested for cytotoxicity. As shown in **Figure 30 a)** and **b)**, both compounds displayed a non-toxic profile when treated alone to the PC12 cells and induced cell proliferation at higher doses tested: compound **76** (**D-614**) slightly increased cell viability at 20 and 30 μM, and compound **62b** (**D-629**) largely increased cell viability at 50 μM.

Then, they were examined for their ability to reverse the toxicity induced by 6-OHDA in PC12 cells. After the PC12 cells were pretreated with increasing doses (1-50 μM) of compound **76** (**D-614**) or **62b** (**D-629**) for 24 h, a single treatment of 75 μM 6-OHDA was given for another 24 h. Cell viability was

assessed by MTT assay. Despite that these two compounds demonstrated comparable results in both *in vitro* receptor assays and MAO inhibition assays, they behaved differently in reversing the 6-OHDA induced cytotoxicity. As shown in **Figure 30**, in contrast to compound **62b** (**D-629**) (**d**), which showed no effect on the 6-OHDA-induced toxicity, compound **76** (**D-614**) (**c**) exerted a dose-dependent neuroprotective effect with the greatest protection (17%) seen at 20 μM dose point. As these two compounds differ only at the accessory binding site moiety, it seems safe to assume that the indole ring could have a critical role in conferring neuroprotective effect.

Following this, compound **76** (**D-614**) was also tested in another neurotoxin induced cytotoxicity model in PC12 cells (**Figure 31**). When the PC12 cells were pre-treated 1 h with **76** (**D-614**) and co-treated with rotenone (1 μM) for additional 24 h, unlike its propyl counterpart **D-512** (unpublished work in lab), this compound failed to exhibit any protective effect. This could result from the increased reactivity of the molecule due to the propargyl replacement in combination with the difference resided in the mechanisms of cytotoxicity between neurotoxins 6-OHDA and rotenone.

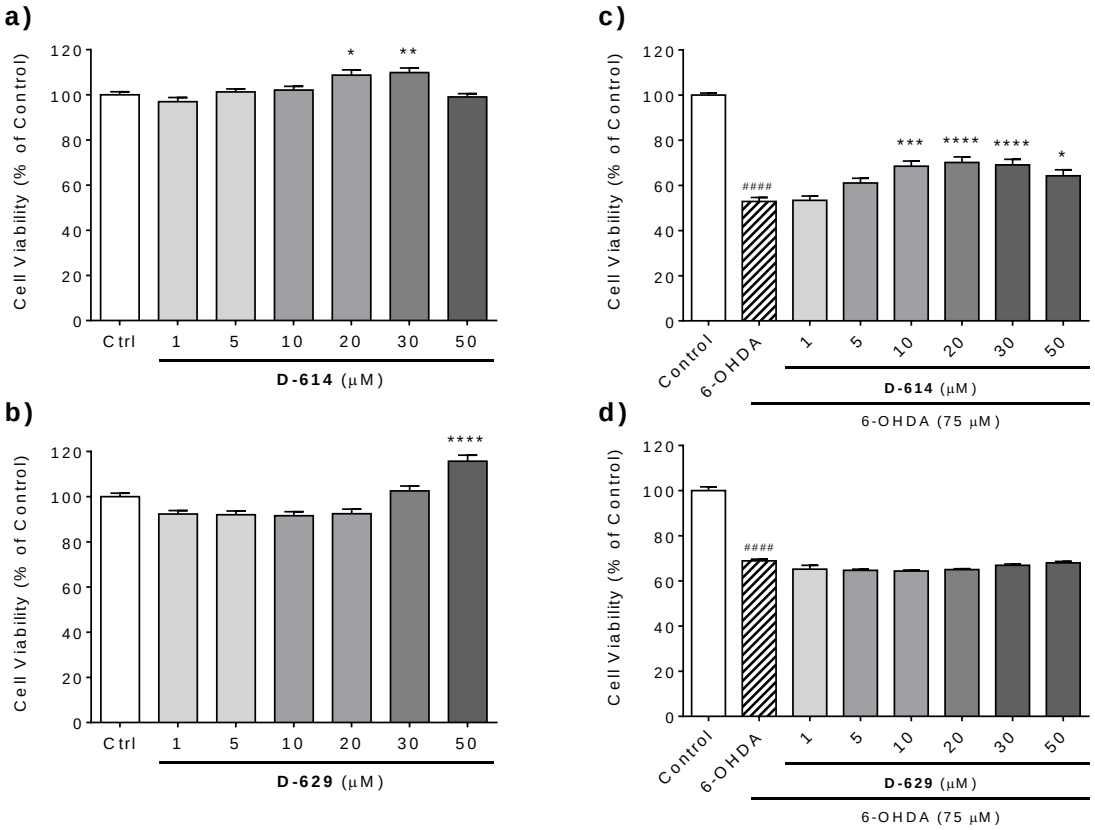

Figure 30. a-b) Dose-dependent effect of compounds **76** (**D-614**) (**a**) and **62b** (**D-629**) (**b**) at various concentrations on the viability of PC12 cells by 24 h treatment. The results shown are means ± SEM of three independent experiments performed in six to eight replicates. One-way ANOVA followed by Tukey's multiple comparison post hoc test was performed (* $p \leq 0.05$, ** $p \leq 0.01$, **** $p \leq 0.0001$ compared to the control). **c-d)** Dose-dependent effect on the viability of PC12 cells by 24 h pretreatment of compounds **76** (**D-614**) (**c**) and **62b** (**D-629**) (**d**) at various concentrations (1-50 µM) followed by the single treatment of 75 µM 6-OHDA. The results shown are means ± SEM of three independent experiments performed in six to eight replicates. One-way ANOVA followed by Tukey's multiple comparison post hoc test was performed (#### $p \leq 0.0001$ compared to the control; * $p \leq 0.05$, *** $p \leq 0.001$, **** $p \leq 0.0001$ compared to the 6-OHDA control).

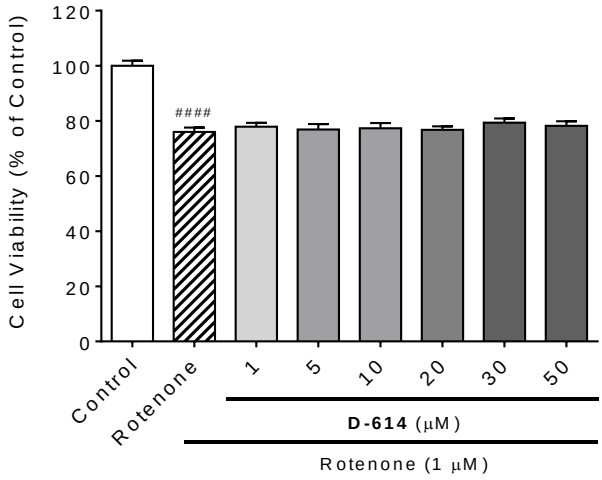

Figure 31. Dose-dependent effect on the viability of PC12 cells by 1 h pretreatment of compound **76** (**D-614**) at various concentrations (1-50 μM) followed by the co-treatment of 1 μM rotenone for 24 h. The results shown are means ± SEM of three independent experiments performed in six to eight replicates. One-way ANOVA followed by Tukey's multiple comparison post hoc test was performed (#### $p \leq 0.0001$ compared to the control).

3.3.5. Reversal of reserpine-induced hypolocomotion in rats with multifunctional MAO-B inhibitors

As mentioned previously, the administration of reserpine, a vesicular monoamine transporter (VMAT) blocker, can generate a hypolocomotion model in rat by inducing the exposure and depletion of monoamines in the synapse of the peripheral sympathetic nerve terminals (Fernandes et al. 2012, Duty and Jenner 2011, Leao et al. 2015). Compound **76** (**D-614**) was selected to assess its ability to reverse the reserpine-induced hypolocomotion, which was established 18 h after administrating reserpine (5 mg/kg, s.c.). At the dose of 10 μmol/kg i.p., compound **76** (**D-614**) has effectively reversed akinesia induced by reserpine

treatment, which is comparable to the reference drug ropinirole and has more continuous effect throughout the assay (**Figure 32**). The observed moderate locomotor stimulation of **76** (**D-614**) is likely to be mediated by the postsynaptic D_2/D_3 receptor activation, which suggests a decent blood-brain barrier penetration profile.

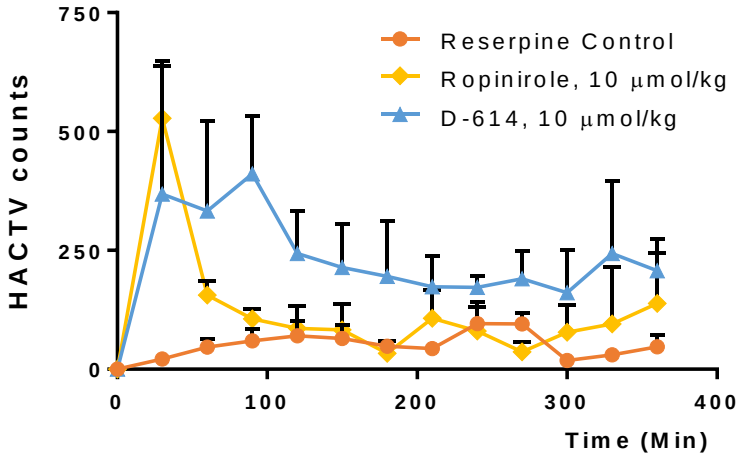

Figure 32. Effect of compound **76** (**D-614**) and ropinirole on reserpine-induced (5.0 mg/kg, s.c.) hypolocomotion in rats. Results are expressed as means ± SEM; n=3 rats per value. Horizontal activity (HACTV), which is the total number of beam interruptions that occurred in the horizontal sensor during a given sample period, was measured as described in Chapter 4. Locomotor data during each 30-min interval after the administration of compound **76** (**D-614**) (i.p.) or ropinirole (i.p.) at the dose of 10 µmol/kg compared to control reserpine treated rats in 18 h post reserpine treatment was plotted. Differences among treatments were significant by one-way ANOVA analysis ($F(2, 36) = 10.57$; $p = 0.0002$). Dunnett's analysis following ANOVA revealed that the effect of compound **76** (**D-614**) ($p < 0.001$) was significantly different when compared to reserpine control (Das et al. 2015).

CHAPTER 4 MATERIALS AND METHODS

4.1. Chemistry

All reagents and solvents were purchased from commercial suppliers and used as received unless otherwise stated. Dry solvents were obtained according to the standard procedure. All reactions were performed under inert atmosphere (N_2) unless otherwise indicated. Analytical silica gel 60 F_{254}-coated TLC plates were obtained from EMD Chemicals, Inc. and were visualized with UV light or by treatment with phosphomolybdic acid (PMA), Dragendorff's reagent, or ninhydrin. Flash column chromatographic purifications were performed using Whatman Purasil 60A silica gel 230−400 mesh. ^{1}H NMR spectra were acquired on a Varian 400 and 600 MHz FT NMR spectrometer using tetramethylsilane (TMS) as the internal standard. The NMR solvent used was $CDCl_3$ or CD_3OD as indicated. Optical rotations were recorded on PerkinElmer 241 polarimeter. Melting points were recorded using a MEL-TEMP II (Laboratory Devices Inc., Placerville, CA) capillary melting point apparatus and were uncorrected. Elemental analyses were performed by Atlantic Microlab, Inc.

Procedure A: (4-Ethoxy-4-oxobutyl)triphenylphosphonium bromide (2)

Triphenylphosphine (3.76 g, 14.34 mmol) and ethyl 4-bromobutyrate (2.0 g, 10.25 mmol) were added to a dried round bottom flask under argon. The reaction mixture was heated to 120 °C under condenser for 16 h, after which the reaction was allowed to come to room temperature. CH_2Cl_2 (10 mL) was added, followed by diethyl ether until no further precipitation of product was observed.

The precipitate was further washed with ether (100 mL) and dried *in vacuo* to give pure compound **2** as a white solid (4.64 g) in quantitative yield. ^{1}H NMR (400 MHz, $CDCl_3$): δ ppm 7.67-7.90 (m, 15 H), 3.98-4.12 (m, 4H), 2.86-2.89 (m, 2H), 1.88-1.94 (m, 2H), 1.22 (t, *J* = 7.2 Hz, 3H).

Procedure B: Ethyl 5-(4-hydroxy-3-methoxyphenyl)pent-4-enoate (4a)

Starting material **2** (6.61 g, 14.45 mmol) was added to dry THF (15 mL) in an oven-dried round bottom flask. The resulting suspension was cooled to −78 °C. Then a solution of NaHMDS (1M in THF, 15.77 mL, 15.77 mmol) was added dropwise, and the reaction mixture was stirred at −78 °C for 1 h. Thereafter, a solution of vanillin **3a** (2.0 g, 13.14 mmol) in dry THF (5 mL) was added dropwise, and reaction stirred at −78 °C for 2 h. Then it was warmed to room temperature and stirred for 48 h. The reaction mixture was then extracted with ethyl acetate (2 ×100 mL) and washed with brine. The combined organic layer was dried over Na_2SO_4 and concentrated *in vacuo*. The crude thus obtained was purified by column chromatography using 10% ethyl acetate in hexanes to yield compound **4a** (1.17 g, 36%) as colorless oil with a preferential *Z*:*E* ratio of > 20:1. ^{1}H NMR (400 MHz, $CDCl_3$): δ ppm 6.88 (d, *J* = 8.2 Hz, 1H), 6.79-6.82 (m, 2H), 6.37 (d, *J* = 11.2 Hz, 1H), 5.64 (s, 1H), 5.49-5.55 (m, 1H), 4.13 (q, *J* = 7.2 Hz, 2H), 3.88 (s, 3H), 2.63-2.69 (m, 2H), 2.45 (t, *J* = 8.0 Hz, 2H), 1.24 (t, *J* = 7.2 Hz, 3H).

Ethyl 5-(2,5-dimethoxyphenyl)pent-4-enoate (4b)

Starting material **2** (7.56 g, 16.53 mmol) was reacted with 2,5-dimethoxy benzaldehyde **3b** (2.5 g, 15.04 mmol) in the presence of NaHMDS 1M in THF (18.05 mmol, 18.05 mL) according to procedure B. The crude was purified by column chromatography using 7-10% ethyl acetate in hexanes to give compound **4b** (1.71 g, 43%). ^{1}H NMR (400 MHz, $CDCl_3$): δ ppm 6.82 (d, J = 2.4 Hz, 1H), 6.74-6.79 (m, 2H), 6.52 (d, J = 11.2 Hz, 1H), 5.65-5.72 (m, 1H), 4.12 (q, J = 7.2 Hz, 2H), 3.78 (s, 3H), 3.77 (s, 3H), 2.55-2.60 (m, 2H), 2.41 (t, J = 7.2 Hz, 2H), 1.23 (t, J = 7.2 Hz, 3H).

Procedure C: Ethyl 5-(4-hydroxy-3-methoxyphenyl)pentanoate (5a)

Intermediate **4a** (1.0 g, 4.00 mmol) was dissolved in ethanol (10 mL) in a round bottom flask, and 10% Pd/C (0.10 g, 10 wt%) was added to it. The reaction flask was degassed, and then the reaction mixture was stirred under hydrogen atmosphere for 2 h at room temperature. After the completion of reaction, the mixture was diluted with ethanol (20 mL) and passed through a short bed of celite. The organic layer was concentrated to afford compound **5a** (0.98 g) in quantitative yield, which was pure enough for the next step. ^{1}H NMR (400 MHz, $CDCl_3$): δ ppm 6.82 (d, J = 8.0 Hz, 1H), 6.65-6.67 (m, 2H), 4.12 (q, J = 7.2 Hz, 2H), 2.55 (t, J = 7.2 Hz, 2H), 3.87 (s, 3H), 2.31 (t, J = 7.2 Hz, 2H), 1.58-1.70 (m,4H), 1.24 (t, J = 7.2 Hz, 3H).

Ethyl 5-(2,5-dimethoxyphenyl)pentanoate (5b)

Intermediate **4b** (1.0 g, 3.78 mmol) was dissolved in ethanol (10 mL) and reacted with 10% Pd/C (0.1 g, 10 wt%) according to procedure C to afford

compound **5b** (0.96 g, 95%), which was used without further purification. ^{1}H NMR (400 MHz, $CDCl_3$): δ ppm 6.75 (d, J = 8.8 Hz, 1H), 6.72 (d, J = 3.2 Hz, 1H), 6.68 (dd, J = 8.4, 2.4 Hz, 1H), 4.12 (q, J = 7.2 Hz, 2H), 3.76 (s, 3H), 3.75 (s, 3H), 2.60 (t, J = 7.4 Hz, 2H), 2.33 (t, J = 7.2 Hz, 2H), 1.56-1.70 (m, 4H), 1.24 (t, J = 7.2 Hz, 3H).

Procedure D: 5-(4-Hydroxy-3-methoxyphenyl)pentanal (6a)

To a solution of compound **5a** (0.66 g, 2.62 mmol) in dry toluene (10 mL) under argon was added DIBALH solution (1M in hexane, 2.87 mL, 2.87 mmol) at −78 °C. The reaction mixture was stirred at −78 °C for 2 h. MeOH (0.20 mL) was added to the reaction mixture, and the reaction mixture was allowed to come to 0 °C. It was then added to a separating funnel containing HCl (1N, 10 mL) and extracted with ethyl acetate (3 × 30 mL). The combined organic layer was washed with brine, dried over Na_2SO_4, and evaporated under reduced pressure. The crude was purified by column chromatography using 11-15% ethyl acetate in hexanes to yield compound **6a** (0.23 g, 42%) as colorless oil.^{1}H NMR (400 MHz, $CDCl_3$): δ ppm 9.75 (t, J = 1.6 Hz, 1H), 6.82 (d, J = 8.0 Hz, 1H), 6.65 (m, 2H), 3.87 (s, 3H), 2.56 (t, J = 7.2 Hz, 2H), 2.44 (td, J_1 = 6.40 Hz, J_2 = 1.60 Hz 2H), 1.59-1.68 (m, 4H).

5-(2,5-Dimethoxyphenyl)pentanal (6b)

Intermediate **5b** (0.6 g, 2.25 mmol) was reduced with DIBALH solution (1M in hexane, 2.47 mL, 2.47 mmol) in dry toluene (10 mL) using procedure D. The crude was purified by column chromatography using 11-15% ethyl acetate in

hexanes to give compound **6b** (0.4 g, 80 %) as yellow oil. ^{1}H NMR (400 MHz, $CDCl_3$): δ ppm 9.74 (d, *J* = 1.6 Hz, 1H), 6.76 (d, *J* = 8.8 Hz, 1H), 6.67-6.71 (m, 2H), 3.76 (s, 3H), 3.75 (s, 3H), 2.60 (t, *J* = 6.4 Hz, 2H), 2.44 (t, *J* = 6.8 Hz, 2H), 1.58-1.37(m, 4H).

Procedure E: 4-(5-((2-Amino-4,5,6,7-tetrahydrobenzo[*d*]thiazol-6-yl)(propyl)amino)pentyl)-2-methoxyphenol ((±)-7a) (D-548).

Into a stirring solution of (±)-pramipexole (0.15 g, 0.71mmol) in CH_2Cl_2 (8 mL) was added aldehyde **6a** (0.148 g, 0.71 mmol), and the mixture stirred for 1 h. $NaBH(OAc)_3$ (0.27 g, 1.27 mmol) was then added portion-wise followed by MeOH (0.8 mL). The reaction was stirred for 36 h at room temperature. The reaction mixture was quenched with a sat. $NaHCO_3$ solution at 0 °C and extracted with CH_2Cl_2 (3 × 25 mL). The combined organic layer was dried over Na_2SO_4, and solvent was removed under reduced pressure. The crude product was purified by column chromatography using 5-7% MeOH in CH_2Cl_2 to give compound (±)-**7a** (0.2 g, 70%).^{1}H NMR (400 MHz, DMSO-d_6): δ ppm 6.64-6.72 (m, 2H), 6.58 (d, *J* = 8.4 Hz, 1H), 3.82 (s, 3H), 3.05 (bs, 1H), 2.50-2.67 (m, 10H), 1.59-1.70 (m, 3H), 1.48-1.53 (m, 4H), 1.28-1.36 (m, 3H), 0.89 (t, *J* = 7.2 Hz, 3H). The free base was converted into its corresponding hydrochloride salt. Mp 224-226 °C. Anal. ($C_{26}H_{43}Cl_2N_3O_4S$) C, H, N.

(*S*)-4-(5-((2-Amino-4,5,6,7-tetrahydrobenzo[*d*]thiazol-6-yl)(propyl)amino)pentyl)-2-methoxyphenol ((−)-7a) (D-591)

Aldehyde **6a** (0.148 g, 0.71 mmol), (−)-pramipexole (0.15 g, 0.71mmol), and $NaBH(OAc)_3$ (0.27 g, 1.27 mmol) in CH_2Cl_2 (8 mL) and MeOH (0.8 mL) were reacted using procedure E, and the resulting crude was purified by column chromatography using 5-7% MeOH in CH_2Cl_2 to give compound (−)-**7a** (0.19 g, 66%). ^{1}H NMR (600 MHz, CD_3OD): δ ppm 6.64-6.72 (m, 2H), 6.58 (d, J = 8.4 Hz, 1H), 3.82 (s, 3H), 3.05 (bs, 1H), 2.65-2.67 (m, 1H), 2.50-2.65 (m, 9H), 1.59-1.70 (m, 3H), 1.48-1.53 (m, 4H), 1.28-1.36 (m, 3H), 0.90 (t, J = 7.2 Hz, 3H). The free base was converted into its corresponding hydrochloride salt. $[\alpha]_D^{25}$ (salt) = −46.8 (c = 0.5 in CH_3OH). Mp 196-198 °C. Anal. ($C_{22}H_{37}Cl_2N_3O_3S$) C, H, N.

N^6-(5-(2,5-Dimethoxyphenyl)pentyl)-N^6-propyl-4,5,6,7-tetrahydrobenzo[*d*]thiazole-2,6-diamine ((±)-7b)

Aldehyde **6b** (0.157 g, 0.71 mmol), (±)-pramipexole (0.15 g, 0.71 mmol), and $NaBH(OAc)_3$ (0.27 g, 1.27 mmol) in CH_2Cl_2 (9 mL) and MeOH (0.8 mL) were reacted using procedure E, and the resulting crude was purified by column chromatography using 5-7% MeOH in CH_2Cl_2 to give compound (±)-**7b** (0.17 g, 58%). ^{1}H NMR (400 MHz, $CDCl_3$): δ ppm 6.75 (d, J = 8.8 Hz, 1H), 6.70 (d, J = 2.4 Hz, 1H), 6.66 (dd, J = 8.8, 2.1 Hz, 1H), 3.75 (s, 3H), 3.74 (s, 3H), 3.07 (bs, 1H), 2.69 (dd, J = 12.0, 4.04 Hz, 2H), 2.47-2.58 (m, 8H), 1.99-2.03(m, 1H), 1.68-1.78 (m, 1H), 1.40-1.61 (m, 6H), 1.31-1.37 (m, 2H), 0.89 (t, J = 7.2 Hz, 3H).

(*S*)-N^6-(5-(2,5-Dimethoxyphenyl)pentyl)-N^6-propyl-4,5,6,7-tetrahydrobenzo[*d*]thiazole-2,6-diamine ((−)-7b)

Aldehyde **6b** (0.105 g, 0. 47 mmol), (−)-pramipexole (0.10 g, 0.47 mmol), and $NaBH(OAc)_3$ (0.18 g, 0.85 mmol) in CH_2Cl_2 (7 mL) and MeOH (0.6 mL) were reacted using procedure E, and the resulting crude was purified by column chromatography using 5-7% MeOH in CH_2Cl_2 to give compound (−)-**7b** (0.105 g, 53%). ^{1}H NMR (600 MHz, $CDCl_3$): *δ* ppm 6.76 (d, *J* = 8.4 Hz, 1H), 6.71 (d, *J* = 1.8 Hz, 1H), 6.67 (dd, *J* = 8.4, 3.0 Hz, 1H), 4.71 (bs, 2H), 3.77 (s, 3H), 3.76 (s, 3H), 3.04 (bs, 1H), 2.69 (d, *J* = 7.2 Hz, 2H), 2.4-2.6 (m, 8H), 2.0 (bs, 1H), 1.62-1.72 (m, 2H), 1.55-1.61 (m, 2H), 1.41-1.52 (m, 3H), 1.33-1.37 (m, 2H), 0.88 (t, *J* = 7.2 Hz, 3H).

Procedure F: 4-(5-((2-Amino-4,5,6,7-tetrahydrobenzo[*d*]thiazol-6-yl)(propyl)amino)pentyl)benzene-1,2-diol ((±)-8a) (D-575)

BBr_3 1M in CH_2Cl_2 (2.66 mL, 2.66 mmol) was added to a solution of compound (±)-**7a** (0.2 g, 0.50 mmol) in CH_2Cl_2 (20 mL) at −78 °C and stirred for 2 h. The reaction mixture was allowed to come to room temperature and stirred for another 4 h. The reaction was then quenched by MeOH (20 mL) at 0 °C, and the solvent was concentrated *in vacuo*. MeOH (20 mL) was added to the residue and again evaporated. This process was repeated three times. The residue obtained was purified by column chromatography using 10-15% MeOH in CH_2Cl_2 to give pure compound (±)-**8a** (0.123 g, 64 %). ^{1}H NMR (400 MHz, CD_3OD): *δ* ppm 6.64 (d, *J* = 8.0 Hz, 1H), 6.60 (d, *J* = 2.4Hz, 1H), 6.47 (dd, *J* = 8.0, 2.4 Hz, 1H), 3.35-3.40 (m, 1H), 2.75-2.85 (m, 5H), 2.62-2.71 (m, 2H), 2.55-2.57 (m, 1H), 2.47 (t, *J* = 7.2 Hz, 2H), 2.09-2.14 (m, 1H), 1.79-1.89 (m, 1H), 1.57-1.64 (m, 6H), 1.31-1.38

(m, 2H), 0.95 (t, *J* = 7.6 Hz, 3H). The free base was converted into its corresponding hydrochloride salt. Mp 196-198 °C. Anal. ($C_{21}H_{34}Cl_3N_3O_2S$) C, H, N.

(*S*)-4-(5-((2-Amino-4,5,6,7-tetrahydrobenzo[*d*]thiazol-6-yl)(propyl)amino)pentyl)benzene-1,2-diol ((−)-8a) (D-593)

BBr_3 1M in CH_2Cl_2 (1.61mL, 1.61 mmol) was reacted with compound (−)-**7a** (0.132 g, 0.33 mmol) in CH_2Cl_2 (10 mL) according to procedure F to afford crude, which was purified by column chromatography using 10-15% MeOH in CH_2Cl_2 to give compound (−)-**8a** (90 mg, 71%). ^{1}H NMR (600 MHz, CD_3OD): *δ* ppm 6.63 (d, *J* = 7.8 Hz, 1H), 6.58 (d, *J* = 1.8 Hz, 1H), 6.45 (dd, *J* = 7.8, 1.8 Hz, 1H), 2.97-3.02 (m, 1H), 2.42-2.62 (m, 10H), 1.95-1.97 (m, 1H), 1.60-1.73 (m, 1H), 1.53-1.58 (quintet, *J* = 7.8Hz, 2H), 1.42-1.48 (septet, *J* = 7.2 Hz, 4H), 1.26-1.31 (quintet, *J* = 7.2 Hz, 2H), 0.88 (t, *J* = 7.2 Hz, 3H). $[\alpha]_D^{25}$ (free base) = − 51.8 (*c* = 1.0 in CH_3OH); the free base was converted into its corresponding hydrochloride salt. Mp 211-212 °C. Anal. ($C_{21}H_{35}Cl_2N_3O_3S$) C, H, N.

2-(5-((2-Amino-4,5,6,7-tetrahydrobenzo[*d*]thiazol-6-yl)(propyl)amino)pentyl)benzene-1,4-diol ((±)-8b) (D-584)

BBr_3 1M in CH_2Cl_2 (2.27 mL, 2.27 mmol) was reacted with compound (±)-**7b** (0.16 g, 0.38 mmol) according to procedure F to afford crude, which was purified by column chromatography using 10-15% MeOH in CH_2Cl_2 to afford compound (±)-**8b** (0.12 g, 80%). ^{1}H NMR (600 MHz, CD_3OD): *δ* ppm 6.55 (d, *J* = 8.4 Hz, 1H), 6.51 (d, *J* = 3.0 Hz, 1H), 6.41 (dd, *J* = 8.4, 3.0 Hz, 1H), 3.0 (m, 1H),

2.44-2.63 61 (m, 10H), 1.98 (d, *J* = 10.2 Hz, 1H), 1.65-1.68 (m, 1H), 1.56-1.61 (m, 2H), 1.44-1.52 (m, 4H), 1.32-1.36 (m, 2H), 0.88 (t, *J* = 7.2 Hz, 3H). The free base was converted into its corresponding hydrochloride salt. Mp 217-219 °C. Anal. ($C_{22}H_{38}Cl_3N_3O_3S$) C, H, N.

(*S*)-2-(5-((2-Amino-4,5,6,7-tetrahydrobenzo[*d*]thiazol-6-yl)(propyl)amino)pentyl)benzene-1,4-diol ((−)-8b) (D-601)

BBr_3 1M in CH_2Cl_2 (1.33 mL, 1.33 mmol) was reacted with compound (−)-**7b** (93 mg, 0.22 mmol) in CH_2Cl_2 (6 mL) according to procedure F to afford crude, which was purified by column chromatography using 10-15% MeOH in CH_2Cl_2 to give compound (−)-**8b** (62 mg, 71%). ^{1}H NMR (600 MHz, CD_3OD): *δ* ppm 6.56 (dd, *J* = 8.4, 1.8 Hz, 1H), 6.52 (d, *J* = 2.4 Hz, 1H), 6.43 (dt, *J* = 8.4, 1.80 Hz, 1H), 2.98-3.03 (m, 1H), 2.44-2.64 (m, 10H), 1.99-2.00 (m, 1H), 1.63-1.71 (m, 1H), 1.57-1.62 (m, 2H), 1.46-1.52 (m, 4H), 1.32-1.37 (m, 2H), 0.90 (t, *J* = 7.2 Hz, 3H). The free base was converted into its corresponding hydrochloride salt. $[\alpha]_D^{25}$ (salt) = −18.4 (*c* = 0.5 in CH_3OH); Mp 222-224 °C. Anal. ($C_{21}H_{34}Cl_3N_3O_2S$) C, H, N.

Procedure G: (*Z*)-Ethyl 5-(4-((tert-butyldimethylsilyl)oxy)-3-methoxyphenyl)pent-4-enoate (9)

The (*Z*)-isomer of **4a** was obtained by further purification of the mixture of (*E*)-, (*Z*)-isomers through column chromatography using 10% ethyl acetate in hexanes. Imidazole (0.35 g, 5.14 mmol) was added to a solution of intermediate **4a** (0.52 g, 2.08 mmol) and *tert*-butyldimethylsilyl chloride (0.37 g, 2.45 mmol) in DMF (5 mL). The solution was stirred at room temperature for 2 h. After the

completion of reaction, sat. $NaHCO_3$ (10 mL) was added and stirred for another 30 min. The reaction mixture was extracted with CH_2Cl_2 (2 x 50 mL). The combined organic layer was dried over Na_2SO_4 and concentrated *in vacuo*. The crude thus obtained was purified by column chromatography using 5% ethyl acetate in hexanes to afford compound **9** (0.75 g) in quantitative yield. ^{1}H NMR (400 MHz, CD_3OD): δ ppm 6.85 (s, 1H), 6.79 (d, *J* = 8.0 Hz, 1H), 6.73 (d, *J* = 8.4 Hz, 1H), 6.37 (d, *J* = 11.2 Hz, 1H), 5.47-5.55 (m, 1H), 4.10 (m, *J* = 7.2 Hz, 2H), 3.78 (s, 3H), 2.63 (q, *J* = 7.2 Hz, 2H), 2.44 (t, *J* = 7.2 Hz, 2H), 1.20 (t, *J* = 7.2 Hz, 3H), 0.99 (s, 9H), 0.13 (s, 6H).

Procedure H: (*Z*)-5-(4-((tert-Butyldimethylsilyl)oxy)-3-methoxyphenyl)pent-4-en-1-ol (10)

Into a stirring solution of compound **9** (0.71 g, 1.95 mmol) in anhydrous THF (15 mL) was added DIBALH solution 1 M in THF (9.73 mL, 9.73 mmol) dropwise at −10 °C. The reaction mixture was stirred at room temperature for 6 h and was quenched with MeOH (1 mL). The mixture was neutralized with 1N HCl (15 mL) solution. The organic layer was separated, and the aqueous layer was extracted with ethyl acetate (2 x 100 mL). The combined organic layer was dried over Na_2SO_4 and concentrated *in vacuo*. The crude product was purified by column chromatography using 11-15% ethyl acetate in hexanes to give compound **10** (0.55 g, 88%). ^{1}H NMR ($CDCl_3$, 400 MHz): δ ppm 6.74-6.85 (m, 3H), 6.37 (d, *J* = 11.2 Hz, 1H), 5.48-5.53 (m, 1H), 3.80 (s, 3H), 2.67 (q, *J* = 7.2

Hz, 2H), 2.43 (t, *J* = 7.2 Hz, 2H), 1.22 (t, *J* = 7.2 Hz, 2H), 1.06 (s, 9H), 0.15 (s, 6H).

Procedure I: (*Z*)-5-(4-((tert-Butyldimethylsilyl)oxy)-3-methoxyphenyl)pent-4-enal (11)

Alcohol **10** (0.9 g, 2.79 mmol) was slowly added to an ice cooled suspension of PCC (pyridinium chlorochromate) (0.80 g, 3.71 mmol) in CH_2Cl_2 (90 mL), and the mixture was stirred at rt for 9 h. The reaction mixture was then filtered over celite, and solvent was evaporated to get residue, which was purified by column chromatography using 10-15% of ethyl acetate in hexanes to give compound **11** (0.36 g, 40%). ^{1}H NMR ($CDCl_3$, 400 MHz): δ ppm 9.78 (s, 1H), 6.74-6.85 (m, 3H), 6.37 (d, *J* = 11.2 Hz, 1H), 5.49-5.52 (m, 1H), 3.80 (s, 3H), 2.56-2.68 (m, 4H), 0.99 (s, 9H), 0.16 (s, 6H).

Procedure J: (*Z*)-4-(5-((2-Amino-4,5,6,7-tetrahydrobenzo[*d*]thiazol-6-yl)(propyl)amino)pent-1-en-1-yl)-2-methoxyphenol ((±)-12) (D-567)

Compound **11** (0.315 g, 0.98 mmol) was dissolved in THF (10 mL) and cooled to 0 °C. TBAF (*n*-tetrabutylammonium fluoride) 1M in THF (1.02 mL, 1.02 mmol) was added, and reaction stirred in ice for 1.5 h. After reaction was complete, 10% $NaHCO_3$ solution (10 mL) was added, and reaction mixture was extracted with CH_2Cl_2 (3 x 50 mL) to obtain aldehyde, which was immediately taken to the next step without further purification. Aldehyde (0.195 g, 0.95 mmol), (±)-pramipexole (0.20 g, 0.95 mmol), and $NaBH(OAC)_3$ (0.36 g, 1.70 mmol) in CH_2Cl_2 (7 mL) and MeOH (1.0 mL) were reacted using procedure E, and the

resulting crude was purified by column chromatography using 5-7% MeOH in CH_2Cl_2 to give compound (±)-**12** (0.148 g, 39%). ^{1}H NMR (400 MHz, CD_3OD): *δ* ppm 6.86 (d, *J* = 8.0 Hz, 1H), 6.76-6.82 (m, 2H), 6.35 (d, *J* = 12.4 Hz, 1H), 5.49-5.56 (m, 1H), 4.98 (bs, 1H), 3.86 (s, 3H), 3.1 (bs, 1H), 2.50-2.71 (m, 8H), 2.37 (q, *J* = 7.2 Hz, 2H), 2.03 (bs, 1H), 1.44-1.70 (m, 5H), 0.88 (t, *J* = 7.2 Hz, 3H). The free base was converted into its corresponding hydrochloride salt. Mp 212-214 °C. Anal. ($C_{22.5}H_{36}Cl_3N_3O_{2.5}S$) C, H, N.

(*S*)-2-Methoxy-4-(5-((5-methoxy-1,2,3,4-tetrahydronaphthalen-2-yl)(propyl)amino)pentyl)phenol ((−)-13)

Aldehyde **6a** (0.12 g, 0.58 mmol), (−)-5-methoxy-*N*-propyl-2-aminotetralin (0.11 g, 0.50 mmol), and $NaBH(OAc)_3$ (0.24 g, 1.13 mmol) in CH_2Cl_2 (8 mL) were reacted using procedure E, and the resulting crude was purified by column chromatography using 5% MeOH in CH_2Cl_2 to give compound (±)-**13** (0.17 g, 82%). ^{1}H NMR (600 MHz, $CDCl_3$): *δ* ppm 7.08 (t, *J* = 7.8 Hz, 1H), 6.81 (d, *J* = 8.4Hz, 1H), 6.70 (d, *J* = 7.8Hz, 1H), 6.67-6.63 (m, 3H), 3.86 (s, 3H), 3.80 (s, 3H), 3.00-2.97 (m, 1H), 2.94-2.90 (m, 1H), 2.84-2.71 (m, 2H), 2.55-2.45 (m, 7H), 2.07-2.01 (m, 1H), 1.62-1.51 (m, 3H), 1.51-1.44 (m, 4H), 1.43-1.32 (m, 2H), 0.88 (t, *J* = 7.2 Hz, 3H).

Procedure K: (*S*)-4-(5-((5-Hydroxy-1,2,3,4-tetrahydronaphthalen-2-yl)(propyl)amino)pentyl)benzene-1,2-diol ((−)-14) (D-644)

Compound (−)-**13** (95 mg, 0.23 mmol) was treated with 48% hydrobromic acid (9.5 mL) and refluxed for 6 h. HBr was removed to obtain the residue, which

was then dissolved in MeOH and filtered through cotton. The filtrate was concentrated and washed with ether for several times followed by drying to give the hydrobromide salt of compound (−)-**14** (72 mg, 66%). ^{1}H NMR (600 MHz, $CDCl_3$): δ ppm 6.96 (t, J = 7.8 Hz, 1H), 6.65-6.60 (m, 4H), 6.47 (d, J = 7.8 Hz, 1H), 3.67 (s, 1H), 3.27-3.23 (m, 2H), 3.11-3.04 (m, 5H), 2.66-2.60 (m, 1H), 2.50 (t, J = 7.2 Hz, 2H), 2.31-2.25 (m, 1H), 1.89-1.83 (m, 1H), 1.76-1.74 (m, 4H), 1.68-1.63 (m, 2H), 1.43-1.39 (m, 2H), 1.03 (t, J = 7.2 Hz, 3H). $[\alpha]_D^{25}$ (salt) = −29.55 (c = 1.0 in CH_3OH). Mp 151-153 °C. Anal. ($C_{25}H_{38}BrNO_4$) C, H, N.

(3-Carboxypropyl)triphenylphosphonium bromide (16)

Triphenylphosphine (7.82 g, 29.81 mmol) was reacted with 4-bromobutanoic acid **15** (4.15 g, 24.85 mmol) according to procedure A to give compound **16** (9.5 g, 89%). ^{1}H NMR (400 MHz, $CDCl_3$): δ ppm 7.89-7.90 (m, 3 H), 7.82-7.85 (m, 6H), 7.76-7.79 (m, 6H), 3.45-3.49 (m, 2H), 2.59-2.61 (m, 2H), 1.92 (t, J = 6.6 Hz, 2H).

Procedure L: 5-(4-Hydroxy-3-methoxyphenyl)pent-4-enoic acid (17)

n-Butyl lithium 2.5 M in hexane (17.4 mL, 43.50 mmol) was added dropwise to a solution of bis(trimethylsilyl)amine (9.91 mL, 47.28 mmol) in THF (45 mL) at 0 °C, and the reaction mixture was stirred for 15 min after completion of addition. Thereafter, the resulting LiHMDS was added to a solution of intermediate **16** (8.46 g, 19.71 mmol) in THF (85 mL). The reaction mixture was stirred at rt for 1 h after the last addition of base. Vanillin **3a** (3.0 g, 19.72 mmol) in THF (10 mL) was then added to the above solution, and the reaction mixture

was stirred at rt for 24 h. After the completion of reaction, water was added, and the layers were separated. The aqueous layer was then acidified to pH=2 with conc. H_2SO_4 and extracted with ethyl acetate (3×150 mL). The combined organic layers were dried over Na_2SO_4 and evaporated *in vacuo*. The residue obtained was purified by column chromatography using 20 % ethyl acetate in hexanes to yield compound **17** (3.0 g, 68%) preferentially as the *E* isomer. ^{1}H NMR (600 MHz, $CDCl_3$): δ ppm 6.92 (s, 1H), 6.76 (d, *J* = 7.8 Hz, 1H), 6.69 (d, *J* = 8.4 Hz, 1H), 6.32 (d, *J* = 15.6 Hz, 1H), 6.04-6.08 (m, 1H), 3.83 (s, 3H), 2.42-2.44 (m, 4H).

Procedure M: (*E*)-Methyl 5-(4-hydroxy-3-methoxyphenyl)pent-4-enoate (18)

To a solution of compound **17** (1.34 g, 6.03 mmol) in MeOH (20 mL) was added acetyl chloride (0.94 mL, 13.22 mmol) at 0 °C, and the reaction mixture was stirred for 1 h. The solution was allowed to come to room temperature and stirred for another 3 h. The reaction was then quenched with saturated $NaHCO_3$ solution and extracted with CH_2Cl_2 (3×50 mL). The organic layer was dried over Na_2SO_4 and evaporated *in vacuo*. The (*E*)-isomer **18** was purified by column chromatography using 15 % ethyl acetate in hexanes (0.72 g, 51%). ^{1}H NMR (600 MHz, $CDCl_3$) δ ppm 6.82-6.86 (m, 3H), 6.34 (d, *J* = 15.6 Hz, 1H), 6.00-6.05 (m, 1H), 3.88 (s, 3H), 3.67 (s, 3H), 2.42-2.52 (m, 4H).

(*E*)-5-(4-Hydroxy-3-methoxyphenyl)pent-4-enal (19)

Intermediate **18** (0.425 g, 1.80 mmol) was reduced with DIBALH solution 1M in hexane (1.97 mL, 1.97 mmol) in dry toluene (8 mL) using procedure D. The crude was purified by column chromatography using 15-25% ethyl acetate in

hexanes to give compound **19** (0.14 g, 38%). ^{1}H NMR (600 MHz, $CDCl_3$): δ ppm 9.80(s, 1H), 6.79-6.86 (m, 3H), 6.32 (d, *J* = 15.6 Hz, 1H), 6.00-6.05 (m, 1H), 3.88 (s, 3H), 2.61 (t, *J* = 7.2 Hz, 2H), 2.52 (q, *J* = 7.2 Hz, 2H).

(*E*)-4-(5-((2-Amino-4,5,6,7-tetrahydrobenzo[*d*]thiazol-6-yl)(propyl)amino)pent-1-en-1-yl)-2-methoxyphenol ((±)-20) (D-604)

Aldehyde **19** (0.11 g, 0.53 mmol), (±)-pramipexole (0.11 g, 0.52 mmol), and $NaBH(OAc)_3$ (0.2 g, 0.94 mmol) in CH_2Cl_2 (7 mL) and MeOH (0.7 mL) were reacted using procedure E, and the resulting crude was purified by column chromatography using 5-7% MeOH in CH_2Cl_2 to give compound (±)-**20** (0.10 g, 48%).^{1}H NMR (600 MHz, $CDCl_3$): δ ppm 6.80-6.85 (m, 3H), 6.29 (d, *J* = 15.6 Hz, 1H), 6.02-6.07 (m, 1H), 4.86 (bs, 1H), 3.87 (s, 3H), 3.02 (bs, 1H), 2.62-2.69 (m, 2H), 2.38-2.54 (m, 6H), 2.17-2.21 (m, 2H), 1.96 (d, *J* = 10.2 Hz, 1H), 1.64-1.71 (m, 1H), 1.59 (t, *J* = 7.2 Hz, 2H), 1.45 (q, *J* = 7.2 Hz, 2H), 0.87 (t, *J* = 7.2 Hz, 3H). The free base was converted into its corresponding hydrochloride salt. Mp 217-219 °C. Anal. ($C_{22}H_{37}Cl_2N_3O_4S$) C, H, N.

(*S*,*E*)-4-(5-((2-Amino-4,5,6,7-tetrahydrobenzo[*d*]thiazol-6-yl)(propyl)amino)pent-1-en-1-yl)-2-methoxyphenol ((−)-20) (D-618)

Aldehyde **19** (55 mg, 0.27 mmol), (−)-pramipexole (56 mg, 0.26 mmol), and $NaBH(OAc)_3$ (0.1 g, 0.47 mmol) in CH_2Cl_2 (15 mL) were reacted using procedure E, and the resulting crude was purified by column chromatography using 10-15% MeOH in CH_2Cl_2 to give compound (−)-**20** (57 mg, 54%). ^{1}H NMR (600 MHz, $CDCl_3$): δ ppm 6.82-6.88 (m, 3H), 6.31 (d, *J* = 15.6 Hz), 6.04-6.09 (m,

1H), 4.77 (bs, 2H), 3.90 (s, 3H), 3.05 (bs, 1H), 2.64-2.71 (m, 2H), 2.41-2.57 (m, 6H), 2.19-2.23 (m, 2H), 1.98 (d, *J* = 10.8 Hz, 1H), 1.67-1.74 (m, 1H), 1.61 (t, *J* = 7.2 Hz, 2H), 1.46 (q, *J* = 7.2 Hz, 2H), 0.89 (t, *J* = 7.2 Hz, 3H). The free base was converted into its corresponding hydrochloride salt. $[\alpha]_D^{25}$ (salt) = −56.00 (c = 1.0 in CH_3OH). Mp 206-209 °C. Anal. ($C_{24.8}H_{41}Cl_3N_3O_{2.7}S$) C, H, N.

6-(4-Hydroxy-3-methoxyphenyl)hex-5-enoic acid (22)

LiHMDS was prepared from *n*-butyl lithium 2.5 M in hexane (17.4 mL, 43.50 mmol) and bis(trimethylsilyl)amine (9.9 mL, 47.23 mmol) in THF (45 mL) at 0 °C for 15 min. Following procedure L, the resulting LiHMDS was added dropwise to a solution of (4-carboxybutyl)triphenylphosphonium bromide **21** (8.7 g, 19.63 mmol) in THF (90 mL). And vanillin **3a** (3 g, 19.72 mmol) in THF (10 mL) was added after 1 h. The crude obtained was purified by column chromatography using 30% ethyl acetate in hexanes to yield compound **22** (1.1 g, 24%). ^{1}H NMR (600 MHz, $CDCl_3$): *δ* ppm 6.90-6.83 (m, 3H), 6.32 (d, *J* = 15.6 Hz, 1H), 6.01 (dt, *J* = 15.6, 7.2 Hz, 1H), 3.87 (s, 3H), 2.41 (t, *J* = 7.2 Hz, 2H), 2.24 (q, *J* = 6.9 Hz, 2H), 1.82 (m, 2H).

6-(4-Hydroxy-3-methoxyphenyl)hexanoic acid (23)

Intermediate **22** (0.5 g, 2.12 mmol) was dissolved in ethanol (25 mL) and reacted with 10% Pd/C (50 mg, 10 wt%) according to procedure C to afford compound **23** (0.46 g, 91%), which was used without further purification. ^{1}H NMR (600 MHz, $CDCl_3$): *δ* ppm 6.81 (d, *J* = 7.8 Hz, 1H), 6.65 (d, *J* = 7.8 Hz, 2H), 3.87

(s, 3H), 2.53 (t, *J* = 7.5 Hz, 2H), 2.35 (t, *J* = 7.5 Hz, 2H), 1.69-1.64 (m, 2H), 1.63-1.58 (m, 2H), 1.40-1.35 (m, 2H).

Methyl 6-(4-hydroxy-3-methoxyphenyl)hexanoate (24)

Intermediate **23** (0.455 g, 1.91 mmol) was esterified with acetyl chloride (0.3 mL, 4.22 mmol) in dry MeOH (12.5 mL) using procedure M. The extract was concentrated to give compound **24** (0.450 g, 93%), which was pure enough for the next step. ^{1}H NMR (600 MHz, $CDCl_3$): *δ* ppm 6.79 (d, *J* = 8.4 Hz, 1H), 6.65 (s, 1H), 6.62 (dd, *J* = 7.8, 1.8 Hz, 1H), 5.85 (bs, 1H), 3.81 (s, 3H),3.63 (s, 3H), 2.50 (t, *J* = 7.8 Hz, 2H), 2.28 (t, *J* = 7.8 Hz, 2H), 1.66-1.61 (m, 2H), 1.60-1.55 (m, 2H), 1.35-1.30 (m, 2H).

6-(4-Hydroxy-3-methoxyphenyl)hexanal (25)

Intermediate **24** (0.314 g, 1.24 mmol) was reduced with DIBALH solution 1M in hexane (1.45 mL, 1.45 mmol) in dry toluene (6 mL) using procedure D. The crude was purified by column chromatography using 15% ethyl acetate in hexanes to give compound **25** (89 mg, 32%). ^{1}H NMR (600 MHz, $CDCl_3$): *δ* ppm 9.75 (t, *J* = 1.5 Hz, 1H), 6.81 (d, *J* = 7.8 Hz, 1H), 6.66-6.64 (m, 2H), 5.49 (s, 1H), 3.86 (s, 3H), 2.53 (t, *J* = 7.8 Hz, 2H), 2.42 (td, *J* = 7.2, 1.8 Hz, 2H), 1.67-1.57 (m, 4H), 1.38-1.33 (m, 2H).

4-(6-((2-Amino-4,5,6,7-tetrahydrobenzo[*d*]thiazol-6-yl)(propyl)amino)hexyl)-2-methoxyphenol ((±)-26) (D-606)

Aldehyde **25** (60 mg, 0.27 mmol), (±)-pramipexole (57 mg, 0.27 mmol), and $NaBH(OAc)_3$ (103 mg, 0.49 mmol) in CH_2Cl_2 (7 mL) were reacted for 48 h

using procedure E, and the resulting crude was purified by column chromatography using 6% MeOH in CH_2Cl_2 to give compound (±)-**26** (35 mg, 31%). ^{1}H NMR (600 MHz, $CDCl_3$): δ ppm 6.80 (d, *J* = 7.8 Hz, 1H), 6.66-6.64 (m, 2H), 4.79 (bs, 2H), 3.85 (s, 3H), 3.04-2.98 (m, 1H), 2.70-2.61 (m, 2H), 2.56-2.50 (m, 4H), 2.48-2.40 (m, 4H), 1.95 (d, *J* = 9.0 Hz, 1H), 1.71-1.65 (qd, *J* = 5.4, 11.4 Hz, 1H), 1.59-1.54 (m, 2H), 1.42 (t, *J* = 6.6 Hz, 4H), 1.31 (t, *J* = 3.0 Hz, 4H), 0.86 (t, *J* = 7.2 Hz, 3H). The free base was converted into its corresponding hydrochloride salt. Mp 170-175 °C. Anal. ($C_{25}H_{45}Cl_2N_3O_4S$) C, H, N.

Ethyl 2-(triphenylphosphoranylidene)acetate (28)

Ethyl bromoacetate **27** (1.98 mL, 17.86 mmol) was slowly added to a stirring solution of triphenylphosphine (5.64 g, 21.50 mmol) in toluene (20 mL). The reaction mixture was refluxed for 16 h and filtered. The filter cake was washed with ethyl acetate (3 x 20 mL) to give phosphonium bromide (6.69 g, 87%). ^{1}H NMR ($CDCl_3$, 400 MHz): δ ppm 7.64-7.91 (m, 15H), 5.54 (d, *J* = 13.6 Hz, 2H), 4.01 (q, *J* = 7.2 Hz, 2H), 1.04 (t, *J* = 7.2 Hz, 3H). Into the solution of phosphonium bromide (6 g, 13.98 mmol) in CH_2Cl_2 (50 mL) was added 1M NaOH aqueous solution (50 mL, 50.00 mmol). The mixture was vigorously stirred for 15 min, and the layers were separated. The aqueous layer was extracted with CH_2Cl_2 (3 x 15 mL). The combined organic phase was dried over Na_2SO_4 and concentrated to give compound **28** (4.28 g, 88%). ^{1}H NMR ($CDCl_3$, 400 MHz): δ ppm 7.40-7.77 (m, 15H), (3.80, minor + 4.01, major) (q, *J* = 7.2 Hz, 2H), (2.70,

minor + 2.92, major) (d, *J* = 22 Hz, 1H), (0.65, minor + 1.21, major) (t, *J* = 7.2 Hz, 3H).

(*E*)-Ethyl 3-(4-hydroxy-3-methoxyphenyl)acrylate (29)

A mixture of vanillin **3a** (0.55 g, 3.61 mmol) and phosphonium ylide **28** (4.28 g, 12.29 mmol) was refluxed in chloroform (30 mL) for 5 h. The solvent was removed, and the crude product was purified by column chromatography using 17% ethyl acetate in hexanes to give compound **29** (0.68 g, 85%). ^{1}H NMR ($CDCl_3$, 400 MHz): δ ppm 7.49 (d, *J* = 15.9 Hz, 1H), 6.75-6.92 (m, 3H), 6.17 (d, *J* = 15.7 Hz, 1H), 4.13 (q, *J* = 7.0 Hz, 2H), 3.70 (s, 3H), 1.19 (t, *J* = 7.2 Hz, 3H).

Ethyl 3-(4-hydroxy-3-methoxyphenyl)propanoate (30)

Intermediate **29** (1.0 g, 4.50 mmol) was dissolved in ethanol (10 mL) in a round bottom flask, and 10% Pd/C (0.10 g, 10 wt%) was added to it. The reaction was continued using procedure C. After the completion of reaction, the mixture was diluted with ethanol (20 mL) and passed through a short bed of celite. The organic layer was concentrated to afford compound **30** (0.95 g) as colorless oil in quantitative yield which was pure enough for the next step. ^{1}H NMR (400 MHz, $CDCl_3$): δ ppm 6.82 (d, *J* = 7.2 Hz, 1H), 6.68 (m, 2H), 4.12 (q, *J* = 7.2 Hz, 2H), 3.84 (s, 3H), 2.87 (t, *J* = 7.6 Hz, 2H), 2.58 (t, *J* = 8.0 Hz, 2H), 1.23 (t, *J* = 7.2 Hz, 3H).

3-(4-Hydroxy-3-methoxyphenyl)propanal (31)

Intermediate **30** (0.60 g, 2.68 mmol) was reduced with DIBALH solution (1M in hexane, 2.93 mL, 2.93 mmol) in dry toluene (10 mL) using procedure D.

The crude was purified by column chromatography using 12-15% ethyl acetate in hexanes to give compound **31** (0.22 g, 46%) as yellow oil. ^{1}H NMR (400 MHz, $CDCl_3$): δ ppm 9.81 (t, *J* = 1.6 Hz, 1H), 6.83 (d, *J* = 7.2 Hz, 1H), 6.68 (m, 2H), 3.87 (s, 3H), 2.89 (t, *J* = 7.6 Hz, 2H), 2.75 (t, *J* = 8.0 Hz, 2H).

4-(3-((2-Amino-4,5,6,7-tetrahydrobenzo[*d*]thiazol-6-yl)(propyl)amino)propyl)-2-methoxyphenol ((±)-32) (D-547)

Aldehyde **31** (0.30 g, 1.66 mmol), (±)-pramipexole (0.369 g, 1.75 mmol), and $NaBH(OAc)_3$ (0.633 g, 2.99 mmol) in CH_2Cl_2 (10 mL) and MeOH (1 mL) were reacted using procedure E, and the resulting crude was purified by column chromatography using 5-7% MeOH in CH_2Cl_2 to give compound (±)-**32** (0.3 g, 48%).^{1}H NMR (400 MHz, CD_3OD): δ ppm 6.79 (s, 1H), 6.71 (d, *J* = 8.0 Hz, 1H), 6.64 (d, *J* = 8.0 Hz, 1H), 3.82 (s, 3H), 2.73-2.89 (m, 5H), 2.57-2.67 (m, 6H), 2.05-2.12 (m, 1H), 1.81-1.92 (m, 3H), 1.59 (m, 2H), 0.95 (t, *J* = 7.2 Hz, 3H). The free base was converted into its corresponding hydrochloride salt. Mp 220-222 °C. Anal. ($C_{21}H_{35}Cl_2N_3O_3S$) C, H, N.

4-(3-((2-Amino-4,5,6,7-tetrahydrobenzo[*d*]thiazol-6-yl)(propyl)amino)propyl)benzene-1,2-diol ((±)-33) (D-573)

BBr_3 1M in CH_2Cl_2 (2.66 mL, 2.66 mmol) was reacted with compound (±)-**32** (0.2 g, 0.53 mmol) according to procedure F to afford crude, which was purified by column chromatography using 15-20% MeOH in CH_2Cl_2 to provide compound (±)-**33** (0.12 g, 62%). ^{1}H NMR (400 MHz, CD_3OD) δ ppm 6.57 (d, *J* = 8.4 Hz, 1H), 6.53 (s, 1H), 6.41 (d, *J* = 8.4 Hz, 1H), 3.13 (bs, 1H), 2.39-2.66 (m,

10H), 1.95 (m, 1H), 1.61-1.75 (m, 3H), 1.41-1.47 (m, 2H), 0.82 (t, *J* = 7.2 Hz, 3H). The free base was converted into its corresponding hydrochloride salt. Mp 192-194 °C. Anal. ($C_{19}H_{31}Cl_3N_3O_{2.5}S$) C, H, N.

(*E*)-Ethyl 3-(4-((tert-butyldimethylsilyl)oxy)-3-methoxyphenyl)acrylate (34)

Compound **29** (1.78g, 8.01 mmol) was reacted with *tert*-butyldimethylsilyl chloride (1.45 g, 9.62 mmol) and imidazole (1.36 g, 19.98 mmol) in DMF (6 mL) according to procedure G. The mixture was extracted with water and diethyl ether. The organic phase was washed with brine and dried over Na_2SO_4. Then it was concentrated to give compound **34**, which was pure enough for the next step (2.42 g, 90%). ^{1}H NMR ($CDCl_3$, 400 MHz): *δ* ppm 7.62 (d, *J* = 15.2 Hz, 1H), 6.99-7.03 (m, 2H), 6.84 (d, *J* = 8.8 Hz, 1H), 6.30 (d, *J* = 16.0 Hz, 1H), 4.25 (q, *J* = 7.1 Hz, 2H), 3.83 (s, 3H), 1.33 (t, *J* = 7.2 Hz, 3H), 0.17 (s, 6H), 0.99 (s, 9H).

(*E*)-3-(4-((tert-Butyldimethylsilyl)oxy)-3-methoxyphenyl)prop-2-en-1-ol (35)

Compound **34** (2.4g, 7.13 mmol) in anhydrous THF (30 mL) was reacted with DIBALH 1 M in THF (35.7 mL, 35.70 mmol) following procedure H to give crude product, which was purified by column chromatography using 25% ethyl acetate in hexanes to give compound **35** (1.97 g, 94%). ^{1}H NMR ($CDCl_3$, 400 MHz): *δ* ppm 6.90 (d, *J* = 1.6 Hz, 1H), 6.84 (dd, *J* = 8.0, 1.6 Hz, 1H), 6.79 (d, *J* = 8.0 Hz, 1H), 6.52 (d, *J* = 15.6 Hz, 1H), 6.22 (dt, *J* = 16.0, 6.0 Hz, 1H), 4.28 (d, *J* = 5.6 Hz, 2H), 3.81 (s, 3H), 0.99 (s, 9H), 0.15 (s, 6H).

(*E*)-3-(4-((tert-Butyldimethylsilyl)oxy)-3-methoxyphenyl)acrylaldehyde (36)

MnO_2 (3.54 g, 40.72 mmol) was added into a solution of compound **35** (0.8 g, 2.72 mmol) in CH_2Cl_2 (15 mL). The mixture was stirred at room temperature for 24 h and was filtered through celite. The filter cake was washed with ethyl acetate, and the filtrate was concentrated to give compound **36** (0.67 g, 84%). ^{1}H NMR ($CDCl_3$, 400 MHz): δ ppm 9.65 (d, J = 7.2 Hz, 1H), 7.40 (d, J = 16.0 Hz, 1H), 7.05-7.08 (m, 2H), 6.88 (d, J = 7.2 Hz, 1H), 6.60 (dd, J = 15.6, 7.6 Hz, 1H), 3.85 (s, 3H), 1.00 (s, 9H), 0.18 (s, 6H).

(*E*)-3-(4-Hydroxy-3-methoxyphenyl)acrylaldehyde (37)

Compound **36** (0.67 g, 2.29 mmol) in THF (10 mL) was reacted with TBAF solution (1 M in THF, 2.52 mL, 2.52 mmol) according to procedure J to obtain the crude, which was purified by column chromatography using 35% ethyl acetate in hexanes to give compound **37** (0.343 g, 84%). It was immediately taken to the next step.

(*E*)-4-(3-((2-Amino-4,5,6,7-tetrahydrobenzo[*d*]thiazol-6-yl)(propyl)amino)prop-1-en-1-yl)-2-methoxyphenol ((±)-38) (D-570)

Aldehyde **37** (0.334 g, 1.87 mmol), (±)-pramipexole (0.395 g, 1.87 mmol), and $NaBH(OAc)_3$ (0.710 g, 3.35 mmol) in CH_2Cl_2 (10 mL) were reacted using procedure E, and the resulting crude was purified by column chromatography using 15% MeOH in CH_2Cl_2 to give compound **38** (0.21g, 30%). ^{1}H NMR (CD_3OD, 400 MHz): δ ppm 7.36 (d, J = 16.4 Hz, 1H), 7.20 (s, 1H), 7.10 (d, J = 8.0 Hz, 1H), 6.92 (dd, J = 15.2, 7.6 Hz, 1H), 6.81 (d, J = 8.4 Hz, 1H), 3.89 (s, 3H), 3.46 (s, 1H), 3.25 (dd, J = 15.6, 5.2 Hz, 1H), 2.99 (t, J = 7.1 Hz, 2H), 2.79-2.90 (m, 3H), 2.58-

2.67 (m, 1H), 2.23-2.33 (m, 1H), 1.81-2.00 (m, 2H), 1.72 (q, *J* = 7.1 Hz, 2H), 1.03 (t, *J* = 7.2 Hz, 3H). The free base was converted into its corresponding hydrochloride salt. Mp 205-207 °C. Anal. ($C_{20}H_{32}Cl_3N_3O_3S$) C, H, N.

3,4-Dihydroxybenzaldehyde (39)

Vanillin **3a** (3.0 g, 19.72 mmol) was reacted with BBr_3 1M in CH_2Cl_2 (36.1 mL, 36.10 mmol) in CH_2Cl_2 (20 mL) following procedure F. The crude obtained was purified by column chromatography using 20-25% ethyl acetate in hexanes to afford compound **39** (2.18 g, 80%). ^{1}H NMR (400 MHz, $CDCl_3$): *δ* ppm 9.67 (s, 1H), 7.29 (m, 2H), 6.89 (d, *J* = 9.2 Hz, 1H).

3,4-bis((tert-Butyldimethylsilyl)oxy)benzaldehyde (40)

Imidazole (5.69 g, 83.58 mmol) was added to a solution of intermediate **39** (2.31 g, 16.72 mmol) and *tert*-butyldimethylsilyl chloride (6.30 g, 41.80 mmol) in DMF (20 mL). The solution was reacted using procedure G. The crude thus obtained was purified by column chromatography using 5% ethyl acetate in hexanes to afford compound **40** (4.10 g, 67%). ^{1}H NMR (400 MHz, $CDCl_3$): *δ* ppm 9.80 (s, 1H), 7.36 (m, 2H), 6.93 (d, *J* = 8.8 Hz, 1H), 0.99 (s, 9H), 0.98 (s, 9H), 0.24 (s, 6H), 0.22 (s, 6H).

(*Z*)-Ethyl 5-(3,4-bis((tert-butyldimethylsilyl)oxy)phenyl)pent-4-enoate (41)

Starting material **2** (5.48 g, 11.98 mmol) was reacted with compound **40** (4.0 g, 10.91 mmol) in the presence of NaHMDS 1M in THF (13.07 mmol, 13.07 mL) according to procedure B. The crude was then purified by column chromatography using 5% ethyl acetate in hexanes to give compound **41** (2.0 g,

39%). ^{1}H NMR (400 MHz, $CDCl_3$): δ ppm 6.81 (m, 2H), 6.73 (d, *J* = 8.4 Hz, 1H), 6.30 (d, *J* = 11.4 Hz, 1H), 5.46-5.50 (m, 1H), 4.12 (q, *J* = 7.3 Hz, 2H), 2.64 (q, *J* = 7.2 Hz, 2H), 2.41 (t, *J* = 7.2 Hz, 2H), 1.24 (t, *J* = 7.2 Hz, 3H), 0.97 (s, 18H), 0.19 (s, 6H), 0.18 (s, 6H).

(*Z*)-5-(3,4-bis((tert-Butyldimethylsilyl)oxy)phenyl)pent-4-enal (42)

Intermediate **41** (1.0 g, 2.15 mmol) was reduced with DIBALH solution 1M in hexane (2.16 mL, 2.16 mmol) in dry toluene (15 mL) using procedure D. The crude was purified by column chromatography using 10% ethyl acetate in hexanes to give compound **42** (0.41 g, 45%) as yellow oil. ^{1}H NMR (600 MHz, $CDCl_3$): δ ppm 9.76 (s, 1H), 6.77-6.79 (m, 2H), 6.73 (td, *J* = 7.2, 2.4 Hz, 1H), 6.33 (d, *J* = 11.4 Hz, 1H), 5.45-5.50 (m, 1H), 2.65 (q, *J* = 7.2 Hz, 2H), 2.56 (t, *J* = 7.2 Hz, 2H), 0.98 (s, 18H), 0.20 (s, 12H).

(*Z*)-*N*^{6}-(5-(3,4-bis((tert-Butyldimethylsilyl)oxy)phenyl)pent-4-en-1-yl)-*N*^{6}-propyl-4,5,6,7-tetrahydrobenzo[*d*]thiazole-2,6-diamine ((±)-43)

Aldehyde **42** (0.3 g, 0.71 mmol), (±)-pramipexole (0.15 g, 0.71mmol), and $NaBH(OAc)_3$ (0.27 g, 1.27 mmol) in CH_2Cl_2 (10 mL) and MeOH (0.8 mL) were reacted using procedure E, and the resulting crude was purified by column chromatography using 5% MeOH in CH_2Cl_2 to give compound (±)-**43** (0.22 g, 50%). ^{1}H NMR (600 MHz, CD_3OD): δ ppm 6.79 (m, 2H), 6.73 (d, *J* = 7.8 Hz, 1H), 6.29 (d, *J* = 11.4 Hz, 1H), 5.52 (m, 1H), 3.09 (bs, 1H), 2.44-2.66 (m, 8H), 2.34-2.37 (m, 2H), 1.96-1.99 (m, 1H), 1.60-1.72 (m, 3H), 1.44-1.51 (m, 2H), 0.97 (s, 18 H), 0.87 (t, *J* = 7.2 Hz, 3H), 0.18 (s, 12H).

(*Z*)-4-(5-((2-Amino-4,5,6,7-tetrahydrobenzo[*d*]thiazol-6-yl)(propyl)amino)pent-1-en-1-yl)benzene-1,2-diol and (*Z*)-4-(5-((2-amino-4,5,6,7-tetrahydrobenzo[*d*]thiazol-6-yl)(propyl)amino)pent-1-en-1-yl)cyclohexa-3,5-diene-1,2-dione (mixture of (±)-44 and (±)-45) (D-592)

Compound (±)-**43** (0.21 g, 0.34 mmol) in THF (5 mL) was reacted with TBAF 1M in THF (1.02 mL, 1.02 mmol) following procedure J. The crude was purified by column chromatography using 15-20% MeOH in CH_2Cl_2 to give a mixture of (±)-**44** and (±)-**45** (95 mg, 72%). ^{1}H NMR (600 MHz, CD_3OD): δ ppm 6.79 (s, 1H), 6.73 (s, 1H), 6.70 (d, *J* = 7.8 Hz, 1H), 6.63 (m, 2H), 6.59 (d, *J* = 8.4 Hz, 1H), 6.20-6.25 (m, 2H), 6.59 (dt, *J* = 15.6, 7.2 Hz, 1H), 5.46 (m, 1H), 3.0 (bs, 2H), 2.40-2.63(m, 16H), 2.32 (m, 2H), 2.16 (m, 2H), 1.95 (m, 2H), 1.56-1.70 (m, 6H), 1.41-1.51 (m, 4H), 0.85-0.90 (m, 6H). The free base was converted into its corresponding hydrochloride salt. HRMS *m/z* $[M + H]^+$: calcd for $C_{21}H_{30}N_3O_2S$, 388.2059; found 388.4567. Mp 212-214 °C. Anal. ($C_{22}H_{34.4}N_3Cl_3O_{2.2}S$) C, H, N.

Procedure N: 2-(4-(2',5'-Dimethoxy-[1,1'-biphenyl]-4-yl)piperazin-1-yl)acetaldehyde (47)

A solution of DMSO (0.11 mL, 1.55 mmol) in CH_2Cl_2 (1 mL) was added into a round-bottom flask containing a stirring solution of oxalyl chloride (76 µL, 0.87 mmol) in CH_2Cl_2 (1 mL) at −78 °C. The mixture was stirred for 0.5 h at the same temperature, and compound **46** (0.15 g, 0.44 mmol) in CH_2Cl_2 (1.5 mL) was added. The stirring of the reaction mixture was continued at −78 °C for another 0.5 h. Thereafter, Et_3N (0.5 mL, 3.59 mmol) was added, and the reaction

was allowed to warm to room temperature and continued for another 1 h. The reaction mixture was quenched by the addition of a saturated solution of $NaHCO_3$ at 0 °C and was extracted with CH_2Cl_2 (3 × 20 mL). The combined organic layer was dried over Na_2SO_4, and the solvent was removed *in vacuo* to produce the crude, which was purified by column chromatography using ethyl acetate to give compound **47** (0.11g, 0.74%). ^{1}H NMR (600 MHz, $CDCl_3$): *δ* ppm 9.75 (s, 1H), 7.45 (d, *J* = 9.0 Hz, 2H), 6.95 (d, *J* = 8.4 Hz, 2H), 6.88 (dd, *J* = 5.4, 3.6 Hz, 2H), 6.79 (dd, *J* = 9.0, 5.0 Hz, 1H), 3.30 (t, *J* = 4.8 Hz, 4H), 3.25 (d, *J* = 1.2 Hz, 2H), 2.70 (t, *J* = 4.8 Hz, 4H).

(*S*)-*N*-(2-(4-(2',5'-dimethoxy-[1,1'-biphenyl]-4-yl)piperazin-1-yl)ethyl)-5-methoxy-*N*-propyl-1,2,3,4-tetrahydronaphthalen-2-amine ((−)-48)

Aldehyde **47** (0.11 g, 0.32 mmol), (−)-5-methoxy-*N*-propyl-2-aminotetralin (0.071 g, 0.32 mmol), and $NaBH(OAc)_3$ (0.137 g, 0.65 mmol) in CH_2Cl_2 (8 mL) were reacted using procedure E, and the resulting crude was purified by column chromatography using ethyl acetate to give compound **(−)-48** (0.061 g, 35%). ^{1}H NMR (600 MHz, $CDCl_3$): *δ* ppm 7.43-7.46 (m, 2H), 7.03 (t, *J* = 7.8 Hz, 1H), 6.94 (d, *J* = 9.0 Hz, 2H), 6.87-6.89 (m, 2H), 6.79 (dd, *J* = 8.4, 3.0 Hz, 1H), 6.70 (d, *J* = 7.8 Hz, 1H), 6.64 (d, *J* = 8.4 Hz, 1H), 3.80 (s, 3H), 3.79 (s, 3H), 3.74 (s, 3H), 3.24 (t, *J* = 5.4 Hz, 4H), 2.81-3.02 (m, 3H), 2.72-2.78 (m, 3H), 2. 66 (bs, 4H), 2.47-2.58 (m, 5H), 2.03-2.12 (m, 1H), 1.52-1.62 (m, 1H), 1.44-1.52 (m, 2H), 0.90 (t, *J* = 7.2 Hz, 3H).

(*S*)-4'-(4-(2-((5-hydroxy-1,2,3,4-tetrahydronaphthalen-2-yl)(propyl)amino)ethyl)piperazin-1-yl)-[1,1'-biphenyl]-2,5-diol ((−)-49)

Intermediate **(−)-48** (35 mg, 0.06 mmol) was treated with 48% hydrobromic acid (4 mL) and refluxed for 6.5 h by following procedure K. The crude was washed with ether for several times followed by drying to give the hydrobromide salt of compound **(−)-49** (42.5 mg, 84%). ^{1}H NMR (600 MHz, $CDCl_3$): δ ppm 7.57 (d, J = 8.4 Hz, 2H), 7.24 (bs, 2H), 6.96 (t, J = 7.8 Hz, 1H), 6.67-6.72 (m, 3H), 6.58- 6.62 (m, 2H), 3.58-3.93 (m, 13H), 3.36-3.48 (m, 1H), 3.27-3.31 (m, 2H), 3.09-3.19 (m, 2H), 2.66-2.76 (m, 1H), 2.46-2.49 (m, 1H), 1.94-1.99 (m, 3H), 1.07 (t, J = 7.2 Hz, 3H). $[\alpha]_D^{25}$ (salt) = −32.40 (c = 0.1 in CH_3OH). Mp 212-214 °C. Anal. ($C_{31}H_{47}Br_3N_3O_{5.5}$) C, H, N.

(*S*)-*N*-(2-amino-4,5,6,7-tetrahydrobenzo[*d*]thiazol-6-yl)-2-nitrobenzenesulfonamide (51)

Into a stirring solution of 2-nitrobenzenesulfonyl chloride (0.488 g, 2.23 mmol) in THF (15 mL), Et_3N (1.38 mL, 9.90 mmol) and (*S*)-4,5,6,7-tetrahydrobenzo[d]thiazole-2,6-diamine **50** (0.41 g, 2.42 mmol) (Brown et al. 2009) were added at −10 °C, and the resulting suspension was then stirred at room temperature for 1.5 h. The suspension was first filtered to remove precipitated triethylammonium chloride, and the filtrate was concentrated *in vacuo*. Water was added, and CH_2Cl_2 (3 × 30 mL) was used to extract the product. The combined organic layer was dried over Na_2SO_4, and the solvent was removed *in vacuo* to obtain sulfonamide **51** (0.7 g, 89%). ^{1}H NMR (600 MHz,

CD_3OD): *δ* ppm 8.11-8.13 (m, 1H), 7.78-7.83 (m, 3H), 3.68-3.76 (m, 1H), 2.70 (dd, *J* = 15.6, 4.2 Hz, 1H), 2.47-2.51 (m, 3H), 1.83-1.91 (m, 1H), 1.78-1.81 (m, 1H).

Procedure O: (*S*)-*N*-(2-amino-4,5,6,7-tetrahydrobenzo[*d*]thiazol-6-yl)-2-nitro-*N*-(prop-2-yn-1-yl)benzenesulfonamide (53)

Sulfonamide **51** (0.52 g, 1.47 mmol), potassium carbonate (1.42 g, 10.27 mmol), and propargyl bromide **52** (0.22 mL, 2.78 mmol) were suspended in acetonitrile (10 mL). The stirring mixture was heated to approximately 50 °C and reacted for 24 h. After cooling to room temperature, the reaction mixture was filtered, and the filtrate was condensed *in vacuo.* Water was added, and CH_2Cl_2 (3 × 20 mL) was used to extract the product. The combined organic layer was dried over Na_2SO_4, and the solvent was removed *in vacuo* to give the crude, which was purified by column chromatography using 1.5% MeOH in CH_2Cl_2 to give intermediate **53** (0.345 g, 60%). ^{1}H NMR (600 MHz, $CDCl_3$): *δ* ppm 8.19 (dd, *J* = 7.8, 1.8 Hz, 1H), 7.67-7.74 (m, 3H), 4.22-4.30 (m, 1H), 4.20 (d, *J* = 2.4 Hz, 2H), 3.04 (t, *J* = 13.2 Hz, 1H), 2.82 (dd, *J* = 15.6, 4.8 Hz, 1H), 2.68-2.77 (m, 2H), 2.21 (t, *J* = 2.4 Hz, 1H), 2.06−2.09 (m, 2H).

Procedure P: (*S*)-*N*^{6}-(prop-2-yn-1-yl)-4,5,6,7-tetrahydrobenzo[*d*]thiazole-2,6-diamine (54)

Potassium carbonate (1.7 g, 12.30 mmol) was first suspended in DMF (6 mL), followed by the addition of thioglycolic acid (0.49 mL, 6.89 mmol) slowly into the suspension at 0 °C. The mixture was stirred at room temperature for 1 h.

Following the addition of intermediate **53** (0.54 g, 1.38 mmol) in DMF (6 mL), the reaction mixture was heated to approximately 55 °C and stirred for another 17 h. Then it was quenched carefully by the adding 1N NaOH at room temperature, and CH_2Cl_2 (4 × 30 mL) was used to extract the product. The combined organic layer was dried over Na_2SO_4, and the solvent was removed *in vacuo* to give the crude, which was purified by column chromatography using 2-5% MeOH in CH_2Cl_2 to give intermediate **54** (0.16 g, 56%). ^{1}H NMR (600 MHz, $CDCl_3$): *δ* ppm 4.79 (bs, 2H), 3.52 (dd, *J* = 4.2, 2.4 Hz, 2H), 3.23-3.27 (m, 1H), 2.85 (dd, *J* = 15.0, 5.4 Hz, 1H), 2.67 (dt, *J* = 17.4, 6.0 Hz, 1H), 2.59-2.63 (m, 1H), 2.39-2.44 (m, 1H), 2.23 (t, *J* = 2.4 Hz, 1H), 1.98-2.02 (m, 1H), 1.69-1.76 (m, 1H).

Pent-4-yn-1-yl 4-methylbenzenesulfonate (56)

Triethylamine (0.66 mL, 4.74 mmol), 4-(dimethylamino)pyridine (29 mg, 0.24 mmol), and toluene-4-sulfonyl chloride (0.498 g, 2.61 mmol) were added to an ice-cooled solution of pent-4-yn-1-ol (0.11 mL, 1.18 mmol) in anhydrous CH_2Cl_2 (5 mL). The mixture was stirred at room temperature for overnight and then diluted with CH_2Cl_2. The organic layer was then washed with water and dried over Na_2SO_4. The solvent was removed *in vacuo*, and the residue was purified by column chromatography using 20% ethyl acetate in hexanes to give compound **56** (0.27 g, 96%). ^{1}H NMR (600 MHz, $CDCl_3$): *δ* ppm 7.78 (dd, *J* = 7.2, 1.8 Hz, 2H), 7.33 (d, *J* = 8.4 Hz, 2H), 4.13 (t, *J* = 6.0 Hz, 2H), 2.43 (s, 3H), 2.23-2.26 (m, 2H), 1.82-1.87 (m, 3H).

(*S*)-*N*-(2-amino-4,5,6,7-tetrahydrobenzo[*d*]thiazol-6-yl)-2-nitro-*N*-(pent-4-yn-1-yl)benzenesulfonamide (57)

In the presence of potassium carbonate (0.257 g, 1.86 mmol), sulfonamide **51** (0.11 g, 0.31 mmol) was reacted with intermediate **56** (0.081 g, 0.34 mmol) in acetonitrile (10 mL) at approximately 85 °C for 36 h by following procedure O, and the resulting crude was purified by column chromatography using 5% MeOH in CH_2Cl_2 to give compound **57** (0.103 g, 79%). ^{1}H NMR (600 MHz, $CDCl_3$): δ ppm 8.09 (dd, J = 7.2, 1.2 Hz, 1H), 7.68−7.74 (m, 2H), 7.65 (dd, J = 7.2, 1.8 Hz, 1H), 4.71 (bs, 2H), 4.16-4.22 (m, 1H), 3.43 (ddd, J = 9.6, 6.0, 1.8 Hz, 2H), 2.67-2.85 (m, 4H), 2.23 (td, J = 6.6, 2.4 Hz, 2H), 1.84-2.01 (m, 5H).

(S)-N^6-(pent-4-yn-1-yl)-4,5,6,7-tetrahydrobenzo[*d*]thiazole-2,6-diamine (58)

Following procedure P, a solution of thioglycolic acid (0.083 mL, 1.17 mmol) in DMF (2 mL) was added into the suspension of potassium carbonate (0.281 g, 2.03 mmol) in DMF (2 mL) at 0 °C and stirred at room temperature for 1h. After the addition of intermediate **57** (0.095 g, 0.23 mmol) in DMF (4 mL), the reaction was heated to approximately 55 °C and stirred for another 20 h. The resulting crude was purified by column chromatography using 5-20% MeOH in CH_2Cl_2 to give compound **58** (0.04 g, 75%). ^{1}H NMR (600 MHz, $CDCl_3$): δ ppm 4.86 (bs, 2H), 3.02−3.03 (m, 1H), 2.89 (dd, J = 15.0, 4.2 Hz, 1H), 2.82 (t, J = 7.2 Hz, 2H), 2.66 (dt, J = 16.8, 5.4 Hz, 1H), 2.56-2.60 (m, 1H), 2.43 (dd, J = 15.6, 8.4 Hz, 1H), 2.29 (td, J = 6.9, 2.2 Hz, 2H), 2.02-2.05 (m, 1H), 1.96 (t, J = 2.7 Hz, 1H), 1.69-1.76 (m, 3H).

Procedure Q: 2-(4-Phenylpiperazin-1-yl)ethan-1-ol (60a)

A suspension of 1-phenylpiperazine **59a** (4.8 mL, 30.47 mmol), 2-bromoethanol (4.37 mL, 61.61 mmol), and potassium carbonate (12.78 g, 92.47 mmol) in acetonitrile (100 mL) was refluxed for 4 h. The reaction mixture was filtered, and the filtrate was evaporated *in vacuo*. The crude product was purified by column chromatography using 5% MeOH in CH_2Cl_2 to give compound **60a** (5.36 g, 85%). ^{1}H NMR ($CDCl_3$, 600 MHZ): δ ppm 7.27 (t, J = 7.2 Hz, 2H), 6.93 (d, J = 7.8 Hz, 2H), 6.87 (t, J = 7.2 Hz, 1H), 3.66 (t, J = 5.4 Hz, 2H), 3.21 (t, J = 5.4 Hz, 4H), 2.68 (t, J = 5.4 Hz, 4H), 2.61 (t, J = 5.4 Hz, 2H).

2-(4-(2,3-Dichlorophenyl)piperazin-1-yl)ethan-1-ol (60b)

1-(2,3-Dichlorophenyl)piperazine hydrochloride salt (1.5 g) was first treated with saturated $NaHCO_3$ solution and extracted with ethyl acetate to obtain the corresponding free base. A solution of the free base **59b** (0.54 g, 2.34 mmol), 2-bromoethanol (0.33 mL, 4.65 mmol), and potassium carbonate (0.97 g, 7.02 mmol) in acetonitrile (10 mL) was refluxed for 4 h by following procedure Q, and the resulting crude was purified by column chromatography using 5% MeOH in CH_2Cl_2 to give compound **60b** (580 mg, 90%). ^{1}H NMR ($CDCl_3$, 400 MHZ): δ ppm 7.14-7.16 (m, 2H), 6.94-6.97 (m, 1H), 3.67 (t, J = 5.6 Hz, 2H), 3.08 (bs, 4H), 2.71 (bs, 4H), 2.63 (t, J = 5.2 Hz, 2H).

2-(4-(2-Methoxyphenyl)piperazin-1-yl)ethan-1-ol (60c)

1-(2-methoxyphenyl)piperazine hydrochloride salt (1.6 g) was first treated with saturated $NaHCO_3$ solution and extracted with ethyl acetate to obtain the

corresponding free base. A solution of the free base **59c** (1.25 g, 6.50 mmol), 2-bromoethanol (0.58 mL, 8.18 mmol), and potassium carbonate (2.25 g, 16.28 mmol) in ethanol (10 mL) was refluxed for 20 h by following procedure Q, and the resulting crude was purified by column chromatography using 5% MeOH in CH_2Cl_2 to give compound **60c** (1.32 g, 86%). ^{1}H NMR ($CDCl_3$, 600 MHZ): δ ppm 7.00-7.03 (m, 1H), 6.91-6.96 (m, 2H), 6.86 (dd, *J* = 7.8, 1.2 Hz, 1H), 3.87 (s, 3H), 3.66 (t, *J* = 5.4 Hz, 2H), 3.10 (bs, 4H), 2.73 (bs, 4H), 2.63 (t, *J* = 5.4 Hz, 2H).

2-(4-(4-Fluorophenyl)piperazin-1-yl)ethan-1-ol (60d)

A solution of 1-(4-fluorophenyl)piperazine **59d** (1.0 g, 5.55 mmol), 2-bromoethanol (0.79 mL, 11.14 mmol), and potassium carbonate (2.3 g, 16.64 mmol) in acetonitrile (20 mL) was refluxed for 18 h by following procedure Q, and the resulting crude was purified by column chromatography using 15% MeOH in CH_2Cl_2 to give compound **60d** (0.95 g, 77%). ^{1}H NMR ($CDCl_3$, 600 MHZ): δ ppm 6.95-6.98 (m, 2H), 6.87-6.89 (m, 2H), 3.66 (t, *J* = 5.4 Hz, 2H), 3.13 (t, *J* = 4.8 Hz, 4H), 2.68 (t, *J* = 4.8 Hz, 4H), 2.62 (t, *J* = 5.4 Hz, 2H).

2-(4-Phenylpiperazin-1-yl)acetaldehyde (61a)

Sulfur trioxide pyridine complex (0.7 g, 4.40 mmol) was dissolved in DMSO (2 mL) and stirred at 0 °C for 15 min. Then this solution was added into a solution of alcohol **60a** (0.2 g, 0.97 mmol) in CH_2Cl_2 (4 mL) dropwise at 0 °C followed by the addition of Et_3N (1.3 mL, 9.33 mmol). The reaction mixture was stirred at room temperature for 2 h. Later it was quenched with water and extracted with CH_2Cl_2 (3 x 20 mL). The combined organic layer was dried over

Na_2SO_4 and condensed *in vacuo*. The resulting crude was purified by column chromatography using ethyl acetate to give compound **61a** (0.12 g, 61%). ^{1}H NMR ($CDCl_3$, 600 MHZ): δ ppm 9.75 (s, 1H), 7.28 (t, *J* = 8.4 Hz, 2H), 6.94 (d, *J* = 7.8 Hz, 2H), 6.88 (t, *J* = 7.2 Hz, 1H), 3.23-3.27 (m, 6H), 2.71 (t, *J* = 4.8 Hz, 4H).

2-(4-(2,3-Dichlorophenyl)piperazin-1-yl)acetaldehyde (61b)

DMSO (0.186 mL, 2.62 mmol, in 1.5 mL of CH_2Cl_2), oxalyl chloride (0.126 mL, 1.44 mmol in 2 mL of CH_2Cl_2), intermediate **60b** (0.2 g, 0.73 mmol, in 1.5 mL of CH_2Cl_2), and Et_3N (0.8 mL, 5.74 mmol) were added in an order and reacted by following procedure N, and the resulting crude was purified by column chromatography using ethyl acetate to give compound **61b** (0.159 g, 80%). ^{1}H NMR (400 MHz, $CDCl_3$): δ ppm 9.75 (s, 1H), 7.13-7.18 (m, 2H), 6.96-6.99 (m, 1H), 3.28 (s, 2H), 3.12 (bs, 4H), 2.74 (bs, 4H).

2-(4-(2-Methoxyphenyl)piperazin-1-yl)acetaldehyde (61c)

DMSO (0.24 mL, 3.38 mmol, in 1 mL of CH_2Cl_2), oxalyl chloride (0.15 mL, 1.72 mmol in 4 mL of CH_2Cl_2), intermediate **60c** (0.2 g, 0.85 mmol, in 2 mL of CH_2Cl_2), and Et_3N (0.7 mL, 5.02 mmol) were added in an order and reacted by following procedure N, and the resulting crude was purified by column chromatography using ethyl acetate to give compound **61c** (0.134 g, 68%). ^{1}H NMR (600 MHz, $CDCl_3$): δ ppm 9.75 (t, *J* = 1.8 Hz, 1H), 6.98-7.01 (m, 1H), 6.91-6.97 (m, 2H), 6.85-6.87 (m, 1H), 3.85 (d, *J* = 1.8 Hz, 3H), 3.25 (t, *J* = 2.4 Hz, 2H), 3.15 (bs, 4H), 2.74 (bs, 4H).

2-(4-(4-Fluorophenyl)piperazin-1-yl)acetaldehyde (61d)

DMSO (0.25 mL, 3.52 mmol, in 2 mL of CH_2Cl_2), oxalyl chloride (0.155 mL, 1.78 mmol in 4 mL of CH_2Cl_2), intermediate **60d** (0.2 g, 0.89 mmol, in 2 mL of CH_2Cl_2), and Et_3N (0.75 mL, 5.38 mmol) were added in an order and reacted by following procedure N, and the resulting crude was purified by column chromatography using ethyl acetate to give compound **61d** (0.138 g, 70%). ^{1}H NMR (600 MHz, $CDCl_3$): *δ* ppm 9.75 (t, *J* = 1.2 Hz, 1H), 6.95-6.97 (m, 2H), 6.87-6.90 (m, 2H), 3.26 (d, *J* = 1.2 Hz, 2H), 3.18 (t, *J* = 4.8 Hz, 4H), 2.71 (t, *J* = 4.8 Hz, 4H).

(*S*)-*N*^{6}-(2-(4-phenylpiperazin-1-yl)ethyl)-*N*^{6}-(prop-2-yn-1-yl)-4,5,6,7-tetrahydrobenzo[*d*]thiazole-2,6-diamine (62a) (D-674)

Aldehyde **61a** (69 mg, 0.34 mmol) and amine **54** (70 mg, 0. 34 mmol) were reacted in the presence of $NaBH(OAc)_3$ (143 mg, 0.67 mmol) in CH_2Cl_2 (10 mL) at room temperature for 48 h by using procedure E, and the resulting crude was purified by column chromatography using 3-10% MeOH in CH_2Cl_2 to give compound **62a** (40 mg, 30%). ^{1}H NMR (400 MHz, $CDCl_3$): *δ* ppm 7.26 (t, *J* = 8.4 Hz, 2H), 6.92 (d, *J* = 8.0 Hz, 2H), 6.85 (t, *J* = 7.2 Hz, 1H), 4.76 (bs, 2H), 3.57 (d, *J* = 2.0 Hz, 2H), 3.21 (t, *J* = 5.2 Hz, 4H), 3.06-3.13 (m, 1H), 2.81-2.88 (m, 3H), 2.62-2.73 (m, 6H), 2.55-2.60 (m, 3H), 2.22 (t, *J* = 2.4 Hz, 1H), 2.11-2.14 (m, 1H), 1.70-1.80 (m, 1H). $[\alpha]_D^{25}$ (free base) = − 45.81 (*c* = 0.62 in CH_3OH); the free base was converted into its corresponding hydrochloride salt. Mp 158-161 °C. Anal. ($C_{23.5}H_{41}Cl_4N_5O_{1.5}S$) C, H, N.

(*S*)-*N*^{6}-(2-(4-(2,3-dichlorophenyl)piperazin-1-yl)ethyl)-*N*^{6}-(prop-2-yn-1-yl)-4,5,6,7-tetrahydrobenzo[*d*]thiazole-2,6-diamine (62b) (D-629)

Aldehyde **61b** (79 mg, 0.29 mmol) and amine **54** (60 mg, 0. 29 mmol) were reacted in the presence of $NaBH(OAc)_3$ (123 mg, 0.58 mmol) in CH_2Cl_2 (10 mL) at room temperature for 48 h by using procedure E, and the resulting crude was purified by column chromatography using 3-5% MeOH in CH_2Cl_2 to give compound **62b** (35 mg, 26%). ^{1}H NMR (600 MHz, $CDCl_3$): δ ppm 7.14 – 7.17 (m, 2H), 6.95-6.97 (dd, *J* = 7.2, 2.4 Hz, 1H), 4.77 (bs, 2H), 3.58 (d, *J* = 1.8 Hz, 2H), 3.08-3.12 (m, 5H), 2.83-2.88 (m, 3H), 2.72-2.82 (m, 4H), 2.60-2.70 (m, 5H), 2.23 (t, *J* = 1.8 Hz, 1H), 2.12-2.14 (m, 1H), 1.74-1.77 (m, 1H). $[\alpha]_D^{25}$ (free base) = − 22.8 (*c* = 1.0 in CH_3OH); the free base was converted into its corresponding hydrochloride salt. Mp 170-172 °C. Anal. ($C_{23.6}H_{35}Cl_6N_5O_{0.4}S$) C, H, N.

(*S*)-*N*^{6}-(2-(4-(2-methoxyphenyl)piperazin-1-yl)ethyl)-*N*^{6}-(prop-2-yn-1-yl)-4,5,6,7-tetrahydrobenzo[*d*]thiazole-2,6-diamine (62c) (D-676)

Aldehyde **61c** (81 mg, 0.35 mmol) and amine **54** (72 mg, 0. 35 mmol) were reacted in the presence of $NaBH(OAc)_3$ (147 mg, 0.69 mmol) in CH_2Cl_2 (10 mL) at room temperature for 48 h by using procedure E, and the resulting crude was purified by column chromatography using 3-8% MeOH in CH_2Cl_2 to give compound **62c** (41 mg, 28%).^{1}H NMR (400 MHz, $CDCl_3$): δ ppm 6.90-7.02 (m, 3H), 6.86 (d, *J* = 8.0 Hz, 1H), 4.77 (bs, 2H), 3.86 (s, 3H), 3.58 (s, 2H), 3.11 (bs, 5H), 2.83-2.89 (m, 3H), 2.72 (bs, 5H), 2.57-2.62 (m, 4H), 2.21 (d, *J* = 2.0 Hz, 1H), 2.12-2.15 (m, 1H), 1.70-1.80 (m, 1H). $[\alpha]_D^{25}$ (free base) = − 25.4 (*c* = 1.0 in

CH_3OH); the free base was converted into its corresponding hydrochloride salt. Mp 163-165 °C. Anal. ($C_{23}H_{38}Cl_4N_5O_{1.5}S$) C, H, N.

(*S*)-*N*^{6}-(2-(4-(4-fluorophenyl)piperazin-1-yl)ethyl)-*N*^{6}-(prop-2-yn-1-yl)-4,5,6,7-tetrahydrobenzo[*d*]thiazole-2,6-diamine (62d) (D-680)

Aldehyde **61d** (45 mg, 0.20 mmol) and amine **54** (42 mg, 0. 20 mmol) were reacted in the presence of $NaBH(OAc)_3$ (86 mg, 0.41 mmol) in CH_2Cl_2 (10 mL) at room temperature for 44 h by using procedure E, and the resulting crude was purified by column chromatography using 3-10% MeOH in CH_2Cl_2 to give compound **62d** (23 mg, 27%). ^{1}H NMR (600 MHz, $CDCl_3$): δ ppm 6.94-6.97 (m, 2H), 6.86-6.88 (m, 2H), 4.87 (bs, 2H), 3.57 (d, *J* = 2.4 Hz, 2H), 3.07-3.14 (m, 5H), 2.82-2.88 (m, 3H), 2.55-2.71 (m, 9H), 2.22 (d, *J* = 2.4 Hz, 1H), 2.11-2.14 (m, 1H), 1.72-1.78 (m, 1H). $[\alpha]_D^{25}$ (free base) = − 39.6 (*c* = 1.0 in CH_3OH); the free base was converted into its corresponding hydrochloride salt. Mp 156-159 °C. Anal. ($C_{24}H_{40}Cl_4FN_5O_2S$) C, H, N.

(*S*)-*N*^{6}-(2-(4-(2,3-dichlorophenyl)piperazin-1-yl)ethyl)-*N*^{6}-(pent-4-yn-1-yl)-4,5,6,7-tetrahydrobenzo[*d*]thiazole-2,6-diamine (62e) (D-664)

Aldehyde **61b** (58 mg, 0.21 mmol) and amine **58** (60 mg, 0.25 mmol) were reacted in the presence of $NaBH(OAc)_3$ (104 mg, 0.49 mmol) in CH_2Cl_2 (8 mL) at room temperature for 48 h by using procedure E, and the resulting crude was purified by column chromatography using 5-10% MeOH in CH_2Cl_2 to give compound **62e** (30 mg, 29%). ^{1}H NMR ($CDCl_3$, 600 MHz): δ ppm 7.13-7.17 (m, 2H), 6.96 (dd, *J* = 7.2, 2.4 Hz, 1H), 4.79 (bs, 2H), 3.01-3.07 (m, 5H), 2.51-2.74 (m,

14H), 2.27 (td, *J* = 6.6, 2.4 Hz, 2H), 1.98-2.00 (m, 1H), 1.95 (t, *J* = 2.4 Hz, 1H), 1.64-1.77 (m, 3H). $[\alpha]_D^{25}$ (free base) = − 20.93 (*c* = 1.0 in CH_3OH); the free base was converted into its corresponding hydrochloride salt. Mp 177-180 °C. Anal. ($C_{24}H_{37}Cl_6N_5S$) C, H, N.

(*S,E*)-4-(5-((2-amino-4,5,6,7-tetrahydrobenzo[*d*]thiazol-6-yl)(prop-2-yn-1-yl)amino)pent-1-en-1-yl)-2-methoxyphenol (63) (D-649)

Aldehyde **61b** (80 mg, 0.39 mmol) and amine **54** (72 mg, 0.35 mmol) were reacted in the presence of $NaBH(OAc)_3$ (164 mg, 0.77 mmol) in CH_2Cl_2 (10 mL) at room temperature for 40 h using procedure E, and the resulting crude was purified by column chromatography using ethyl acetate to give compound **62e** (48.4 mg, 35%). ^{1}H NMR ($CDCl_3$, 600 MHz): *δ* ppm 6.83-6.87 (m, 3H), 6.31 (d, *J* = 15.6 Hz, 1H), 6.06 (dt, *J* = 15.6, 7.2 Hz, 1H), 4.75 (bs, 2H), 3.90 (s, 3H), 3.49 (dd, *J* = 13.8, 2.4 Hz, 2H), 3.06-3.10 (m, 1H), 2.80 (dd, *J* = 15.6, 5.4 Hz, 1H), 2.70 (t, *J* = 6.6 Hz, 3H), 2.56-2.65 (m, 2H), 2.22 (q, *J* = 6.6 Hz, 2H), 2.20 (t, *J* = 2.4 Hz, 1H), 2.11-2.13 (m, 1H), 1.74 (dq, *J* = 11.4, 5.4 Hz, 1H), 1.63-1.68 (m, 2H). $[\alpha]_D^{25}$ (free base) = − 46.25 (*c* = 1.0 in CH_3OH); the free base was converted into its corresponding hydrochloride salt. Mp 202-205 °C. Anal. ($C_{24}H_{39}Cl_3N_3O_{3.5}S$) C, H, N.

1-(2-((*tert*-Butyldimethylsilyl)oxy)ethyl)piperazine (66)

A suspension of piperazine **64** (10.0 g, 116.09 mmol), (2-bromoethoxy)(tert-butyl)dimethylsilane **65** (11.1 g, 46.4 mmol), and potassium carbonate (48.13 g, 348.27 mmol) in acetonitrile (100 mL) was refluxed for 15 h.

The reaction mixture was filtered, and the filtrate was condensed *in vacuo*. The residue was then diluted with ether, washed with water, dried over Na_2SO_4, filtered, and concentrated to produce intermediate **66** (10.7 g, 95%). ^{1}H NMR ($CDCl_3$, 600 MHz): δ ppm 3.73 (t, J = 6.0 Hz, 2H), 2.86 (t, J = 4.8 Hz, 4H), 2.46−2.50 (m, 6H), 0.86 (s, 9H), 0.03 (s, 6H).

***tert*-Butyl 6-bromo-1H-indole-1-carboxylate (68)**

Into a stirring solution of 6-bromo-1*H*-indole **67** (2.0 g, 10.2 mmol) in THF (20 mL) were added $(Boc)_2O$ (2.45 g, 11.22 mmol) and DMAP (1.37 g, 11.22 mmol) at room temperature. The reaction mixture was stirred at the same temperature for 12 h, and then was condensed *in vacuo*. After the extraction with ethyl acetate (3 × 20 mL) in water, the combined organic layer was dried over Na_2SO_4, filtered, and concentrated *in vacuo.* The crude was purified by column chromatography using 5% ethyl acetate in hexanes to give compound **68** (2.98 g, 99%). ^{1}H NMR ($CDCl_3$, 600 MHz): δ ppm 8.36 (bs, 1H), 7.55 (s, 1H), 7.40 (d, J = 8.4 Hz, 1H), 7.33 (dd, J = 7.2, 1.2 Hz, 1H), 6.52 (d, J = 4.2 Hz, 1H), 1.67 (s, 9H).

***tert*-Butyl 6-(4-(2-((tert-butyldimethylsilyl)oxy)ethyl)piperazin-1-yl)-1H-indole-1-carboxylate (69)**

The mixture of intermediate **68** (0.382 g, 1.29 mmol), intermediate **66** (0.63 g, 2.58 mmol), BINAP (79.7 mg, 0.13 mmol), and Cs_2CO_3 (1.26 g, 3.87 mmol) in toluene (15 mL) was degassed by bubbling N_2 for 5 min. Then $Pd(OAc)_2$ (21.6 mg, 0.10 mmol) was added quickly followed by degassing for another 5 min. The reaction mixture was refluxed for 24 h under inert condition.

Afterward, it was cooled to room temperature, filtered through a pad of celite, washed with CH_2Cl_2, and concentrated *in vacuo*. The resulting crude was purified by column chromatography using 30% ethyl acetate in hexanes to give compound **69** (0.35 g, 59%). ^{1}H NMR ($CDCl_3$, 600 MHz): δ ppm 7.77 (bs, 1H), 7.44 (s, 1H), 7.40 (d, *J* = 8.4 Hz, 1H), 6.93 (dd, *J* = 6.6, 2.4 Hz, 1H), 6.45 (d, *J* = 3.6 Hz, 1H), 3.81 (t, *J* = 6.6 Hz, 2H), 3.25 (t, *J* = 4.8 Hz, 4H), 2.72 (t, *J* = 4.8 Hz, 4H), 2.60 (t, *J* = 6.0 Hz, 2H), 1.65 (s, 9H), 0.91 (s, 9H), 0.08 (s, 6H).

***tert*-Butyl 6-(4-(2-hydroxyethyl)piperazin-1-yl)-1H-indole-1-carboxylate (70)**

Compound **69** (0.57 g, 1.24 mmol) was reacted with TBAF 1M in THF (1.49 mL, 1.49 mmol) in THF (10 mL) following procedure J for 2 h. The crude was purified by silica gel column chromatography using 20% MeOH in ethyl acetate to give compound **69** (0.31 g, 72%). ^{1}H NMR ($CDCl_3$, 600 MHz): δ ppm 7.78 (bs, 1H), 7.45 (s, 1H), 7.41 (dd, *J* = 5.4, 3.0 Hz, 1H), 6.91−6.93 (m, 1H), 6.45 (d, *J* = 3.6 Hz, 1H), 3.68 (t, *J* = 6.0 Hz, 2H), 3.25−3.26 (m, 4H), 2.72−2.73 (m, 4H), 2.60−2.64 (m, 2H), 1.66 (s, 9H).

***tert*-Butyl 7-chloro-6-(4-(2-oxoethyl)piperazin-1-yl)-1H-indole-1-carboxylate (71)**

DMSO (0.33 mL, 4.63 mmol, in 1.5 mL of CH_2Cl_2), oxalyl chloride (0.22 mL, 2.55 mmol, in 2 mL of CH_2Cl_2), intermediate **70** (0.4 g, 1.16 mmol, in 5 mL of CH_2Cl_2), and Et_3N (0.97 mL, 6.95 mmol) were added in order and reacted following procedure N, and the resulting crude was purified by column chromatography using 40% ethyl acetate in hexanes to give compound **71** (0.21

g, 48%). ^{1}H NMR ($CDCl_3$, 600 MHz): *δ* ppm 9.76 (s, 1H), 7.44 (d, *J* = 3.6 Hz, 1H), 7.41 (d, *J* = 8.4 Hz, 1H), 7.02 (d, *J* = 8.4 Hz, 1H), 6.49 (d, *J* = 3.6 Hz, 1H), 3.24−3.29 (m, 4H), 3.20 (m, 4H), 2.76 (m, 2H), 1.64 (s, 9H).

tert-Butyl (_S_)-6-(4-(2-((2-amino-4,5,6,7-tetrahydrobenzo[_d_]thiazol-6-yl)(prop-2-yn-1-yl)amino)ethyl)piperazin-1-yl)-7-chloro-1H-indole-1-carboxylate (72)

Aldehyde **71** (0.2 g, 0.53 mmol) and amine **54** (0.1 g, 0.48 mmol) were reacted in the presence of $NaBH(OAc)_3$ (0.22 g, 1.06 mmol) in CH_2Cl_2 (20 mL) at room temperature for 65 h using procedure E, and the resulting crude was purified by column chromatography using 10% MeOH in CH_2Cl_2 to give compound **72** (0.06 g, 23%).^{1}H NMR ($CDCl_3$, 600 MHz): *δ* ppm 7.43 (d, *J* = 3.0 Hz, 1H), 7.39 (d, *J* = 7.8 Hz, 1H), 7.01 (d, *J* = 8.4 Hz, 1H), 6.48 (d, *J* = 3.6 Hz, 1H), 4.77 (bs, 2H), 3.58 (d, *J* = 2.4 Hz, 2H), 3.10-3.16 (m, 5H), 2.83-2.88 (m, 3H), 2.59-2.73 (m, 9H), 2.23 (t, *J* = 1.8 Hz, 1H), 2.13-2.15 (m, 1H), 1.73-1.79 (m, 1H), 1.64 (s, 9H). $[\alpha]_D^{25}$ (free base) = − 28.0 (*c* = 1.0 in CH_3OH).

Procedure R: (_S_)-_N_^{6}-(2-(4-(7-chloro-1H-indol-6-yl)piperazin-1-yl)ethyl)-_N_^{6}-(prop-2-yn-1-yl)-4,5,6,7-tetrahydrobenzo[_d_]thiazole-2,6-diamine (73) (D-635)

Into a stirred solution of compound **72** (0.017 g, 0.03 mmol) in CH_2Cl_2 (2 mL) at 0 °C, trifluoroacetic acid (TFA) (2 mL) was added slowly and the reaction mixture was stirred for another 2 h at room temperature. Unreacted TFA and solvent were removed *in vacuo*, and the obtained solid was washed with ether for several times followed by drying to yield the TFA salt of **73** (0.017 g, 79%). ^{1}H NMR (CD_3OD, 600 MHz): *δ* ppm 7.48 (d, *J* = 7.8 Hz, 1H), 7.26 (d, *J* = 3.0 Hz, 1H),

6.95 (d, *J* = 8.4 Hz, 1H), 6.45 (d, *J* = 3.6 Hz, 1H), 3.63 (d, *J* = 2.4 Hz, 2H), 3.42 (t, *J* = 6.0 Hz, 2H), 3.34 (s, 3H), 3.29-3.30 (m, 5H), 3.18-3.24 (m, 3H), 2.80 (dd, *J* = 15.6, 4.8 Hz, 1H), 2.78 (t, *J* = 2.4 Hz, 1H), 2.67-2.71 (m, 2H), 2.58-2.62 (m, 1H), 2.19 (d, *J* = 10.8 Hz, 1H), 1.84-1.91 (m, 1H). HRMS m/z $[M + H]^+$: calcd for $C_{24}H_{29}ClN_6SH$, 469.1941; found, 469.1930. $[\alpha]_D^{25}$ = −21.33 (c = 1.0 in CH_3OH). Mp 118-122 °C. Anal. ($C_{28.8}H_{37}ClF_6N_6O_{6.2}S$) C, H, N.

***tert*-Butyl (*S*)-5-(4-(2-((2-amino-4,5,6,7-tetrahydrobenzo[*d*]thiazol-6-yl)(prop-2-yn-1-yl)amino)ethyl)piperazin-1-yl)-4-chloro-1H-indole-1-carboxylate (75)**

Aldehyde **74** (0.22 g, 0.58 mmol), which was obtained according to literature (Johnson et al. 2012, 2013), and amine **54** (0.11 g, 0.52 mmol) were reacted in the presence of $NaBH(OAc)_3$ (0.25 g, 1.16 mmol) in CH_2Cl_2 (12 mL) at room temperature for 40 h using procedure E, and the resulting crude was purified by column chromatography using 5% MeOH in CH_2Cl_2 to give compound **75** (0.08 g, 29%). ^{1}H NMR ($CDCl_3$, 600 MHz): *δ* ppm 7.98 (bs, 1H), 7.59 (s, 1H), 7.09 (dd, *J* = 6.6, 2.4 Hz, 1H), 6.67 (d, *J* = 3.6 Hz, 1H), 5.07 (bs, 2H), 3.58 (d, *J* = 2.4 Hz, 2H), 3.11-3.15 (m, 5H), 2.82-2.89 (m, 3H), 2.68-2.74 (m, 4H), 2.56-2.65 (m, 4H), 2.51 (s, 1H), 2.24 (t, *J* = 2.4 Hz, 1H), 2.12-2.14 (m, 1H), 1.71-1.78 (m, 1H), 1.66 (s, 10H). $[\alpha]_D^{25}$ = −28.3 (c = 1.0 in CH_2Cl_2).

(*S*)-*N*^{6}-(2-(4-(4-chloro-1H-indol-5-yl)piperazin-1-yl)ethyl)-*N*^{6}-(prop-2-yn-1-yl)-4,5,6,7-tetrahydrobenzo[d]thiazole-2,6-diamine (76) (D-614)

Compound **75** (0.07 g, 0.12 mmol) was reacted with trifluoroacetic acid (3 mL) in CH_2Cl_2 (3 mL) following procedure R to produce the TFA salt of **76** (0.1 g,

90%). ^{1}H NMR (CD_3OD, 600 MHz): δ ppm 7.29 (dd, J = 6.0, 3.0 Hz, 1H), 7.24 (dd, J = 6.6, 3.0 Hz, 1H), 7.00 (q, J = 8.4 Hz, 1H), 6.47 (d, J = 3.0 Hz, 1H), 3.59 (d, J = 2.4 Hz, 2H), 3.33 (s, 1H), 3.10-3.15 (m, 5H), 2.95-2.99 (m, 5H), 2.77-2.85 (m, 3H), 2.66-2.67 (m, 1H), 2.59-2.64 (m, 2H), 2.48-2.53 (m, 2H), 2.11-2.13 (m, 1H), 1.72-1.80 (m, 1H). LRMS m/z $[M + H]^+$: calcd for $C_{24}H_{29}ClN_6SH$, 469.19; found, 469.19. $[\alpha]_D^{25}$ = −19.6 (c = 1.0 in CH_3OH). Mp 165-170 °C. Anal. ($C_{31}H_{34}Cl_3F_9N_6O_6S$) C, H, N.

1,6-Dimethoxynaphthalene (78)

Intermediates **78**-**81** were synthesized based on a published procedure with slight modification (Hirayama, Ikunaka, and Matsumoto 2005). Into a stirring suspension of 1,6-dihydroxynaphthalene **77** (20 g, 124.87 mmol) and potassium carbonate (63.8 g, 461.62 mmol) in acetone (80 mL), dimethyl sulfate (41.5 mL, 437.60 mmol) was added slowly over 15 min at room temperature. The mixture was refluxed for 4h and was cooled to room temperature afterwards. It was filtered, and the filtrate was evaporated *in vacuo*. The resulting crude was purified by column chromatography using 5% ethyl acetate in hexanes to give compound **78** (15.9 g, 68%). ^{1}H NMR ($CDCl_3$, 600 MHz): δ ppm 8. 25 (d, J = 9.6 Hz, 1H), 7.38-7.42 (m, 2H), 7.21 (dd, J = 10.8, 1.8 Hz, 1H), 7.16 (d, J = 2.4 Hz, 1H), 6.72 (d, J = 7.2 Hz, 1H), 4.01 (s, 3H), 3.94 (s, 3H).

5-Methoxy-3,4-dihydronaphthalen-2(1*H*)-one (79)

Slices of sodium (14.7 g, 639.41 mmol) was added into a stirring solution of intermediate **78** (10 g, 53.13 mmol) in EtOH (250 mL) over 45 min at 40-60 °C,

and the reaction mixture was refluxed for 2h. Then it was gradually cooled 0 °C, and water (100 mL) was added with caution. Concentrated aqueous hydrochloric acid (approximately 50 mL) was added drop wise into the mixture to reduce the pH of solution to around 2, and it was refluxed for another 1 h. The solvents were removed in vacuo, and CH_2Cl_2 (4 x 200 mL) was used to extract the product. The resulting crude was purified by column chromatography using 3-4% ethyl acetate in hexanes to give compound **79** (5.71 g, 61%). ^{1}H NMR ($CDCl_3$, 600 MHz): δ ppm 7.18 (t, J = 7.8 Hz, 1H), 6.78 (d, J = 7.8 Hz, 1H), 6.74 (d, J = 7.8 Hz, 1H), 3.85 (s, 3H), 3.57 (s, 2H), 3.09 (t, J = 6.6 Hz, 2H), 2.53 (t, J = 6.6 Hz, 2H).

(*E*)-5-methoxy-3,4-dihydronaphthalen-2(1*H*)-one O-methyl oxime (80)

Methoxyamine hydrochloride (3.87 g, 46.34 mmol) was first dissolved in 60% (v/v) aqueous solution of MeOH (50 mL), and then sodium acetate (3.8 g, 46.32 mmol) was added at room temperature to render the mixture pH neutral. A solution of **79** (4.9 f, 27.81 mmol) in the same MeOH aqueous solution (50 mL) was added slowly, and the reaction mixture was continued to stir at room temperature for 2 h. The solvents were evaporated to one third in vacuo, and ethyl acetate (3 x 100 mL) was used extracted the product. The obtained crude was purified by column chromatography using 2% ethyl acetate in hexanes to give compound **80** (5.06 g, 89%). ^{1}H NMR ($CDCl_3$, 600 MHz): δ ppm 7.14 (t, J = 7.8 Hz, 1H), 6.70-6.80 (m, 2H), 3.89 and 3.84 (s, total 3H), 3.83 (s, 3H), 3.75 and 3.49 (s, total 2H), 2.87 (dt, J = 9.6, 6.6 Hz, 2H), 2.62 and 2.51 (t, J = 6.6 Hz, total 2H).

5-Methoxy-1,2,3,4-tetrahydronaphthalen-2-amine hydrochloride (81)

Into a solution of intermediate **80** (1.28 g, 6.24 mmol) in MeOH (25 mL) and 10% (w/v) solution of HCl in MeOH (11 mL), 10% Pd/C (128 mg, 10% of wt) was added in portions with caution. The resultant suspension was placed at a shaker hydrogenation apparatus and shaken under an atmosphere of hydrogen (initial pressure 2.0 bar) at room temperature for 2.5 h. The reaction mixture was filtered through celite to remove the catalyst and washed with MeOH (3 x 20 mL). The combined filtrate was concentrated in vacuo, and recrystallized with ethyl acetate (25 mL). The precipitated solid was filtered and dried to give compound **81** (0.94 g, 71%). ^{1}H NMR ($CDCl_3$, 600 MHz): δ ppm 7.12 (t, J = 7.8 Hz, 1H), 6.76 (d, J = 8.4 Hz, 1H), 6.70 (d, J = 7.8 Hz, 1H), 3.80 (s, 3H), 3.47-3.50 (m, 1H), 3.10 (dd, J = 15.6, 4.8 Hz, 1H), 2.95 (dt, J = 18.0, 5.4 Hz, 1H), 2.81 (dd, J = 15.6, 9.6 Hz, 1H), 2.63-2.69 (m, 1H), 2.19-2.23 (m, 1H), 1.75-1.82 (m, 1H).

***N*-(2-(4-(2,3-dichlorophenyl)piperazin-1-yl)ethyl)-5-methoxy-1,2,3,4-tetrahydronaphthalen-2-amine (82)**

Aldehyde **61b** (270 mg, 0.99 mmol) and amine **81** (175 mg, 0. 99 mmol) were reacted in the presence of $NaBH(OAc)_3$ (419 mg, 1.98 mmol) in CH_2Cl_2 (15 mL) at room temperature for 40 h by using procedure E, and the resulting crude was purified by column chromatography using 5% MeOH in CH_2Cl_2 to give compound **82** (359 mg, 84%). ^{1}H NMR ($CDCl_3$, 600 MHz): δ ppm 7.13-7.17 (m, 2H), 7.10 (t, J = 7.8 Hz, 1H), 6.95 (dd, J = 7.2, 3.0 Hz, 1H), 6.71 (d, J = 7.8 Hz,

1H), 6.66 (d, *J* = 8.4 Hz, 1H), 3.81 (s, 3H), 3.49 (t, *J* = 1.8 Hz, 3H), 3.01-3.04 (m, 5H), 2.87-2.96 (m, 4H), 2.56-2.68 (m, 8H), 2.10-2.12 (m, 1H), 1.16-1.65 (m, 1H).

_N_-(2-(4-(2,3-dichlorophenyl)piperazin-1-yl)ethyl)-5-methoxy-_N_-(prop-2-yn-1-yl)-1,2,3,4-tetrahydronaphthalen-2-amine (83)

Intermediate **82** (57 mg, 0.13 mmol) was reacted with propargyl bromide **52** (15 µL, 0.19 mmol) in the presence of potassium carbonate (127 mg, 0.92 mmol) in acetonitrile (10 mL) at 50-60 °C for 4 h by following procedure O, and the resulting crude was purified by column chromatography using ethyl acetate to give compound **83** (33 mg, 53%). ^{1}H NMR ($CDCl_3$, 600 MHz): δ ppm 7.12-7.16 (m, 2H), 7.09 (t, *J* = 7.8 Hz, 1H), 6.96 (dd, *J* = 7.2, 2.4 Hz, 1H), 6.71 (d, *J* = 7.8 Hz, 1H), 6.65 (d, *J* = 7.8 Hz, 1H), 3.80 (s, 3H), 3.61 (d, *J* = 2.4 Hz, 2H), 2.94-3.04 (m, 7H), 2.89 (t, *J* = 7.2 Hz, 2H), 2.70-2.82 (m, 5H), 2.53-2.64 (m, 3H), 2.17-2.20 (m, 2H), 1.59-1.64 (m, 1H).

6-((2-(4-(2,3-dichlorophenyl)piperazin-1-yl)ethyl)(prop-2-yn-1-yl)amino)-5,6,7,8-tetrahydronaphthalen-1-ol (84) (D-675)

Intermediate **83** (70 mg, 0.15 mmol) was reacted with BBr_3 (1M in CH_2Cl_2) (0.44 mL, 0.44 mmol) in CH_2Cl_2 (10 mL) at −40 °C for 2h and room temperature for another 2 h by following procedure F. The crude obtained was purified by column chromatography using ethyl acetate to afford compound **84** (57 mg, 84%). ^{1}H NMR ($CDCl_3$, 600 MHz): δ ppm 7.13-7.17 (m, 2H), 6.95-7.00 (m, 2H), 6.65 (d, *J* = 7.8 Hz, 1H), 6.56 (d, *J* = 7.8 Hz, 1H), 3.57 (d, *J* = 2.4 Hz, 2H), 3.10 (bs, 4H),

2.86-2.98 (m, 5H), 2.66-2.75 (m, 5H), 2.62 (t, *J* = 7.2 Hz, 2H), 2.53-2.58 (m, 1H), 2.21 (t, *J* = 2.4 Hz, 1H), 2.14-2.18 (m, 1H), 1.55-1.60 (m, 1H).

4.2. Dopamine D_2 and D_3 Receptor Assays

The binding assay was carried out to determine the inhibition constants (K_i) of the synthesized compounds by observing the inhibition of [^{3}H] spiroperidol (15 Ci/mmol, PerkinElmer) binding to rD_2 or rD_3 receptors expressed in HEK-293 cells in a buffer containing 0.9% NaCl (Ghosh et al. 2010, Zhen et al. 2010). The Cheng–Prusoff equation was used to convert the observed IC_{50} into inhibition constants (K_i) (Zhen et al. 2010). The functional activity of selected compounds was assessed by measuring stimulation of [^{35}S]GTPγS (1,250 Ci/mmol, PerkinElmer) binding in comparison to dopamine, the full agonist, to evaluate their ability of activating hD_2 and hD_3 receptors expressed in CHO cells as described by us previously (Ghosh et al. 2010, Zhen et al. 2010).

4.3. Reagents for biological evaluations

Dulbecco's phosphate-buffered saline, thioflavin T (ThT), thiazolyl blue tetrazolium bromide (MTT), human recombinant monoamine oxidase (MAO) enzymes, kynuramine, and pargyline were purchased from Sigma-Aldrich. Uranyl acetate and formvar-coated carbon-stabilized copper grid (400 mesh) were purchased from Electron Microscopy Sciences (EMS). Dimethyl sulfoxide (DMSO) and methanol were purchased from Fischer Scientific.

4.4. *In vitro* αSN anti-aggregation study

Selected novel multifunctional D_2/D_3 dopamine agonists were tested in an *in vitro* assay to determine their ability to inhibit αSN aggregation. The plasmid pET28 containing αSN expressing cDNA was used for recombinant synthesis and purification of the protein by following the published procedure (Huang et al. 2005, Shevchik, Condemine, and Robertbaudouy 1994). The purified protein was aliquoted, lyophilized, and then stored at −80 °C.

4.4.1. Shaking study

All the samples were prepared in sterilized PBS (pH = 7.4). The lyophilized recombinant αSN was first dissolved in PBS and filtered through a 0.22 μm filter to remove preformed aggregates. Samples of αSN (60 μM) were shaken (1,400 rpm) in the presence or absence of test compound (120 μM), **(−)-8a (D-593)**, in a Thermomixer R shaker (Eppendorf, Hamburg, Germany) at 37 °C for a period of 6 days. **D-520** was used as the reference compound here. Drugs were also tested alone (120 μM) to show any direct effect on assays. Aliquots were collected at the beginning (0D) and at the endpoint (6D) of the experiment, which were analyzed by transmission electron microscope (TEM), circular dichroism (CD) spectra to gain information on the morphology and protein structure of αSN. In addition, thioflavin T (ThT) assay and cell viability assay were used to determine the effect of compounds on αSN fibrilization and toxicity. Assays were carried out in three independent experiments.

4.4.2. Preparation of αSN preformed fibrils (PFF)

The lyophilized recombinant αSN was dissolved in sterilized PBS (pH = 7.4). and filtered through a 0.22 μm filter to remove preformed aggregates. Then a solution of αSN (5 mg/mL) was shaken (1,000 rpm) at 37ºC in a Thermomix R shaker (Eppendorf, Hamburg, Germany) for a period of 5 days, which was aliquoted and stored at -80ºC until use (Volpicelli-Daley et al. 2011).

4.4.3. Seeding study

All the samples were prepared in sterilized PBS (pH = 7.4). The lyophilized recombinant αSN was first dissolved in PBS and filtered through a 0.22 μm filter to remove preformed aggregates. Monomeric αSN at 1.25 mg/mL (86.45 μM) was seeded with 0.5% (v/v) of PFFs at 37ºC in the presence or absence of test compounds (−)-**8a** (**D-593**), (−)-**20** (**D-618**), and (−)-**14** (**D-644**) at 172.9 μM without agitation. Monomeric αSN (86.45 μM) without seeding and drugs alone (172.9 μM) were also tested. Aliquots were collected at 0D, 10D time points. For compound (−)-**49** (**D-670**), an extended seeding experiment was carried out for 30 days in comparison to its parent compound **D-520**, and aliquots were collected at 0D, 10D, 20D, and 30D time points. TEM and CD spectra were used to characterize the morphology and structure of αSN in the seeded aggregation. The aliquots were analyzed by ThT assay and cell viability assay to determine the effect of compounds on αSN fibrilization and toxicity. Assays were carried out in three independent experiments.

4.4.4. Transmission electron microscope (TEM)

The aliquots obtained from the shaking and seeding studies were characterized by TEM. Protein aliquots (4 µL) were applied to the formvar-coated carbon-stabilized copper grids (400 mesh) and absorbed for 4 min. The grids were then rinsed briefly with distilled water twice, negatively stained with 2% aqueous uranyl acetate solution, air-dried, and examined with a JEOL (JEM 2010) transmission electron microscope at an accelerating voltage of 200 kV and 80,000 magnification.

4.4.5. Circular dichroism (CD)

CD spectra were obtained using a Jasco J-1500 CD spectrophotometer to characterize the secondary structure of collected αSN aliquots. αSN samples were diluted to 20 µM by ultrapure water to minimize the absorption caused by buffer for CD spectra measurements. Spectra were recorded in a 0.1 mm path-length cuvette from 260 to 190 nm with a step size of 1 nm and a bandwidth of 1 or 3 nm. For all spectra, an average of five scans was obtained. CD spectra of the appropriate buffer was recorded and subtracted from the protein spectra.

4.4.6. Thioflavin T (ThT) assay

The extent of fibrillization of αSN was evaluated with ThT fluorescence assay (Narkiewicz, Giachin, and Legname 2014). The assay was carried out following a published protocol (Modi et al. 2014). 10 µL of the aliquots were mixed with 10 µL of ThT solution (40 µM in PBS) in a 384 well black plate (solid bottom, Corning). ThT fluorescence level was measured in duplicates immediately after addition by using the Synergy Hybrid H1 fluorescence

microplate reader (BioTek) at 440/485 nm (excitation/emission) wavelength with auto-sensitivity mode. Assays were carried out in three independent experiments.

4.4.7. Cell viability

PC12 cells were seeded at 17,000 cells/well density in a 96-well plate and allowed to attach for 24 h. The collected αSN aliquots were diluted with cell medium and treated to the cells for 24 h; the final concentration resulted from dilution were 10 μM for αSN and 20 μM for the compounds. The cell viability was measured by MTT assay, which will be described in details in the section 4.6.1.

4.5. Human monoamine oxidase (hMAO) inhibition studies

To determine the ability of selected compounds in inhibiting MAO enzyme, a fluorometric screening was carried out following published protocols with some modifications (Yan et al. 2004, Novaroli et al. 2005, Chimenti et al. 2013). The activity of enzyme was determined by measuring the fluorescence generated from the MAO catalyzed oxidation of kynuramine to 4-hydroxyquinoline (4-HQ). Commercially available microsomes from insect cells containing recombinant hMAO-A and hMAO-B (Sigma-Aldrich) were used as the enzyme source in this study. They were pre-aliquoted to avoid repeated freeze-thaw cycles and stored at −80 °C. During experiment preparation, they were thawed rapidly in a 37 °C water bath and kept on ice until use. Kynuramine was used as the substrate for both MAO-A and MAO-B, and potassium phosphate buffer (0.1 M, pH 7.4, made isotonic with KCl 20.2 mM) was used as the assay buffer. The final volume of the

reaction was set to 200 µL. Pargyline, a potent MAO-B inhibitor, was included in the assay as a reference compound.

4.5.1. Initial hMAO-B inhibition screening

Selected compounds were first examined at a dose of 25 µM for their inhibitory activity against hMAO-B. The final concentration of enzyme and substrate were set to 15 µg/mL and 25 µM, respectively. Stocks of compounds (50 mM) were prepared in DMSO, whose percentage was kept at 0.05% in the final assay reaction mixture. Substrate (50 µL/well) and compound solutions (100 µL/well) were added into a black 96-well plate and pre-incubated at 37 °C for 10 min. The control wells received assay buffer instead of compound solutions. The enzymatic reaction was initiated by the addition of hMAO-B solution (50 µL/well). The reaction mixture was then incubated at 37 °C for 20 min, and subsequently 2N NaOH aqueous solution (75 µL/well) was added to terminate the reaction. The fluorescence of 4-HQ, was measured in triplicates using the Synergy Hybrid H1 fluorescence microplate reader (BioTek) at the wavelength pair of 310/400 nm (excitation/emission), and the readings were averaged and normalized with respect to the control. Assays were carried out in three independent experiments.

4.5.2. IC_{50} values determination

Compounds, which reduced the hMAO-B activity to near half in the initial screening were considered hit molecules and were tested further for the IC_{50} values for both hMAO-A and hMAO-B to determine their selectivity index. Seven doses of test compounds (0-250 µM) were used, and the final concentration of

enzyme was set to 15 µg/mL. The final concentrations of substrate for measuring either hMAO-A or hMAO-B activity were set to 40 µM and 25 µM, respectively. The fluorescence was measured in either duplicates or triplicates, and the IC_{50} values were determined from non-linear regression of dose-response curves using GraphPad Prism 6.0 (GraphPad Software, San Diego, CA, USA). Assays were carried out in three independent experiments.

4.6. Cell culture and treatments

PC12 Adh cells (ATCC® CRL1721.1™, Manassas, VA, USA), a rat adrenal pheochromocytoma cell line, were cultured in T-75 flasks (Greiner Bio One, Frickenhausen, Germany) and maintained in RPMI 1640 medium supplemented with 10% heat-inactivated horse serum, 5% fetal bovine serum, 100 units/mL penicillin, and 100 µg/mL streptomycin at 37 °C in 5% CO_2 atmosphere. Stock solutions of compounds (−)-**8a** (**D-593**), (−)-**20** (**D-618**), (−)-**14** (**D-644**), (−)-**49** (**D-670**), **76** (**D-614**), **62b** (**D-629**) (100 mM) and rotenone (40 mM) were prepared in DMSO and stored at −20 °C. Stock solution (1 M) of 6-hydroxydopamine (6-OHDA) was prepared in DMSO and aliquots were stored at −80 °C.

4.6.1. Cytotoxicity assay in PC12 cells

The effect of compounds (−)-**8a** (**D-593**), (−)-**20** (**D-618**), (−)-**14** (**D-644**), (−)-**49** (**D-670**), **76** (**D-614**), and **62b** (**D-629**) on the viability of PC12 cells were tested. 24 h after plating the cells at 17,000 cells/well density in a 96-well plate, increasing doses of the selected compounds were added resulting the final

concentrations to be 0.1-50 µM. Control cells received 0.01% DMSO containing medium instead. After 24 h of treatment, MTT assay was performed. Following the addition of 5 mg/mL MTT solution (prepared in Dulbecco's phosphate-buffered saline) to the cells to a final concentration of 0.5 mg/mL, the plates were further incubated at 37 °C in 5% CO_2 atmosphere for 3−4 h to produce dark-blue formazan crystals. Then the plates were centrifuged for 10 min at 450 rpm, and the supernatants were carefully removed. Formazan crystals were then dissolved in MeOH:DMSO (1:1) mixture and shaken gently at 400 rpm for 30 min at room temperature on a Thermomix R shaker (Eppendorf, Hamburg, Germany). The absorbance (*A*) was measured at a dual wavelength of 570 nm and 690 nm on a microplate reader (Biotek Epoch, Winooski, VT, USA) and adjusted with a background correction (A_{570}-A_{690}). Cell viability was normalized and plotted as percentage of background corrected values compared to untreated controls. Assays were carried out in three independent experiments.

4.6.2. Neuroprotection against 6-OHDA-induced toxicity in PC12 cells

For assessing the neuroprotective effects of test compounds (−)-**8a** (**D-593**), (−)-**20** (**D-618**), (−)-**14** (**D-644**), (−)-**49** (**D-670**), **76** (**D-614**), and **62b** (**D-629**) on 6-OHDA mediated cell death, a quantitative colorimetric MTT assay was used. PC12 cells were seeded at 17,000 cells/well density in a 96-well plate and allowed to adhere for 24 h. Increasing concentrations of compounds were added to the cells to make the final concentration to be 0.1-50 µM. Control cells and 6-OHDA control cells received 0.01% DMSO containing medium. After 24 h of pre-

treatment, the drug containing medium was removed. Cells were exposed to 75 μM 6-OHDA and control cells were treated with 0.01% DMSO containing medium for additional 24 h. Afterward, MTT assay was performed as described previously. Assays were carried out in three independent experiments.

4.6.3. Neuroprotection against rotenone-induced toxicity in PC12 cells

Compound **76** (**D-614**) was also tested in another neurotoxin induced cytotoxicity model in PC12 cells. PC12 cells were seeded at 10,000 cells/well density in a 96-well plate and allowed to adhere for 24 h. Increasing doses of compound **76** (**D-614**) was pre-treated to the cells for 1 h to make the final concentrations to be 1-50 μM. Then 1 μM of rotenone was cotreated to the cells for another 24 h. Afterward, MTT assay was performed as described previously. Assays were carried out in three independent experiments.

4.7. Animal experiments

4.7.1. Drugs and chemicals

The following commercially available drugs were used in the experiment: reserpine hydrochloride (Alfa Aesar) and ropinirole (Sigma-Aldrich). Reserpine was dissolved in 10−25 μL of glacial acetic acid and further diluted with 5.5% glucose solution. The hydrochloride salts of compound (−)-**8a** (**D-593**), (−)-**20** (**D-618**), **76** (**D-614**), and ropinirole were dissolved in DI water. The hydrobromic salt of compounds (−)-**49** (**D-670**) and **D-520** were dissolved in 3% and 5% (2-hydroxypropyl)-β-cyclodextrin, respectively, due to low solubility in DI water. All compounds for this study were administered in a volume of 0.1−0.2 mL for

subcutaneous administration and 0.5−0.7 mL for intraperitoneal administration into each rat.

4.7.2. Animals

In rodent studies, animals were male Sprague−Dawley rats from Harlan (Indianapolis, IN) weighing 220−225 g unless otherwise noted. Animals were maintained in sawdust-lined cages in a temperature and humidity controlled environment at 22 ± 1 °C and 60 ± 5%, respectively. A 12 h light/dark cycle was also maintained, with lights on from 6:00 a.m. to 6:00 p.m. They were group-housed with unrestricted access to food and water. All experiments were performed during the light component. All animal use procedures were in compliance with the Wayne State University Investigation Committee consistent with AALAC guidelines.

4.7.3. Reversal of reserpine-induced hypolocomotion in rats

Administrating reserpine, the irreversible inhibitor of the vesicular monoamine transporter (VMAT), blocks the internalization of monoamines into vesicles and leads to the loss of storage capacity. Unprotected monoamines in the cytosol undergo metabolism, resulting in the depletion of monoamines in the synapse of the peripheral sympathetic nerve terminals, which induces catalepsy in rodents (Fernandes et al. 2012, Duty and Jenner 2011, Leao et al. 2015). The effects of compounds (−)-**8a** (**D-593**), (−)-**20** (**D-618**), **76** (**D-614**) and (−)-**49** (**D-670**) in reversing reserpine-induced hypolocomotion were tested following a reported procedure (McCall et al. 2005). Ropinirole was used as a reference

D_2/D_3 agonist in this study. Reserpine (5.0 mg/kg, s.c.) was administered to isoflurane-anaesthetized rats 18 h before the injection of drugs or vehicle. Prior to administration of test compounds, reference drug or vehicle, the rats were placed individually in the chambers for 1 h for acclimatization. Immediately after administration of either drugs or vehicle, animals were individually placed in an Opto-Varimex-4 animal activity monitor chamber (Columbus Instruments, Ohio, USA), and locomotor activity was monitored for 6 h. Horizontal activity (HACTV) was recorded as consecutive interruption of two infrared beams, situated 50 cm apart and 4 cm above the cage floor in the monitor chamber. The effect of drugs on locomotor activity was compared with respect to saline treated controls (means ± SEM).

4.8. Statistical analysis

Statistical analyses were performed using GraphPad Prism 6.0 (GraphPad Software, San Diego, CA, USA). For all the *in vitro* assays, the data were analyzed by one-way analysis of variance (ANOVA) analysis followed by Tukey's multiple comparison post hoc test unless otherwise specified. And for the *in vivo* assays, one-way ANOVA analysis followed by Dunnett's analysis was used. The effect was considered significant if the difference from control group was observed at $p < 0.05$.

CHAPTER 5 CONCLUSION

The pathogenesis of Parkinson's disease (PD) has been found to be multifactorial, and its complexity suggests that multifunctional therapeutics could be beneficial for its treatment. Therefore, it is hypothesized that the incorporation of pharmacological properties targeting α-synuclein (αSN) aggregation and monoamine oxidase-B (MAO-B) activity into the dopamine D_2/D_3 agonistic components may confer disease-modifying as well as symptom-relieving effects.

The first main objective was to generate a series of novel dopamine D_2/D_3 receptor agonists that can potentially modulate αSN aggregation by incorporating the dihydroxy or hydroxy-methoxy component to the D_2/D_3 agonist fragments via various linkers based on the hybrid molecular template. In this current structure-activity relationship (SAR) study, the effects of linker length and stereochemistry on D_2/D_3 receptors binding were first assessed: compounds with elongated five- or six-carbon linkers were found to considerably enhance the binding affinity towards both D_2/D_3 receptors. Overall, it has been found that variation of linker lengths and the changes in the stereochemistry at the linker region may either increase or decrease the binding affinity. Afterwards, the influence of terminal dihydroxy or hydroxy-methoxy component on D_2/D_3 receptors affinity was also analyzed: the dihydroxy substitutions generally gave enhanced binding profiles comparing to their corresponding hydroxy-methoxy analogs. Then, the effect of agonist binding head group was briefly examined. In consistent to the previous findings, all the (−)-isomers tested displayed higher binding affinities for both

D_2/D_3 receptors, in comparison to their racemic counterparts. Furthermore, the bioisosteric replacement of the 2-aminothiazole head group in compound (−)-**8a** (**D-593**) with aminotetralin moiety in compound (−)-**14** (**D-644**) was found to produce a greater enhancement in the D_2/D_3 receptor binding. Five compounds (−)-**7a** (**D-591**)**,** (−)-**8a** (**D-593**), (−)-**8b** (**D-601**)**,** (−)-**14** (**D-644**), and (−)-**20** (**D-618**) with desirable binding profiles were further selected to test for their agonist activity through *in vitro* functional assay, and these compounds were found to be comparably potent and full agonist at both D_2 and D_3 receptors.

In addition, compound (−)-**49** (**D-670**), which is the para-dihydroxy analog of the previous lead compound **D-520**, was tested and compared with its parent compound. Although a reduction in binding affinities was found in the binding assay, compound (−)-**49** (**D-670**) demonstrated an improved potency in the functional assay. Moreover, while the efficacy of (−)-**49** (**D-670**) to the D_2 receptor maintained, the compound was found to exhibit enhanced potency at the D_3 receptor.

Following the characterization of receptors activities, selected compounds were studied for their ability to modulate αSN aggregation through *in vitro* shaking and seeding studies. During the process of either shaking or seeding, changes in both morphology and secondary protein structure of αSN were observed through transmission electron microscope (TEM) and circular dichroism (CD) spectra, and the increased fibrilization and cytotoxicity of αSN were observed through thioflavin T (ThT) assay and cell viability assay. In the shaking

assay, test compound (−)-**8a** (**D-593**) was found to inhibit the fibrilization; however, its ability to reverse αSN induced toxicity was not significant. In the seeding assays, compounds (−)-**8a** (**D-593**), (−)-**20** (**D-618**), and (−)-**14** (**D-644**) were able to inhibit the αSN aggregation and reversed αSN induced cytotoxicity to various extents; the compounds (−)-**14** (**D-644**) and (−)-**8a** (**D-593**) were found to be more prominent. In addition, compound (−)-**49** (**D-670**) displayed an anti-aggregation activity comparable to its parent compound **D-520** in the context of fibrilization and cytotoxicity.

Furthermore, compounds (−)-**8a** (**D-593**), (−)-**20** (**D-618**), (−)-**14** (**D-644**), and (−)-**49** (**D-670**) were evaluated for their neuroprotective effect against the 6-OHDA induced toxicity in PC12 cells. All the test compounds were able to reverse the cytotoxicity induced by 6-OHDA. Thereafter, compounds (−)-**8a** (**D-593**), (−)-**20** (**D-618**), and (−)-**49** (**D-670**) were selected for *in vivo* animal study. The compound (−)-**8a** (**D-593**) was found to effectively reverse the hypolocomotion induced by reserpine treatment, whereas the compound (−)-**20** (**D-618**) displayed only a slight effect. In contrast, compound (−)-**49** (**D-670**) failed to reverse the reserpine-induced akinesia. Thus, compounds (−)-**8a** (**D-593**) and (−)-**14** (**D-644**), which are promising D_2/D_3 agonists with neuroprotective activity, were identified as the lead compounds in this SAR study and may have the potential to provide symptom-relieving and disease-modifying effect for the treatment of PD.

This work has provided a systematic evaluation on the effect of alkyl linkers and hydroxyphenol or methoxyphenol components on dopamine D_2/D_3 receptor activities, which can guide in the design of future multifunctional D_2/D_3 agonist. In addition, through a line of biological assays, lead compounds were successfully identified, which require further mechanistic study to investigate the modulatory effect of compounds on αSN aggregation. Techniques such as size exclusion high-performance liquid chromatograph (SEC-HPLC) in combination with mass spectrometry could be applied to study the mode of interaction between αSN protein and compounds.

The second main objective was to design and synthesize a series of novel dopamine D_2/D_3 receptor agonists that may potentially selectively inhibit MAO-B activity by replacing the propyl group with the propargyl group. In this SAR study, the synthesized compounds were first compared in regards to their binding activity towards D_2/D_3 receptors with their propyl parent compounds. A general reduction in D_2/D_3 binding affinity was observed with most of the compounds except for (−)-**62c (D-676)** and (−)-**73** (**D-635**). In the case of functional activities, while propargyl compounds generally became partial D_2 agonists with reduced potency due to the propargyl replacement, they remained full agonists at D_3 receptor with reduced potency. However, (−)-**73** (**D-635**) retained nearly full D_2 agonistic activity and exerted a slight improvement in the potency at the D_3 receptor. Moreover, a pentynyl analog (−)-**62e** (**D-664**) was also included in this

SAR study. This replacement deprived the agonistic activity at both D_2 and D_3 receptors despite the its binding affinity at the receptors.

When tested in the *in vitro* enzymatic assays, compounds (−)-**62b** (**D-629**), (−)-**63** (**D-649**), and (−)-**76** (**D-614**) were shown to be the most active compounds and reduced the MAO-B activity by approximately half in the assay conditions. This assay also revealed that substitutions on the phenyl ring in the accessory binding site moiety may play a role in altering the MAO inhibitory effect. The determination of IC_{50} values suggested that while compound (−)-**62b** (**D-629**) is slightly selective for MAO-B, compound (−)-**76** (**D-614**) is non-selective towards both MAO isoforms.

Afterwards, compounds (−)-**76** (**D-614**) and (−)-**62b** (**D-629**) were evaluated for their neuroprotective ability in PC12 cells. In contrast to compound (−)-**62b** (**D-629**), which failed in the 6-OHDA model, compound (−)-**76** (**D-614**) exerted a dose-dependent neuroprotective effect. However, this effect was not replicated in the rotenone neuroprotection model.

Finally, compound (−)-**76** (**D-614**) was tested in the PD animal model, and it effectively reversed reserpine-induced hypolocomotion in rat. Thus, compound (−)-**76** (**D-614**), a promising D_2/D_3 agonist that exerted neuroprotective and MAO-B inhibitory activity, was identified as the lead compound from this SAR study.

This initial SAR study explored the potential of incorporating additional MAO-B inhibitory effect into D_2/D_3 agonist molecules via the replacement of the propyl group by a propargyl group in the headgroup moiety. A relatively low

compatibility of the structural preference and conformational requirements for D_2/D_3 agonistic activity and MAO-B inhibitory activity has been observed in the current molecular template. Thus, an expanded SAR study with further structural modifications in the hybrid template is required to improve the receptor activities and enzyme inhibition profile. Molecular modeling could also be applied to assist with the drug design and compound screening. In addition, a mechanistic study could be carried out to further characterize the identified MAO-B inhibitors.

REFERENCES

Acharya, S., B. M. Safaie, P. Wongkongkathep, M. I. Ivanova, A. Attar, F. G. Klarner, T. Schrader, J. A. Loo, G. Bitan, and L. J. Lapidus. 2014. "Molecular basis for preventing alpha-synuclein aggregation by a molecular tweezer." *J Biol Chem* 289 (15):10727-37. doi: 10.1074/jbc.M113.524520.

Alves, G., E. B. Forsaa, K. F. Pedersen, M. Dreetz Gjerstad, and J. P. Larsen. 2008. "Epidemiology of Parkinson's disease." *J Neurol* 255 Suppl 5:18-32. doi: 10.1007/s00415-008-5004-3.

Alves, G., E. B. Forsaa, K. F. Pedersen, M. D. Gjerstad, and J. P. Larsen. 2008. "Epidemiology of Parkinson's disease." *Journal of Neurology* 255:18-32. doi: 10.1007/s00415-008-5004-3.

Ardah, M. T., K. E. Paleologou, G. Lv, S. B. Abul Khair, A. S. Kazim, S. T. Minhas, T. H. Al-Tel, A. A. Al-Hayani, M. E. Haque, D. Eliezer, and O. M. El-Agnaf. 2014. "Structure activity relationship of phenolic acid inhibitors of alpha-synuclein fibril formation and toxicity." *Front Aging Neurosci* 6:197. doi: 10.3389/fnagi.2014.00197.

Ascherio, A., and M. A. Schwarzschild. 2016. "The epidemiology of Parkinson's disease: risk factors and prevention." *Lancet Neurol* 15 (12):1257-1272. doi: 10.1016/S1474-4422(16)30230-7.

Bar-Am, O., T. Amit, L. Kupershmidt, Y. Aluf, D. Mechlovich, H. Kabha, L. Danovitch, V. R. Zurawski, M. B. Youdim, and O. Weinreb. 2015.

"Neuroprotective and neurorestorative activities of a novel iron chelator-brain selective monoamine oxidase-A/monoamine oxidase-B inhibitor in animal models of Parkinson's disease and aging." *Neurobiol Aging* 36 (3):1529-42. doi: 10.1016/j.neurobiolaging.2014.10.026.

Barrett, P. J., and J. Timothy Greenamyre. 2015. "Post-translational modification of alpha-synuclein in Parkinson's disease." *Brain Res* 1628 (Pt B):247-53. doi: 10.1016/j.brainres.2015.06.002.

Bartels, T., J. G. Choi, and D. J. Selkoe. 2011. "alpha-Synuclein occurs physiologically as a helically folded tetramer that resists aggregation." *Nature* 477 (7362):107-U123. doi: 10.1038/nature10324.

Binda, C., P. Newton-Vinson, F. Hubalek, D. E. Edmondson, and A. Mattevi. 2002. "Structure of human monoamine oxidase B, a drug target for the treatment of neurological disorders." *Nat Struct Biol* 9 (1):22-6. doi: 10.1038/nsb732.

Biswas, S., S. Hazeldine, B. Ghosh, I. Parrington, E. Kuzhikandathil, M. E. A. Reith, and A. K. Dutta. 2008. "Bioisosteric heterocyclic versions of 7-{[2-(4-phenyl-piperazin-1-yl)ethyl]propylamino}-5,6,7,8-tetrahydronaphthalen-2-ol: Identification of highly potent and selective agonists for dopamine D3 receptor with potent in vivo activity." *Journal of Medicinal Chemistry* 51 (10):3005-3019. doi: 10.1021/jm701524h.

Biswas, S., S. H. Zhang, F. Fernandez, B. Ghosh, J. Zhen, E. Kuzhikandathil, M. E. A. Reith, and A. K. Dutta. 2008. "Further structure-activity relationships

study of hybrid 7-{[2-(4-phenylpiperazin-1-yl)ethyl]propylamino}-5,6,7,8-tetrahydronaphthalen-2-ol analogues: Identification of a high-affinity D3-preferring agonist with potent in vivo activity with long duration of action." *Journal of Medicinal Chemistry* 51 (1):101-117. doi: 10.1021/jm070860r.

Blandini, F., and M. T. Armentero. 2014. "Dopamine receptor agonists for Parkinson's disease." *Expert Opin Investig Drugs* 23 (3):387-410. doi: 10.1517/13543784.2014.869209.

Blesa, J., I. Trigo-Damas, A. Quiroga-Varela, and V. R. Jackson-Lewis. 2015. "Oxidative stress and Parkinson's disease." *Frontiers in Neuroanatomy* 9. doi: 10.3389/fnana.2015.00091.

Blum, D., S. Torch, M. F. Nissou, A. L. Benabid, and J. M. Verna. 2000. "Extracellular toxicity of 6-hydroxydopamine on PC12 cells." *Neurosci Lett* 283 (3):193-6.

Bonifacio, M. J., P. N. Palma, L. Almeida, and P. Soares-Da-Silva. 2007. "Catechol-O-methyltransferase and its inhibitors in Parkinson's disease." *Cns Drug Reviews* 13 (3):352-379. doi: DOI 10.1111/j.1527-3458.2007.00020.x.

Bose, A., and M. F. Beal. 2016. "Mitochondrial dysfunction in Parkinson's disease." *J Neurochem* 139 Suppl 1:216-231. doi: 10.1111/jnc.13731.

Braak, H., K. Del Tredici, U. Rub, R. A. de Vos, E. N. Jansen Steur, and E. Braak. 2003. "Staging of brain pathology related to sporadic Parkinson's disease." *Neurobiol Aging* 24 (2):197-211.

Breydo, L., J. W. Wu, and V. N. Uversky. 2012. "Alpha-synuclein misfolding and Parkinson's disease." *Biochim Biophys Acta* 1822 (2):261-85. doi: 10.1016/j.bbadis.2011.10.002.

Brown, D. A., M. Mishra, S. Zhang, S. Biswas, I. Parrington, T. Antonio, M. E. A. Reith, and A. K. Dutta. 2009. "Investigation of various N-heterocyclic substituted piperazine versions of 5/7-{[2-(4-aryl-piperazin-1-yl)-ethyl]-propyl-amino}-5,6,7,8-tetrahydro-naphthalen-2-ol: Effect on affinity and selectivity for dopamine D3 receptor." *Bioorganic & Medicinal Chemistry* 17 (11):3923-3933. doi: 10.1016/j.bmc.2009.04.031.

Burbulla, L. F., and R. Kruger. 2011. "Converging environmental and genetic pathways in the pathogenesis of Parkinson's disease." *Journal of the Neurological Sciences* 306 (1-2):1-8. doi: 10.1016/j.jns.2011.04.005.

Burre, J., S. Vivona, J. Diao, M. Sharma, A. T. Brunger, and T. C. Sudhof. 2013. "Properties of native brain alpha-synuclein." *Nature* 498 (7453):E4-6; discussion E6-7. doi: 10.1038/nature12125.

Butler, B., D. Sambo, and H. Khoshbouei. 2016. "Alpha-synuclein modulates dopamine neurotransmission." *J Chem Neuroanat*. doi: 10.1016/j.jchemneu.2016.06.001.

Calo, L., M. Wegrzynowicz, J. Santivanez-Perez, and M. Grazia Spillantini. 2016. "Synaptic failure and alpha-synuclein." *Mov Disord* 31 (2):169-77. doi: 10.1002/mds.26479.

Can, O. D., D. Osmaniye, U. Demir Ozkay, B. N. Saglik, S. Levent, S. Ilgin, M. Baysal, Y. Ozkay, and Z. A. Kaplancikli. 2017. "MAO enzymes inhibitory activity of new benzimidazole derivatives including hydrazone and propargyl side chains." *Eur J Med Chem* 131:92-106. doi: 10.1016/j.ejmech.2017.03.009.

Carradori, S., and R. Silvestri. 2015. "New Frontiers in Selective Human MAO-B Inhibitors." *J Med Chem* 58 (17):6717-32. doi: 10.1021/jm501690r.

Caudle, W. M., R. E. Colebrooke, P. C. Emson, and G. W. Miller. 2008. "Altered vesicular dopamine storage in Parkinson's disease: a premature demise." *Trends Neurosci* 31 (6):303-8. doi: 10.1016/j.tins.2008.02.010.

Chartier-Harlin, M. C., J. Kachergus, C. Roumier, V. Mouroux, X. Douay, S. Lincoln, C. Levecque, L. Larvor, J. Andrieux, M. Hulihan, N. Waucquier, L. Defebvre, P. Amouyel, M. Farrer, and A. Destee. 2004. "Alpha-synuclein locus duplication as a cause of familial Parkinson's disease." *Lancet* 364 (9440):1167-9. doi: 10.1016/S0140-6736(04)17103-1.

Chau, K. Y., J. M. Cooper, and A. H. V. Schapira. 2013. "Pramipexole Reduces Phosphorylation of alpha-Synuclein at Serine-129." *Journal of Molecular Neuroscience* 51 (2):573-580. doi: 10.1007/s12031-013-0030-8.

Chen, X., H. A. de Silva, M. J. Pettenati, P. N. Rao, P. St George-Hyslop, A. D. Roses, Y. Xia, K. Horsburgh, K. Ueda, and T. Saitoh. 1995. "The human NACP/alpha-synuclein gene: chromosome assignment to 4q21.3-q22 and TaqI RFLP analysis." *Genomics* 26 (2):425-7.

Chimenti, P., A. Petzer, S. Carradori, M. D'Ascenzio, R. Silvestri, S. Alcaro, F. Ortuso, J. P. Petzer, and D. Secci. 2013. "Exploring 4-substituted-2-thiazolylhydrazones from 2-, 3-, and 4-acetylpyridine as selective and reversible hMAO-B inhibitors." *European Journal of Medicinal Chemistry* 66:221-227. doi: 10.1016/j.ejmech.2013.05.032.

Coelho-Cerqueira, E., P. Carmo-Goncalves, A. S. Pinheiro, J. Cortines, and C. Follmer. 2013. "alpha-Synuclein as an intrinsically disordered monomer - fact or artefact?" *Febs Journal* 280 (19):4915-4927. doi: 10.1111/febs.12471.

Collier, T. J., D. E. Redmond, Jr., K. Steece-Collier, J. W. Lipton, and F. P. Manfredsson. 2016. "Is Alpha-Synuclein Loss-of-Function a Contributor to Parkinsonian Pathology? Evidence from Non-human Primates." *Front Neurosci* 10:12. doi: 10.3389/fnins.2016.00012.

Constantinescu, R. 2008. "Update on the use of pramipexole in the treatment of Parkinson's disease." *Neuropsychiatr Dis Treat* 4 (2):337-52.

Corti, O., S. Lesage, and A. Brice. 2011. "What Genetics Tells Us About the Causes and Mechanisms of Parkinson's Disease." *Physiological Reviews* 91 (4):1161-1218. doi: 10.1152/physrev.00022.2010.

Das, B., S. Vedachalam, D. Luo, T. Antonio, M. E. Reith, and A. K. Dutta. 2015. "Development of a Highly Potent D2/D3 Agonist and a Partial Agonist from Structure-Activity Relationship Study of N(6)-(2-(4-(1H-Indol-5-yl)piperazin-1-yl)ethyl)-N(6)-propyl-4,5,6,7-tetrahydroben zo[d]thiazole-

2,6-diamine Analogues: Implication in the Treatment of Parkinson's Disease." *J Med Chem* 58 (23):9179-95. doi: 10.1021/acs.jmedchem.5b01031.

Dauer, W., and S. Przedborski. 2003. "Parkinson's disease: mechanisms and models." *Neuron* 39 (6):889-909.

Davidson, W. S., A. Jonas, D. F. Clayton, and J. M. George. 1998. "Stabilization of alpha-synuclein secondary structure upon binding to synthetic membranes." *Journal of Biological Chemistry* 273 (16):9443-9449. doi: DOI 10.1074/jbc.273.16.9443.

de Lau, L. M., and M. M. Breteler. 2006. "Epidemiology of Parkinson's disease." *Lancet Neurol* 5 (6):525-35. doi: 10.1016/S1474-4422(06)70471-9.

Dehay, B., M. Bourdenx, P. Gorry, S. Przedborski, M. Vila, S. Hunot, A. Singleton, C. W. Olanow, K. M. Merchant, E. Bezard, G. A. Petsko, and W. G. Meissner. 2015. "Targeting alpha-synuclein for treatment of Parkinson's disease: mechanistic and therapeutic considerations." *Lancet Neurol* 14 (8):855-66. doi: 10.1016/S1474-4422(15)00006-X.

Dettmer, U., A. J. Newman, V. E. von Saucken, T. Bartels, and D. Selkoe. 2015. "KTKEGV repeat motifs are key mediators of normal alpha-synuclein tetramerization: Their mutation causes excess monomers and neurotoxicity." *Proceedings of the National Academy of Sciences of the United States of America* 112 (31):9596-9601. doi: 10.1073/pnas.1505953112.

Dias, V., E. Junn, and M. M. Mouradian. 2013. "The Role of Oxidative Stress in Parkinson's Disease." *Journal of Parkinsons Disease* 3 (4):461-491. doi: 10.3233/Jpd-130230.

Duty, S., and P. Jenner. 2011. "Animal models of Parkinson's disease: a source of novel treatments and clues to the cause of the disease." *British Journal of Pharmacology* 164 (4):1357-1391. doi: 10.1111/j.1476-5381.2011.01426.x.

Edmondson, D. E., C. Binda, and A. Mattevi. 2007. "Structural insights into the mechanism of amine oxidation by monoamine oxidases A and B." *Archives of Biochemistry and Biophysics* 464 (2):269-276. doi: 10.1016/j.abb.2007.05.006.

Edmondson, D. E., C. Binda, J. Wang, A. K. Upadhyay, and A. Mattevi. 2009. "Molecular and mechanistic properties of the membrane-bound mitochondrial monoamine oxidases." *Biochemistry* 48 (20):4220-30. doi: 10.1021/bi900413g.

Eisenhofer, G., I. J. Kopin, and D. S. Goldstein. 2004. "Catecholamine metabolism: a contemporary view with implications for physiology and medicine." *Pharmacol Rev* 56 (3):331-49. doi: 10.1124/pr.56.3.1.

Esposito, G., F. Ana Clara, and P. Verstreken. 2012. "Synaptic vesicle trafficking and Parkinson's disease." *Dev Neurobiol* 72 (1):134-44. doi: 10.1002/dneu.20916.

Factor, S. A. 2008. "Current status of symptomatic medical therapy in Parkinson's disease." *Neurotherapeutics* 5 (2):164-180. doi: DOI 10.1016/j.nurt.2007.12.001.

Fernandes, V. S., J. R. Santos, A. H. F. F. Leao, A. M. Medeiros, T. G. Melo, G. S. Izidio, A. Cabral, R. A. Ribeiro, V. C. Abilio, A. M. Ribeiro, and R. H. Silva. 2012. "Repeated treatment with a low dose of reserpine as a progressive model of Parkinson's disease." *Behavioural Brain Research* 231 (1):154-163. doi: 10.1016/j.bbr.2012.03.008.

Ferreira, M., and J. Massano. 2017. "An updated review of Parkinson's disease genetics and clinicopathological correlations." *Acta Neurol Scand* 135 (3):273-284. doi: 10.1111/ane.12616.

Finberg, J. P. 2014. "Update on the pharmacology of selective inhibitors of MAO-A and MAO-B: focus on modulation of CNS monoamine neurotransmitter release." *Pharmacol Ther* 143 (2):133-52. doi: 10.1016/j.pharmthera.2014.02.010.

Fusco, G., A. De Simone, T. Gopinath, V. Vostrikov, M. Vendruscolo, C. M. Dobson, and G. Veglia. 2014. "Direct observation of the three regions in alpha-synuclein that determine its membrane-bound behaviour." *Nat Commun* 5:3827. doi: 10.1038/ncomms4827.

Gal, S., M. Fridkin, T. Amit, H. Zheng, and M. B. Youdim. 2006. "M30, a novel multifunctional neuroprotective drug with potent iron chelating and brain

selective monoamine oxidase-ab inhibitory activity for Parkinson's disease." *J Neural Transm Suppl* (70):447-56.

Gallegos, S., C. Pacheco, C. Peters, C. M. Opazo, and L. G. Aguayo. 2015. "Features of alpha-synuclein that could explain the progression and irreversibility of Parkinson's disease." *Frontiers in Neuroscience* 9. doi: 10.3389/fnins.2015.00059.

Gautam, S., S. Karmakar, R. Batra, P. Sharma, P. Pradhan, J. Singh, B. Kundu, and P. K. Chowdhury. 2017. "Polyphenols in combination with beta-cyclodextrin can inhibit and disaggregate alpha-synuclein amyloids under cell mimicking conditions: A promising therapeutic alternative." *Biochim Biophys Acta*. doi: 10.1016/j.bbapap.2017.02.014.

Gautam, S., S. Karmakar, A. Bose, and P. K. Chowdhury. 2014. "beta-cyclodextrin and curcumin, a potent cocktail for disaggregating and/or inhibiting amyloids: a case study with alpha-synuclein." *Biochemistry* 53 (25):4081-3. doi: 10.1021/bi500642f.

Gershanik, O. S. 2015. "Improving L-dopa therapy: the development of enzyme inhibitors." *Mov Disord* 30 (1):103-13. doi: 10.1002/mds.26050.

Ghosh, B., T. Antonio, B. Gopishetty, M. Reith, and A. Dutta. 2010. "Further delineation of hydrophobic binding sites in dopamine D-2/D-3 receptors for N-4 substituents on the piperazine ring of the hybrid template 5/7-{[2-(4-aryl-piperazin-1-yl)-ethyl]-propyl-amino}-5,6,7,8-tetrahydro-naphthalen-2-

ol." *Bioorganic & Medicinal Chemistry* 18 (15):5661-5674. doi: 10.1016/j.bmc.2010.06.025.

Giasson, B. I., I. V. Murray, J. Q. Trojanowski, and V. M. Lee. 2001. "A hydrophobic stretch of 12 amino acid residues in the middle of alpha-synuclein is essential for filament assembly." *J Biol Chem* 276 (4):2380-6. doi: 10.1074/jbc.M008919200.

Goedert, M. 2015. "Alzheimer's and Parkinson's diseases: The prion concept in relation to assembled A beta, tau, and alpha-synuclein." *Science* 349 (6248). doi: 10.1126/science.1255555.

Goedert, M., F. Clavaguera, and M. Tolnay. 2010. "The propagation of prion-like protein inclusions in neurodegenerative diseases." *Trends Neurosci* 33 (7):317-25. doi: 10.1016/j.tins.2010.04.003.

Goedert, M., M. G. Spillantini, K. Del Tredici, and H. Braak. 2013. "100 years of Lewy pathology." *Nat Rev Neurol* 9 (1):13-24. doi: 10.1038/nrneurol.2012.242.

Goldman, S. M. 2014. "Environmental Toxins and Parkinson's Disease." *Annual Review of Pharmacology and Toxicology, Vol 54* 54:141-164. doi: 10.1146/annurev-pharmtox-011613-135937.

Gooch, C. L., E. Pracht, and A. R. Borenstein. 2017. "The Burden of Neurological Disease in the United States: A Summary Report and Call to Action." *Ann Neurol*. doi: 10.1002/ana.24897.

Grosch, J., J. Winkler, and Z. Kohl. 2016. "Early Degeneration of Both Dopaminergic and Serotonergic Axons - A Common Mechanism in Parkinson's Disease." *Frontiers in Cellular Neuroscience* 10. doi: 10.3389/fncel.2016.00293.

Halliwell, B. 2006. "Oxidative stress and neurodegeneration: where are we now?" *Journal of Neurochemistry* 97 (6):1634-1658. doi: 10.1111/j.1471-4159.2006.03907.x.

Hasegawa, M., T. Nonaka, and M. Masuda-Suzukake. 2017. "Prion-like mechanisms and potential therapeutic targets in neurodegenerative disorders." *Pharmacol Ther* 172:22-33. doi: 10.1016/j.pharmthera.2016.11.010.

Hastings, T. G. 2009. "The role of dopamine oxidation in mitochondrial dysfunction: implications for Parkinson's disease." *J Bioenerg Biomembr* 41 (6):469-72. doi: 10.1007/s10863-009-9257-z.

Hauser, D. N., and T. G. Hastings. 2013. "Mitochondrial dysfunction and oxidative stress in Parkinson's disease and monogenic parkinsonism." *Neurobiology of Disease* 51:35-42. doi: 10.1016/j.nbd.2012.10.011.

Hawkes, C. H., K. Del Tredici, and H. Braak. 2007. "Parkinson's disease: a dual-hit hypothesis." *Neuropathol Appl Neurobiol* 33 (6):599-614. doi: 10.1111/j.1365-2990.2007.00874.x.

Helguera, A. M., G. Perez-Machado, M. N. Cordeiro, and F. Borges. 2012. "Discovery of MAO-B inhibitors - present status and future directions part I: oxygen heterocycles and analogs." *Mini Rev Med Chem* 12 (10):907-19.

Hernandez, D. G., X. Reed, and A. B. Singleton. 2016. "Genetics in Parkinson disease: Mendelian versus non-Mendelian inheritance." *J Neurochem* 139 Suppl 1:59-74. doi: 10.1111/jnc.13593.

Hirayama, Y., M. Ikunaka, and J. Matsumoto. 2005. "An expeditious scalable synthesis of (S)-2-amino-5-methoxytetralin via resolution." *Organic Process Research & Development* 9 (1):30-38. doi: 10.1021/op0498363.

Hirsch, L., N. Jette, A. Frolkis, T. Steeves, and T. Pringsheim. 2016. "The Incidence of Parkinson's Disease: A Systematic Review and Meta-Analysis." *Neuroepidemiology* 46 (4):292-300. doi: 10.1159/000445751.

Hu, Q., V. N. Uversky, M. Huang, H. Kang, F. Xu, X. Liu, L. Lian, Q. Liang, H. Jiang, A. Liu, C. Zhang, F. Pan-Montojo, and S. Zhu. 2016. "Baicalein inhibits alpha-synuclein oligomer formation and prevents progression of alpha-synuclein accumulation in a rotenone mouse model of Parkinson's disease." *Biochim Biophys Acta* 1862 (10):1883-90. doi: 10.1016/j.bbadis.2016.07.008.

Huang, C. J., G. P. Ren, H. Zhou, and C. C. Wang. 2005. "A new method for purification of recombinant human alpha-synuclein in Escherichia coli." *Protein Expression and Purification* 42 (1):173-177. doi: 10.1016/j.pep.2005.02.014.

Huleatt, P. B., M. L. Khoo, Y. Y. Chua, T. W. Tan, R. S. Liew, B. Balogh, R. Deme, F. Goloncser, K. Magyar, D. P. Sheela, H. K. Ho, B. Sperlagh, P. Matyus, and C. L. Chai. 2015. "Novel arylalkenylpropargylamines as neuroprotective, potent, and selective monoamine oxidase B inhibitors for the treatment of Parkinson's disease." *J Med Chem* 58 (3):1400-19. doi: 10.1021/jm501722s.

Hwang, O. 2013. "Role of oxidative stress in Parkinson's disease." *Exp Neurobiol* 22 (1):11-7. doi: 10.5607/en.2013.22.1.11.

Jain, N., K. Bhasne, M. Hemaswasthi, and S. Mukhopadhyay. 2013. "Structural and Dynamical Insights into the Membrane-Bound alpha-Synuclein." *Plos One* 8 (12). doi: 10.1371/journal.pone.0083752.

Jankovic, J. 2008. "Parkinson's disease: clinical features and diagnosis." *J Neurol Neurosurg Psychiatry* 79 (4):368-76. doi: 10.1136/jnnp.2007.131045.

Jankovic, J., and L. G. Aguilar. 2008. "Current approaches to the treatment of Parkinson's disease." *Neuropsychiatr Dis Treat* 4 (4):743-57.

Jiang, T., Q. Sun, and S. Chen. 2016. "Oxidative stress: A major pathogenesis and potential therapeutic target of antioxidative agents in Parkinson's disease and Alzheimer's disease." *Prog Neurobiol* 147:1-19. doi: 10.1016/j.pneurobio.2016.07.005.

Jo, E., J. McLaurin, C. M. Yip, P. St George-Hyslop, and P. E. Fraser. 2000. "alpha-Synuclein membrane interactions and lipid specificity." *J Biol Chem* 275 (44):34328-34. doi: 10.1074/jbc.M004345200.

Johnson, M., T. Antonio, M. E. Reith, and A. K. Dutta. 2012. "Structure-activity relationship study of N(6)-(2-(4-(1H-Indol-5-yl)piperazin-1-yl)ethyl)-N(6)-propyl-4,5,6,7-tetrahydroben zo[d]thiazole-2,6-diamine analogues: development of highly selective D3 dopamine receptor agonists along with a highly potent D2/D3 agonist and their pharmacological characterization." *J Med Chem* 55 (12):5826-40. doi: 10.1021/jm300268s.

Johnson, M., T. Antonio, M. E. Reith, and A. K. Dutta. 2013. "Correction to Structure-Activity Relationship Study of N(6)-(2-(4-(1H-Indol-5-yl)piperazin-1-yl)ethyl)-N(6)-propyl-4,5,6,7-tetrahydroben zo[d]thiazole-2,6-diamine Analogues: Development of Highly Selective D3 Dopamine Receptor Agonists along with a Highly Potent D2/D3 Agonist and Their Pharmacological Characterization." *J Med Chem* 56 (2):589-90. doi: 10.1021/jm301634c.

Johnson, W. M., A. L. Wilson-Delfosse, and J. J. Mieyal. 2012. "Dysregulation of glutathione homeostasis in neurodegenerative diseases." *Nutrients* 4 (10):1399-440. doi: 10.3390/nu4101399.

Jones, D. R., S. Moussaud, and P. McLean. 2014. "Targeting heat shock proteins to modulate alpha-synuclein toxicity." *Ther Adv Neurol Disord* 7 (1):33-51. doi: 10.1177/1756285613493469.

Kim, G. H., J. E. Kim, S. J. Rhie, and S. Yoon. 2015. "The Role of Oxidative Stress in Neurodegenerative Diseases." *Exp Neurobiol* 24 (4):325-40. doi: 10.5607/en.2015.24.4.325.

Kordower, J. H., Y. P. Chu, R. A. Hauser, T. B. Freeman, and C. W. Olanow. 2008. "Lewy body-like pathology in long-term embryonic nigral transplants in Parkinson's disease." *Nature Medicine* 14 (5):504-506. doi: 10.1038/nm1747.

Kowal, S. L., T. M. Dall, R. Chakrabarti, M. V. Storm, and A. Jain. 2013. "The current and projected economic burden of Parkinson's disease in the United States." *Mov Disord* 28 (3):311-8. doi: 10.1002/mds.25292.

Kruger, R., W. Kuhn, T. Muller, D. Woitalla, M. Graeber, S. Kosel, H. Przuntek, J. T. Epplen, L. Schols, and O. Riess. 1998. "Ala30Pro mutation in the gene encoding alpha-synuclein in Parkinson's disease." *Nat Genet* 18 (2):106-8. doi: 10.1038/ng0298-106.

Labenski, M. T., A. A. Fisher, H. H. Lo, T. J. Monks, and S. S. Lau. 2009. "Protein electrophile-binding motifs: lysine-rich proteins are preferential targets of quinones." *Drug Metab Dispos* 37 (6):1211-8. doi: 10.1124/dmd.108.026211.

Lashuel, H. A., C. R. Overk, A. Oueslati, and E. Masliah. 2013. "The many faces of alpha-synuclein: from structure and toxicity to therapeutic target." *Nat Rev Neurosci* 14 (1):38-48. doi: 10.1038/nrn3406.

Leao, A. H. F. F., A. J. Sarmento-Silva, J. R. Santos, A. M. Ribeiro, and R. H. Silva. 2015. "Molecular, Neurochemical, and Behavioral Hallmarks of Reserpine as a Model for Parkinson's Disease: New Perspectives to a Long-Standing Model." *Brain Pathology* 25 (4):377-390. doi: 10.1111/bpa.12253.

Lee, V. M., and J. Q. Trojanowski. 2006. "Mechanisms of Parkinson's disease linked to pathological alpha-synuclein: new targets for drug discovery." *Neuron* 52 (1):33-8. doi: 10.1016/j.neuron.2006.09.026.

Lesage, S., M. Anheim, F. Letournel, L. Bousset, A. Honore, N. Rozas, L. Pieri, K. Madiona, A. Durr, R. Melki, C. Verny, A. Brice, and Group French Parkinson's Disease Genetics Study. 2013. "G51D alpha-synuclein mutation causes a novel parkinsonian-pyramidal syndrome." *Ann Neurol* 73 (4):459-71. doi: 10.1002/ana.23894.

Lesage, S., and A. Brice. 2009. "Parkinson's disease: from monogenic forms to genetic susceptibility factors." *Human Molecular Genetics* 18:R48-R59. doi: 10.1093/hmg/ddp012.

Lev, N., R. Djaldetti, and E. Melamed. 2007. "Initiation of symptomatic therapy in Parkinson's disease: dopamine agonists versus levodopa." *Journal of Neurology* 254:19-26. doi: 10.1007/s00415-007-5004-8.

Li, H. T., D. H. Lin, X. Y. Luo, F. Zhang, L. N. Ji, H. N. Du, G. Q. Song, J. Hu, J. W. Zhou, and H. Y. Hu. 2005. "Inhibition of alpha-synuclein fibrillization by dopamine analogs via reaction with the amino groups of alpha-synuclein.

Implication for dopaminergic neurodegeneration." *FEBS J* 272 (14):3661-72. doi: 10.1111/j.1742-4658.2005.04792.x.

Li, J. Y., E. Englund, J. L. Holton, D. Soulet, P. Hagell, A. J. Lees, T. Lashley, N. P. Quinn, S. Rehncrona, A. Bjorklund, H. Widner, T. Revesz, O. Lindvall, and P. Brundin. 2008. "Lewy bodies in grafted neurons in subjects with Parkinson's disease suggest host-to-graft disease propagation." *Nature Medicine* 14 (5):501-503. doi: 10.1038/nm1746.

Li, J., M. Zhu, S. Rajamani, V. N. Uversky, and A. L. Fink. 2004. "Rifampicin inhibits alpha-synuclein fibrillation and disaggregates fibrils." *Chem Biol* 11 (11):1513-21. doi: 10.1016/j.chembiol.2004.08.025.

Limongi, D., and S. Baldelli. 2016. "Redox Imbalance and Viral Infections in Neurodegenerative Diseases." *Oxid Med Cell Longev* 2016:6547248. doi: 10.1155/2016/6547248.

Lipton, S. A. 2007. "Pathologically activated therapeutics for neuroprotection." *Nat Rev Neurosci* 8 (10):803-8. doi: 10.1038/nrn2229.

Lorenzen, N., S. B. Nielsen, Y. Yoshimura, B. S. Vad, C. B. Andersen, C. Betzer, J. D. Kaspersen, G. Christiansen, J. S. Pedersen, P. H. Jensen, F. A. A. Mulder, and D. E. Otzen. 2014. "How Epigallocatechin Gallate Can Inhibit alpha-Synuclein Oligomer Toxicity in Vitro." *Journal of Biological Chemistry* 289 (31):21299-21310. doi: 10.1074/jbc.M114.554667.

Lotharius, J., and P. Brundin. 2002. "Pathogenesis of Parkinson's disease: Dopamine, vesicles and alpha-synuclein." *Nature Reviews Neuroscience* 3 (12):932-942. doi: 10.1038/nrn983.

Luna, E., and K. C. Luk. 2015. "Bent out of shape: alpha-Synuclein misfolding and the convergence of pathogenic pathways in Parkinson's disease." *FEBS Lett* 589 (24 Pt A):3749-59. doi: 10.1016/j.febslet.2015.10.023.

Luo, D., H. Sharma, D. Yedlapudi, T. Antonio, M. E. Reith, and A. K. Dutta. 2016. "Novel multifunctional dopamine D2/D3 receptors agonists with potential neuroprotection and anti-alpha synuclein protein aggregation properties." *Bioorg Med Chem* 24 (21):5088-5102. doi: 10.1016/j.bmc.2016.08.021.

Luo, J. H., and J. P. Abrahams. 2014. "Cyclic Peptides as Inhibitors of Amyloid Fibrillation." *Chemistry-a European Journal* 20 (9):2410-2419. doi: 10.1002/chem.201304253.

Luo, Y., A. Hoffer, B. Hoffer, and X. Qi. 2015. "Mitochondria: A Therapeutic Target for Parkinson's Disease?" *International Journal of Molecular Sciences* 16 (9):20704-20730. doi: 10.3390/ijms160920704.

Ma, M. W., J. Wang, Q. Zhang, R. Wang, K. M. Dhandapani, R. K. Vadlamudi, and D. W. Brann. 2017. "NADPH oxidase in brain injury and neurodegenerative disorders." *Mol Neurodegener* 12 (1):7. doi: 10.1186/s13024-017-0150-7.

Majd, S., J. H. Power, and H. J. Grantham. 2015. "Neuronal response in Alzheimer's and Parkinson's disease: the effect of toxic proteins on

intracellular pathways." *BMC Neurosci* 16:69. doi: 10.1186/s12868-015-0211-1.

Martin, H. L., and P. Teismann. 2009. "Glutathione-a review on its role and significance in Parkinson's disease." *Faseb Journal* 23 (10):3263-3272. doi: 10.1096/fj.08-125443.

McCall, R. B., K. J. Lookingland, P. J. Bedard, and R. M. Huff. 2005. "Sumanirole, a highly dopamine D2-selective receptor agonist: in vitro and in vivo pharmacological characterization and efficacy in animal models of Parkinson's disease." *J Pharmacol Exp Ther* 314 (3):1248-56. doi: 10.1124/jpet.105.084202.

Meiser, J., D. Weindl, and K. Hiller. 2013. "Complexity of dopamine metabolism." *Cell Commun Signal* 11 (1):34. doi: 10.1186/1478-811X-11-34.

Mercuri, N. B., and G. Bernardi. 2005. "The 'magic' of L-dopa: why is it the gold standard Parkinson's disease therapy?" *Trends in Pharmacological Sciences* 26 (7):341-344. doi: 10.1016/j.tips.2005.05.002.

Mirecka, E. A., H. Shaykhalishahi, A. Gauhar, S. Akgul, J. Lecher, D. Willbold, M. Stoldt, and W. Hoyer. 2014. "Sequestration of a beta-Hairpin for Control of alpha-Synuclein Aggregation." *Angewandte Chemie-International Edition* 53 (16):4227-4230. doi: 10.1002/anie.201309001.

Modi, G., C. Voshavar, S. Gogoi, M. Shah, T. Antonio, M. E. Reith, and A. K. Dutta. 2014. "Multifunctional D2/D3 agonist D-520 with high in vivo

efficacy: modulator of toxicity of alpha-synuclein aggregates." *ACS Chem Neurosci* 5 (8):700-17. doi: 10.1021/cn500084x.

Moore, D. J., A. B. West, V. L. Dawson, and T. M. Dawson. 2005. "Molecular pathophysiology of Parkinson's disease." *Annual Review of Neuroscience* 28:57-87. doi: 10.1146/annurev.neuro.28.061604.135718.

Mor, D. E., S. E. Ugras, M. J. Daniels, and H. Ischiropoulos. 2016. "Dynamic structural flexibility of alpha-synuclein." *Neurobiol Dis* 88:66-74. doi: 10.1016/j.nbd.2015.12.018.

Moreira, P. I., X. Zhu, X. Wang, H. G. Lee, A. Nunomura, R. B. Petersen, G. Perry, and M. A. Smith. 2010. "Mitochondria: a therapeutic target in neurodegeneration." *Biochim Biophys Acta* 1802 (1):212-20. doi: 10.1016/j.bbadis.2009.10.007.

Moustafa, A. A., S. Chakravarthy, J. R. Phillips, A. Gupta, S. Keri, B. Polner, M. J. Frank, and M. Jahanshahi. 2016. "Motor symptoms in Parkinson's disease: A unified framework." *Neurosci Biobehav Rev* 68:727-40. doi: 10.1016/j.neubiorev.2016.07.010.

Muller, T. 2015. "Catechol-O-methyltransferase inhibitors in Parkinson's disease." *Drugs* 75 (2):157-74. doi: 10.1007/s40265-014-0343-0.

Narkiewicz, J., G. Giachin, and G. Legname. 2014. "In vitro aggregation assays for the characterization of alpha-synuclein prion-like properties." *Prion* 8 (1):19-32. doi: 10.4161/pri.28125.

Nicotra, A., F. Pierucci, H. Parvez, and O. Senatori. 2004. "Monoamine oxidase expression during development and aging." *Neurotoxicology* 25 (1-2):155-65. doi: 10.1016/S0161-813X(03)00095-0.

Novaroli, L., M. Reist, E. Favre, A. Carotti, M. Catto, and P. A. Carrupt. 2005. "Human recombinant monoamine oxidase B as reliable and efficient enzyme source for inhibitor screening." *Bioorganic & Medicinal Chemistry* 13 (22):6212-6217. doi: 10.1016/j.bmc.2005.06.043.

O'Carroll, A. M., C. J. Fowler, J. P. Phillips, I. Tobbia, and K. F. Tipton. 1983. "The deamination of dopamine by human brain monoamine oxidase. Specificity for the two enzyme forms in seven brain regions." *Naunyn Schmiedebergs Arch Pharmacol* 322 (3):198-202.

Oueslati, A., M. Ximerakis, and K. Vekrellis. 2014. "Protein Transmission, Seeding and Degradation: Key Steps for alpha-Synuclein Prion-Like Propagation." *Exp Neurobiol* 23 (4):324-36. doi: 10.5607/en.2014.23.4.324.

Parkinson's Disease Foundation. "Statistics on Parkinson's." http://www.pdf.org/en/parkinson_statistics.

Parkinson, J. 2002. "An essay on the shaking palsy. 1817." *J Neuropsychiatry Clin Neurosci* 14 (2):223-36; discussion 222. doi: 10.1176/jnp.14.2.223.

Pasanen, P., L. Myllykangas, M. Siitonen, A. Raunio, S. Kaakkola, J. Lyytinen, P. J. Tienari, M. Poyhonen, and A. Paetau. 2014. "Novel alpha-synuclein mutation A53E associated with atypical multiple system atrophy and

Parkinson's disease-type pathology." *Neurobiol Aging* 35 (9):2180 e1-5. doi: 10.1016/j.neurobiolaging.2014.03.024.

Patel, M. 2016. "Targeting Oxidative Stress in Central Nervous System Disorders." *Trends Pharmacol Sci* 37 (9):768-78. doi: 10.1016/j.tips.2016.06.007.

Poewe, W., A. Antonini, J. C. M. Zijlmans, P. R. Burkhard, and F. Vingerhoets. 2010. "Levodopa in the treatment of Parkinson's disease: an old drug still going strong." *Clinical Interventions in Aging* 5:229-238. doi: 10.2147/Cia.86456.

Politis, M., K. Wu, S. Molloy, P. G. Bain, K. R. Chaudhuri, and P. Piccini. 2010. "Parkinson's Disease Symptoms: The Patient's Perspective." *Movement Disorders* 25 (11):1646-1651. doi: 10.1002/mds.23135.

Polymeropoulos, M. H., C. Lavedan, E. Leroy, S. E. Ide, A. Dehejia, A. Dutra, B. Pike, H. Root, J. Rubenstein, R. Boyer, E. S. Stenroos, S. Chandrasekharappa, A. Athanassiadou, T. Papapetropoulos, W. G. Johnson, A. M. Lazzarini, R. C. Duvoisin, G. DiIorio, L. I. Golbe, and R. L. Nussbaum. 1997. "Mutation in the alpha-synuclein gene identified in families with Parkinson's disease." *Science* 276 (5321):2045-2047. doi: DOI 10.1126/science.276.5321.2045.

Priyadarshi, A., S. A. Khuder, E. A. Schaub, and S. S. Priyadarshi. 2001. "Environmental risk factors and Parkinson's disease: a metaanalysis." *Environ Res* 86 (2):122-7. doi: 10.1006/enrs.2001.4264.

Proukakis, C., C. G. Dudzik, T. Brier, D. S. MacKay, J. M. Cooper, G. L. Millhauser, H. Houlden, and A. H. Schapira. 2013. "A novel alpha-synuclein missense mutation in Parkinson disease." *Neurology* 80 (11):1062-4. doi: 10.1212/WNL.0b013e31828727ba.

Rascol, O., S. Perez-Lloret, and J. J. Ferreira. 2015. "New treatments for levodopa-induced motor complications." *Mov Disord* 30 (11):1451-60. doi: 10.1002/mds.26362.

Ray, P. D., B. W. Huang, and Y. Tsuji. 2012. "Reactive oxygen species (ROS) homeostasis and redox regulation in cellular signaling." *Cell Signal* 24 (5):981-90. doi: 10.1016/j.cellsig.2012.01.008.

Recasens, A., and B. Dehay. 2014. "Alpha-synuclein spreading in Parkinson's disease." *Front Neuroanat* 8:159. doi: 10.3389/fnana.2014.00159.

Reis, J., I. Encarnacao, A. Gaspar, A. Morales, N. Milhazes, and F. Borges. 2012. "Parkinson's disease management. Part II- discovery of MAO-B inhibitors based on nitrogen heterocycles and analogues." *Curr Top Med Chem* 12 (20):2116-30.

Rey, N. L., S. George, and P. Brundin. 2016. "Review: Spreading the word: precise animal models and validated methods are vital when evaluating prion-like behaviour of alpha-synuclein." *Neuropathol Appl Neurobiol* 42 (1):51-76. doi: 10.1111/nan.12299.

Robakis, D., and S. Fahn. 2015. "Defining the Role of the Monoamine Oxidase-B Inhibitors for Parkinson's Disease." *CNS Drugs* 29 (6):433-41. doi: 10.1007/s40263-015-0249-8.

Schapira, A. H. V. 2006. "Etiology of Parkinson's disease." *Neurology* 66 (10):S10-S23.

Schapira, A. H. V. 2009. "Neurobiology and treatment of Parkinson's disease." *Trends in Pharmacological Sciences* 30 (1):41-47. doi: 10.1016/j.tips.2008.10.005.

Schulte, C., and T. Gasser. 2011. "Genetic basis of Parkinson's disease: inheritance, penetrance, and expression." *Appl Clin Genet* 4:67-80. doi: 10.2147/TACG.S11639.

Shevchik, V. E., G. Condemine, and J. Robertbaudouy. 1994. "Characterization of Dsbc, a Periplasmic Protein of Erwinia-Chrysanthemi and Escherichia-Coli with Disulfide-Isomerase Activity." *Embo Journal* 13 (8):2007-2012.

Siddiqui, I. J., N. Pervaiz, and A. A. Abbasi. 2016. "The Parkinson Disease gene SNCA: Evolutionary and structural insights with pathological implication." *Sci Rep* 6:24475. doi: 10.1038/srep24475.

Singleton, A. B., M. Farrer, J. Johnson, A. Singleton, S. Hague, J. Kachergus, M. Hulihan, T. Peuralinna, A. Dutra, R. Nussbaum, S. Lincoln, A. Crawley, M. Hanson, D. Maraganore, C. Adler, M. R. Cookson, M. Muenter, M. Baptista, D. Miller, J. Blancato, J. Hardy, and K. Gwinn-Hardy. 2003.

"alpha-Synuclein locus triplication causes Parkinson's disease." *Science* 302 (5646):841. doi: 10.1126/science.1090278.

Sorce, S., K. H. Krause, and V. Jaquet. 2012. "Targeting NOX enzymes in the central nervous system: therapeutic opportunities." *Cell Mol Life Sci* 69 (14):2387-407. doi: 10.1007/s00018-012-1014-5.

Soto-Otero, R., E. Mendez-Alvarez, A. Hermida-Ameijeiras, A. M. Munoz-Patino, and J. L. Labandeira-Garcia. 2000. "Autoxidation and neurotoxicity of 6-hydroxydopamine in the presence of some antioxidants: Potential implication in relation to the pathogenesis of Parkinson's disease." *Journal of Neurochemistry* 74 (4):1605-1612. doi: DOI 10.1046/j.1471-4159.2000.0741605.x.

Spillantini, M. G., R. A. Crowther, R. Jakes, M. Hasegawa, and M. Goedert. 1998. "alpha-Synuclein in filamentous inclusions of Lewy bodies from Parkinson's disease and dementia with lewy bodies." *Proc Natl Acad Sci U S A* 95 (11):6469-73.

Spillantini, M. G., M. L. Schmidt, V. M. Lee, J. Q. Trojanowski, R. Jakes, and M. Goedert. 1997. "Alpha-synuclein in Lewy bodies." *Nature* 388 (6645):839-40. doi: 10.1038/42166.

Stefanis, L. 2012. "alpha-Synuclein in Parkinson's Disease." *Cold Spring Harbor Perspectives in Medicine* 2 (2). doi: 10.1101/cshperspect.a009399.

Stocchi, F., and M. Torti. 2016. "Adjuvant therapies for Parkinson's disease: critical evaluation of safinamide." *Drug Design Development and Therapy* 10:609-618. doi: 10.2147/Dddt.S77749.

Subramaniam, S. R., and M. F. Chesselet. 2013. "Mitochondrial dysfunction and oxidative stress in Parkinson's disease." *Progress in Neurobiology* 106:17-32. doi: 10.1016/j.pneurobio.2013.04.004.

Tarazi, F. I., Z. T. Sahli, M. Wolny, and S. A. Mousa. 2014. "Emerging therapies for Parkinson's disease: from bench to bedside." *Pharmacol Ther* 144 (2):123-33. doi: 10.1016/j.pharmthera.2014.05.010.

Tatton, W., R. Chalmers-Redman, and N. Tatton. 2003. "Neuroprotection by deprenyl and other propargylamines: glyceraldehyde-3-phosphate dehydrogenase rather than monoamine oxidase B." *J Neural Transm (Vienna)* 110 (5):509-15. doi: 10.1007/s00702-002-0827-z.

Teo, K. C., and S. L. Ho. 2013. "Monoamine oxidase-B (MAO-B) inhibitors: implications for disease-modification in Parkinson's disease." *Transl Neurodegener* 2 (1):19. doi: 10.1186/2047-9158-2-19.

The Food and Drug Administration. "FDA approves drug to treat Parkinson's disease." Last Modified 03/24/2017, accessed 05/15/2017. https://www.fda.gov/newsevents/newsroom/pressannouncements/ucm547852.htm.

Theillet, F. X., A. Binolfi, B. Bekei, A. Martorana, H. M. Rose, M. Stuiver, S. Verzini, D. Lorenz, M. van Rossum, D. Goldfarb, and P. Selenko. 2016.

"Structural disorder of monomeric alpha-synuclein persists in mammalian cells." *Nature* 530 (7588):45-+. doi: 10.1038/nature16531.

Tong, J., J. H. Meyer, Y. Furukawa, I. Boileau, L. J. Chang, A. A. Wilson, S. Houle, and S. J. Kish. 2013. "Distribution of monoamine oxidase proteins in human brain: implications for brain imaging studies." *J Cereb Blood Flow Metab* 33 (6):863-71. doi: 10.1038/jcbfm.2013.19.

Tuttle, M. D., G. Comellas, A. J. Nieuwkoop, D. J. Covell, D. A. Berthold, K. D. Kloepper, J. M. Courtney, J. K. Kim, A. M. Barclay, A. Kendall, W. Wan, G. Stubbs, C. D. Schwieters, V. M. Lee, J. M. George, and C. M. Rienstra. 2016. "Solid-state NMR structure of a pathogenic fibril of full-length human alpha-synuclein." *Nat Struct Mol Biol* 23 (5):409-15. doi: 10.1038/nsmb.3194.

Tyson, T., J. A. Steiner, and P. Brundin. 2016. "Sorting out release, uptake and processing of alpha-synuclein during prion-like spread of pathology." *J Neurochem* 139 Suppl 1:275-289. doi: 10.1111/jnc.13449.

Venda, L. L., S. J. Cragg, V. L. Buchman, and R. Wade-Martins. 2010. "alpha-Synuclein and dopamine at the crossroads of Parkinson's disease." *Trends in Neurosciences* 33 (12):559-568. doi: 10.1016/j.tins.2010.09.004.

Volpicelli-Daley, L. A., K. C. Luk, T. P. Patel, S. A. Tanik, D. M. Riddle, A. Stieber, D. F. Meaney, J. Q. Trojanowski, and V. M. Y. Lee. 2011. "Exogenous alpha-Synuclein Fibrils Induce Lewy Body Pathology Leading to Synaptic

Dysfunction and Neuron Death." *Neuron* 72 (1):57-71. doi: 10.1016/j.neuron.2011.08.033.

Wang, C., C. Zhao, D. Li, Z. Tian, Y. Lai, J. Diao, and C. Liu. 2016. "Versatile Structures of alpha-Synuclein." *Front Mol Neurosci* 9:48. doi: 10.3389/fnmol.2016.00048.

Wang, W., I. Perovic, J. Chittuluru, A. Kaganovich, L. T. T. Nguyen, J. L. Liao, J. R. Auclair, D. Johnson, A. Landeru, A. K. Simorellis, S. L. Ju, M. R. Cookson, F. J. Asturias, J. N. Agar, B. N. Webb, C. H. Kang, D. Ringe, G. A. Petsko, T. C. Pochapsky, and Q. Q. Hoang. 2011. "A soluble alpha-synuclein construct forms a dynamic tetramer." *Proceedings of the National Academy of Sciences of the United States of America* 108 (43):17797-17802. doi: 10.1073/pnas.1113260108.

Weinreb, O., T. Amit, O. Bar-Am, and M. B. Youdim. 2010. "Rasagiline: a novel anti-Parkinsonian monoamine oxidase-B inhibitor with neuroprotective activity." *Prog Neurobiol* 92 (3):330-44. doi: 10.1016/j.pneurobio.2010.06.008.

Weinreb, P. H., W. Zhen, A. W. Poon, K. A. Conway, and P. T. Lansbury, Jr. 1996. "NACP, a protein implicated in Alzheimer's disease and learning, is natively unfolded." *Biochemistry* 35 (43):13709-15. doi: 10.1021/bi961799n.

Winklhofer, K. F., and C. Haass. 2010. "Mitochondrial dysfunction in Parkinson's disease." *Biochim Biophys Acta* 1802 (1):29-44. doi: 10.1016/j.bbadis.2009.08.013.

Winklhofer, K. F., J. Tatzelt, and C. Haass. 2008. "The two faces of protein misfolding: gain- and loss-of-function in neurodegenerative diseases." *EMBO J* 27 (2):336-49. doi: 10.1038/sj.emboj.7601930.

Wirdefeldt, K., H. O. Adami, P. Cole, D. Trichopoulos, and J. Mandel. 2011. "Epidemiology and etiology of Parkinson's disease: a review of the evidence." *European Journal of Epidemiology* 26:S1-S58. doi: 10.1007/s10654-011-9581-6.

Wong, Y. C., and D. Krainc. 2017. "alpha-synuclein toxicity in neurodegeneration: mechanism and therapeutic strategies." *Nat Med* 23 (2):1-13. doi: 10.1038/nm.4269.

World Health Organization. 2006. *Neurological disorders: public health challenges*: World Health Organization.

Xu, Y., Y. Deng, and H. Qing. 2015. "The phosphorylation of alpha-synuclein: development and implication for the mechanism and therapy of the Parkinson's disease." *J Neurochem* 135 (1):4-18. doi: 10.1111/jnc.13234.

Yacoubian, T. A., and D. G. Standaert. 2009. "Targets for neuroprotection in Parkinson's disease." *Biochim Biophys Acta* 1792 (7):676-87. doi: 10.1016/j.bbadis.2008.09.009.

Yan, Z. Y., G. W. Caldwell, B. Y. Zhao, and A. B. Reitz. 2004. "A high-throughput monoamine oxidase inhibition assay using liquid chromatography with tandem mass spectrometry." *Rapid Communications in Mass Spectrometry* 18 (8):834-840. doi: 10.1002/rcm.1415.

Yedlapudi, D., G. S. Joshi, D. Luo, S. V. Todi, and A. K. Dutta. 2016. "Inhibition of alpha-synuclein aggregation by multifunctional dopamine agonists assessed by a novel in vitro assay and an in vivo Drosophila synucleinopathy model." *Sci Rep* 6:38510. doi: 10.1038/srep38510.

Youdim, M. B., and Y. S. Bakhle. 2006. "Monoamine oxidase: isoforms and inhibitors in Parkinson's disease and depressive illness." *Br J Pharmacol* 147 Suppl 1:S287-96. doi: 10.1038/sj.bjp.0706464.

Youdim, M. B., D. Edmondson, and K. F. Tipton. 2006. "The therapeutic potential of monoamine oxidase inhibitors." *Nat Rev Neurosci* 7 (4):295-309. doi: 10.1038/nrn1883.

Youdim, M. B., and P. F. Riederer. 2004. "A review of the mechanisms and role of monoamine oxidase inhibitors in Parkinson's disease." *Neurology* 63 (7 Suppl 2):S32-5.

Zarranz, J. J., J. Alegre, J. C. Gomez-Esteban, E. Lezcano, R. Ros, I. Ampuero, L. Vidal, J. Hoenicka, O. Rodriguez, B. Atares, V. Llorens, E. Gomez Tortosa, T. del Ser, D. G. Munoz, and J. G. de Yebenes. 2004. "The new mutation, E46K, of alpha-synuclein causes Parkinson and Lewy body dementia." *Ann Neurol* 55 (2):164-73. doi: 10.1002/ana.10795.

Zhao, J., S. Yu, Y. Zheng, H. Yang, and J. Zhang. 2017. "Oxidative Modification and Its Implications for the Neurodegeneration of Parkinson's Disease." *Mol Neurobiol* 54 (2):1404-1418. doi: 10.1007/s12035-016-9743-3.

Zhen, J., T. Antonio, S. Ali, K. A. Neve, A. K. Dutta, and M. E. A. Reith. 2015. "Use of radiolabeled antagonist assays for assessing agonism at D-2 and D-3 dopamine receptors: Comparison with functional GTR(gamma)S assays." *Journal of Neuroscience Methods* 248:7-15. doi: 10.1016/j.jneumeth.2015.03.028.

Zhen, J., T. Antonio, A. K. Dutta, and M. E. A. Reith. 2010. "Concentration of receptor and ligand revisited in a modified receptor binding protocol for high-affinity radioligands: [H-3]Spiperone binding to D-2 and D-3 dopamine receptors." *Journal of Neuroscience Methods* 188 (1):32-38. doi: 10.1016/j.jneumeth.2010.01.031.

Zivec, M., B. Anzic, and S. Gobec. 2010. "A Novel Scalable Synthesis of Pramipexole." *Organic Process Research & Development* 14 (5):1125-1129. doi: 10.1021/op1000989.

ABSTRACT

APPROACH TOWARDS THE DEVELOPMENT OF NOVEL DISEASE MODIFYING THERAPEUTICS FOR PARKINSON'S DISEASE

by

DAN LUO

August 2017

Advisor: Dr. Aloke Dutta

Major: Pharmaceutical Sciences

Degree: Doctor of Philosophy

Parkinson’s disease (PD) is an age-related neurodegenerative disease, which is characterized by the progressive loss of dopaminergic neurons in the substantia nigra pars compacta (SNpc) and the presence of intraneuronal proteinaceous deposits named Lewy bodies (LBs) or Lewy neurites (LNs). A broad spectrum of motor and non-motor symptoms has been observed in PD, with bradykinesia, resting tremor, rigidity, and postural instability as its key clinical features. Although the etiology of PD is still not well-understood, multiple pathological factors including oxidative stress, mitochondrial dysfunction, α-synuclein (αSN) protein aggregation, as well as genetic and environmental aspects are strongly implicated in the disease progression. The present treatments available for PD generally fall into four major categories, namely levodopa/carbidopa, monoamine oxidase B (MAO-B) inhibitors, catechol-*O*-methyl transferase (COMT) inhibitors, and dopamine agonists. However, these current clinical treatments are only able to provide symptomatic relief and fail to

delay the disease progression. Furthermore, the long-term use of levodopa leads to motor complications including the development of dyskinesia. Thus, there is still a great unmet need for effective treatment of PD which should involve disease modification. Due to the complexity observed in the disease pathogenesis, treatments that incorporates the pathogenic factors involved in PD might offer an advantage in combating the disease by modifying the disease progression. The hypothesis of this project is that the incorporation of dopamine D_2/D_3 agonistic binding component to accessory moieties targeting either αSN aggregation or MAO-B enzyme may lead to multifunctional drugs with a potential to provide both symptom-relieving and disease-modifying effects as a promising approach for new generation PD treatment.

In this dissertation, two library of compounds have been developed based on the previously established hybrid structure approach, and the initial structure-activity relationship (SAR) study has been perused to identify possible lead compounds through *in vitro* and *in vivo* evaluations. The first main objective is to design and develop a series of novel dopamine D_2/D_3 receptor agonists that can potentially modulate α-synuclein (αSN) aggregation by combining the dihydroxy or hydroxy-methoxy component with D_2/D_3 agonist fragment through various linkers according to the hybrid molecular template. Based on the results of *in vitro* receptor assays, compounds (−)-**8a** (**D-593**), (−)-**20** (**D-618**), (−)-**14** (**D-644**), and (−)-**49** (**D-670**) were selected and further evaluated to determine their potential αSN aggregation modulatory properties and neuroprotective effect.

Subsequently, compound (−)-**8a** (**D-593**) was identified as a lead compound by using a well-established Parkinson's disease (PD) animal model. The second main objective is to design and synthesize a series of novel dopamine D_2/D_3 receptor agonists that may potentially inhibit monoamine oxidase B (MAO-B) activity by introducing the propargyl group into the hybrid molecular template. An initial SAR study was conducted based on the generated compound library through *in vitro* receptor assays and enzymatic studies which led to the identification of compounds (−)-**62b** (**D-629**) and (−)-**76** (**D-614**) as potential candidates. Moreover, *in vitro* neuroprotection models and a PD animal model were used to further evaluate them, and (−)-**76** (**D-614**) was identified as the lead compound that requires further modification.

AUTOBIOGRAPHICAL STATEMENT

DAN LUO

Education

Bachelor of Medicine, Pharmacology 2011
Anhui University of Traditional Chinese Medicine, Hefei, China

Awards and Honors

Wayne State University

Frank O. Taylor Scholarship	2017
Thomas C. Rumble University Graduate Fellowship	2016
Graduate Research Assistantship	2012-2016

Anhui University of Traditional Chinese Medicine

Guangdong Yifang Scholarship	2010
Second-class People's Scholarship	2008-2009

Publications

1. **Luo, D.**; Sharma, H.; Yedlapudi, D.; Antonio, T.; Reith, M. E.; Dutta, A. K., Novel multifunctional dopamine D2/D3 receptors agonists with potential neuroprotection and anti-alpha synuclein protein aggregation properties. *Bioorg Med Chem* **2016,** *24* (21), 5088-5102.
2. Das, B.; Rajagopalan, S.; Joshi, G. S.; Xu, L.; **Luo, D.**; Andersen, J. K.; Todi, S. V.; Dutta, A. K., A novel iron (II) preferring dopamine agonist chelator D-607 significantly suppresses alpha-syn- and MPTP-induced toxicities in vivo. *Neuropharmacology* **2017,** *123*, 88-99.
3. Yedlapudi, D.; Joshi, G. S.; **Luo, D.**; Todi, S. V.; Dutta, A. K., Inhibition of alpha-synuclein aggregation by multifunctional dopamine agonists assessed by a novel in vitro assay and an in vivo Drosophila synucleinopathy model. *Sci Rep* **2016,** *6*, 38510.
4. Das, B.; Vedachalam, S.; **Luo, D.**; Antonio, T.; Reith, M. E.; Dutta, A. K., Development of a Highly Potent D2/D3 Agonist and a Partial Agonist from Structure-Activity Relationship Study of N(6)-(2-(4-(1H-Indol-5-yl)piperazin-1-yl)ethyl)-N(6)-propyl-4,5,6,7-tetrahydrobenzo[d]thiazole-2,6-diamine Analogues: Implication in the Treatment of Parkinson's Disease. *J Med Chem* **2015,** *58* (23), 9179-95.

Published Abstract and Presentation

1. **Luo, D.**; Sharma, H.; Antonio, T.; Reith, M. E.; Dutta, A. K., Design, synthesis, and initial structure-activity relationship (SAR) study of novel multifunctional dopamine D_2/D_3 agonists with modulatory property against α-synuclein aggregation and toxicity. 250th American Chemical Society National Meeting and Exposition, Boston, MA, USA, August 16-20, 2015.